



This work is protected by copyright and other intellectual property rights and duplication or sale of all or part is not permitted, except that material may be duplicated by you for research, private study, criticism/review or educational purposes. Electronic or print copies are for your own personal, non-commercial use and shall not be passed to any other individual. No quotation may be published without proper acknowledgement. For any other use, or to quote extensively from the work, permission must be obtained from the copyright holder/s.

"THE SOLID GEOLOGY OF THE AREA BETWEEN BINIC AND BREHEC,
CÔTES DU NORD, FRANCE."

A thesis

VOL 2

By: PAUL DESMOND RYAN, B.A.

Submitted to the University of Keele for the Degree of Ph.D.

September 1973.



IMAGING SERVICES NORTH


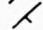




Boston Spa, Wetherby

West Yorkshire, LS23 7BQ

www.bl.uk

**CONTAINS
PULLOUTS**

STRUCTURAL MAP OF THE
"SERIES DE BINIC"

- K E Y
-  S_{2C}
 -  S_B
 -  axial trace F_{2C}
 -  antiform
 -  axial trace F_{1C}
 -  synform

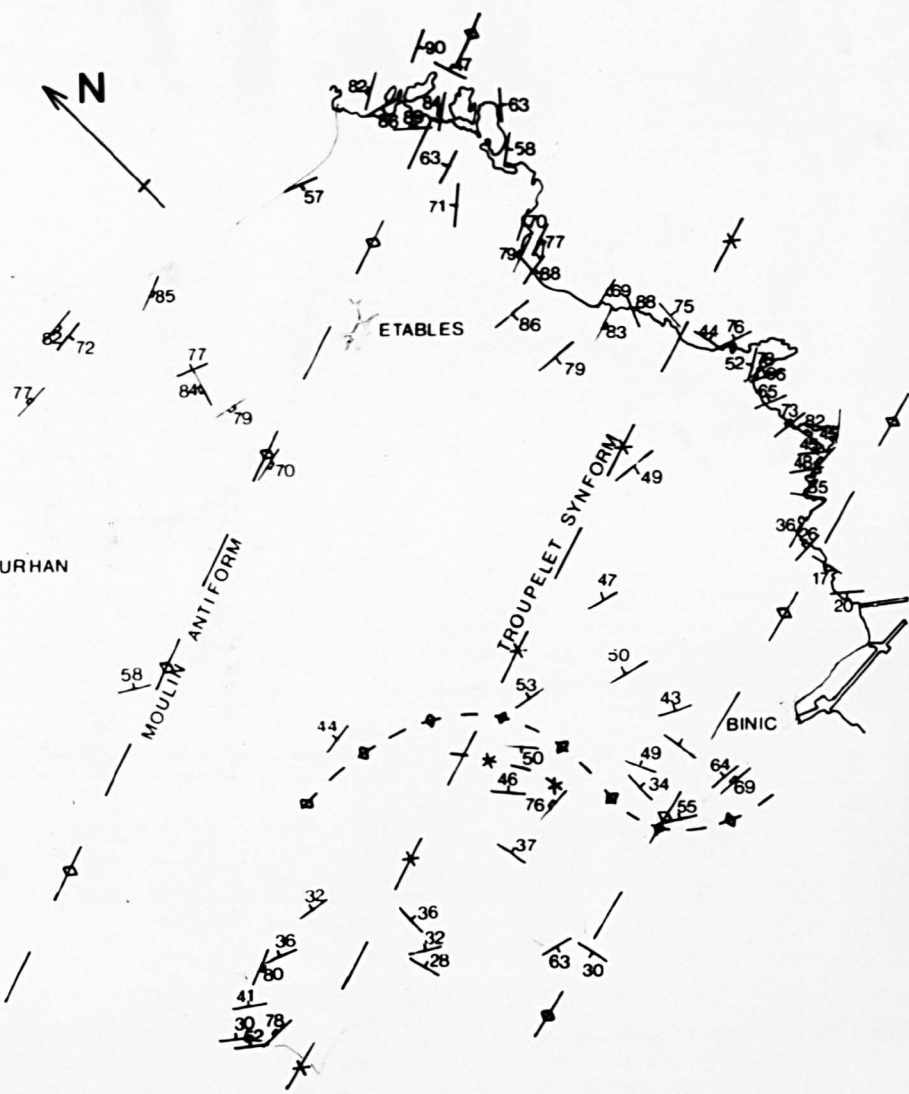
PLOURHAN

ETABLES

BINIC

MOULIN ANTIFORM

TROUPELET SYNFORM



CHAPTER IV

THE CADOMIAN OROGENY

A. Introduction

This orogeny, which Adams (1967) and Roach et al (1972) have shown to have occurred between 690 - 570 m.y. ago, has deformed and metamorphosed the Brioverian sediments and, to a variable degree, the Pentevrian basement. A detailed study of the structures and metamorphic assemblages developed during this event has been undertaken. A particular effort has been made to evaluate the history of events for the Cadomian orogeny in this region as there has been considerable disagreement amongst previous authors (see page 1.6) as to the complexity of the structural history and its relationship to metamorphic events.

The tectonic and metamorphic history of the Cadomian orogeny for this area has been evaluated for three separate lithological sequences each of which yield slightly different stories. These are:

The Binic-Bréhec Series. This sequence includes the Brioverian sediments of the Series de Binic, the Brioverian of Pointe de la Tour and the Brioverian of Bréhec.

The Palus plage Brioverian. These are Brioverian metasediments and metavolcanics that outcrop in the region of Palus plage where they can be seen to lie unconformably upon Pentevrian basement. (see Chapter III).

The Pentevrian. This includes all rocks found in the area that are thought to belong to the pre-Brioverian crystalline basement.

The chapter consists of first a description of the Cadomian structures found in each of these sequences, then an account of the metamorphic history for each area, and finally a summary and synthesis of all these events.

Deformation	Fold phase	Style	Foliation	Lineation	Metamorphism	Mineral assemblage
D _{1C}	F _{1C}	? tight or isoclinal folds with some overturning and approximately N-S striking axial surfaces.
D _{2C}	F _{2C}	Close to isoclinal upright folds with 75°-255° striking axial surfaces	S _{2C}	...	M _{2C} (? continuous crystallisation ?) ↓	Quartz, albite, biotite and zoisite (in calcareous bands).
D _{3C}	F _{3C}	tight small scale similar folds, whose axial surfaces are parallel to S _{2C}	S _{2C}	...		
D _{4C}	...	crenulation lineation of local development	...	L _{4C}		
D _{5,6,7C}	K _A , K _B , K _C	conjugate kink bands		
...	M _{5C}	metasomatic muscovite

Table 4.1. Structural and Metamorphic History of the Binic-Bréhec Series.

Figure 4.3. Stereographic projections showing late Cadomian brittle structures developed throughout the area studies: A) 96 poles to actual surfaces of kink bands; B) 71 poles to epidotised and quartz-filled shear zones; C) maxima from A indicating 3 conjugate sets of kinks A1, 2; B1,2; c1,2. See text for further explanation.

shear zones (Plates 4.6 and 4.7). The kink bands are only well developed in the Series de Binic, where they cut the S_{2C} foliation. The other structures are found elsewhere in the region, the epidotized shears being restricted to the Pentevrian and the Saint Quay intrusion. Within the Series de Binic the kink bands pass into quartz veins along their axial planes and 'en echelon' quartz veins are often formed as a result of dilation of the cleavage during the formation of the kink band.

Figure 4.3A is a stereographic projection of the poles to the axial planes of the kink bands found within the Series de Binic. When this is compared with figure 4.3B, which is a stereographic projection of poles to quartz veins, epidotised shears, and to the axial surfaces of 'en echelon' quartz veins it will be seen that although the two diagrams are complex all the maxima are coincident. This would suggest that the stress fields that gave rise to the kinks within the Series de Binic were also responsible for the formation of these other late structures.

It has been possible to recognise three sets of conjugate kink bands in the Series de Binic, the poles to the axial planes of these being represented by the maxima A_1 and A_2 , B_1 and B_2 and C_1 and C_2 in Figure 4.3C. The other two maxima may represent a fourth set of conjugate kink bands but this has not been seen in the field. Both sets A and B are seen to have overall monoclinic symmetry with respect to the cleavage S_{2C} as the axes of intersection of the two axial surfaces A_1 and A_2 (A) and B_1 and B_2 (B) lie within the plane of the cleavage (Figure 4.3C). See C show overall triclinic symmetry with respect to the cleavage S_{2C} , as the axis of intersection of the two axial planes (c) does not lie within S_{2C} .

Each of these sets of conjugate kink bands is found to be more well developed in one particular area. Set A are common around Binic, set B are common at Moulin plage and set C are common in the northern half of

Deformation	Fold phase	Style	Foliation	Lineation	Metamorphism	Mineral assemblages
D _{1C}	F _{1C}	isoclinal folds with NE - SW trending axial surfaces which are associated with the development of shear zones or slides?	S _{1C}	...	M _{1C}	biotite + actinolite + (quartz + plagioclase)
D _{2C}	F _{2C}	isoclinal folds which die out in basement and have axial surfaces that strike 80°-260°	S _{2C}	L _{2C}	M _{2C}	andesine + quartz + biotite + hornblende
...	M _{3C}	andesine + quartz + biotite + hornblende + garnet + cordierite + anthophyllite + magnetite
D _{3C}	...	retrograde shear zones which are associated with flattening and tightening of earlier structures	S _{3C}	L _{3C}	M _{4C}	quartz + albite + chlorite + sericite + epidote
...	M _{5C}	muscovite (calcite + haematite + garnet + sphene in veins?)

Table 4.2. The structural and metamorphic history of the Palus plage Brioverian.

the Series.

2. Cadomian Structures in the Palus Brioverian

(a) Introduction

This sequence of meta-volcanics and meta-sediments which are described in the previous Chapter (page 3.18ff) is seen to rest unconformably upon the Pentevrian basement along the east side of Palus plage. The geological map for this region (Figure 3.16) shows the outcrop pattern of the unconformity to be complex. This is the result of polyphase deformation of the Brioverian cover and the Pentevrian basement during the Cadomian orogeny. While the Cadomian deformation events in this area are similar to those recorded in the rest of the region studied the metamorphic textures differ from those recorded elsewhere.

The following sequence of deformational events can be shown to have been operative: (Table 4.2):

1. A phase of folding F_{1C} that produced large and small scale folds with a locally developed axial surface foliation S_{1C} . Northeast-southeast trending shear belts may also have developed during this event.
2. A phase of folding F_{2C} that produced structures with east-northeast - west-southwest striking axial surfaces. An associated axial surface foliation S_{2C} is developed throughout the area.
3. A phase of flattening D_{3C} that caused tightening of the earlier structures. Shear belts with a cataclastic foliation S_{3C} are locally developed.

The late phases of kinking that are found elsewhere in the region are not present within this sequence.

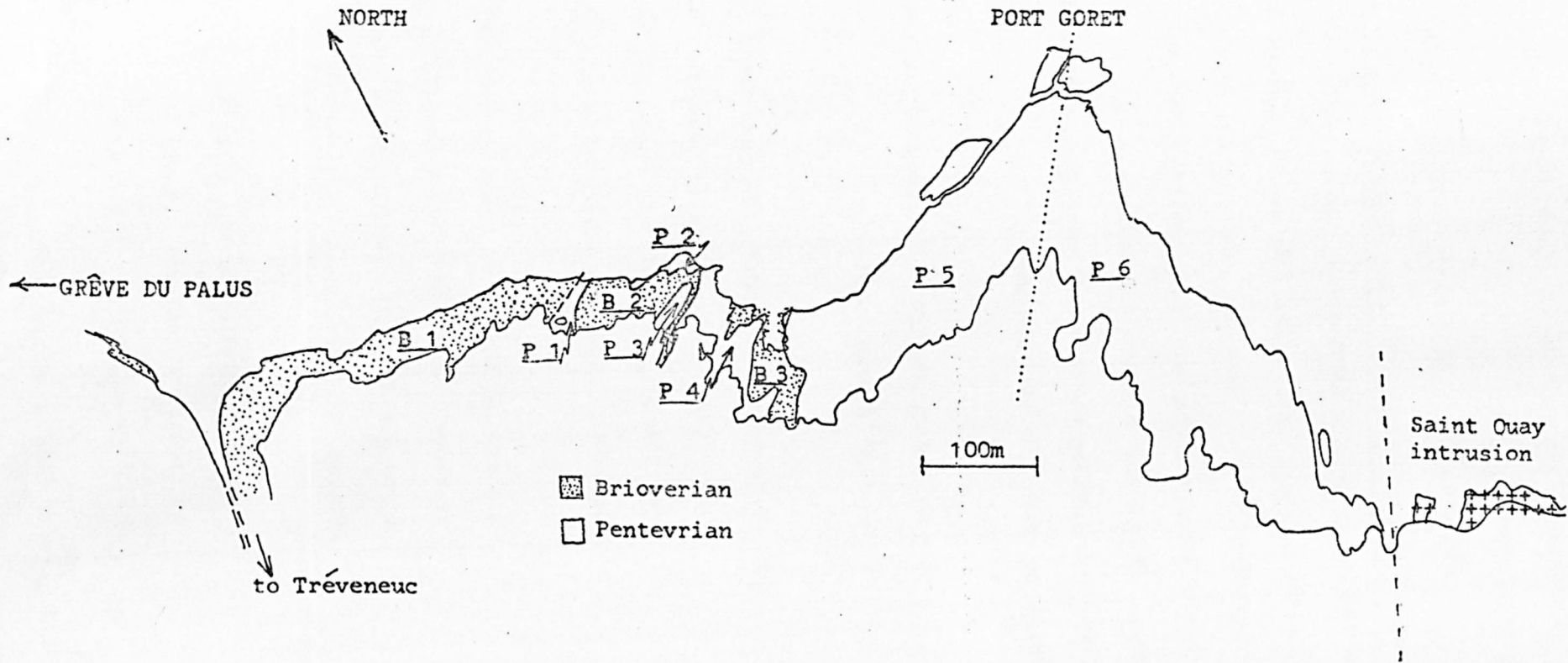
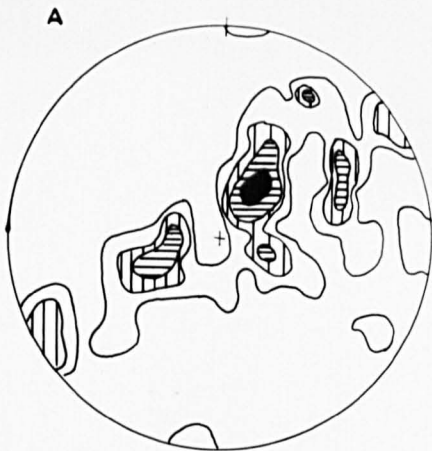
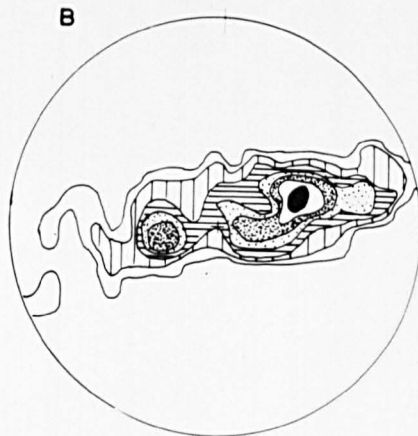


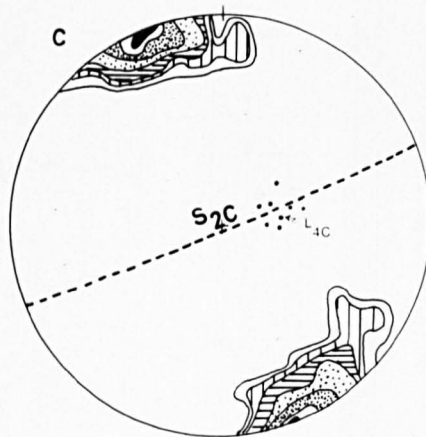
Figure 4.1. Structural map of the Series de Binic.



67 axes small scale F_{2C} folds
[contours at 1,3,5,8%]



89 $S_B \setminus S_{2C}$ intersections
[contours at 1,2,4,6,8,10,12%]



121 poles to S_{2C} , Series de Binic.
[contours at 1,2,4,8,16,22,30%]

Figure 4.2. Stereographic projections of structures found within the Binic - Brehec Series:

- A) 67 axes of small scale F_{2C} folds;
- B) Cleavage S_{2C} / bedding intersections;
- c) Contoured stereogram showing 121 poles to S_{2C} within the Series de Binic.

B. Cadomian Structures

1. Cadomian structures in the Binic-Brehec Series.

The Brioverian turbidites have been effected by the following structural events (Table 4:1).

- (a) A phase of folding, termed F_{1C} , that produced tight to isoclinal overturned folds.
- (b) A phase of folding termed F_{2C} that produced tight to isoclinal folds about east-west axial surfaces.
- (c) A phase of deformation, termed F_{3C} , that resulted in the formation of small scale folds and the tightening of previous structures by displacement along the S_{2C} cleavage.
- (d) A phase of crinkling that resulted in the local formation of a marked lineation termed L_{4C} .
- (e) Several late phases of kinking that have produced at least three conjugate sets of kink bands.

(a) First phase of folding F_{1C}

This phase of folding does not have any associated penetrative metamorphic fabric and fold closures and minor structures developed during this event are difficult to identify, but where these are found they are clearly deformed by folds of the second Cadomian fold phase F_{2C} (Figure 4.1). It is only from a study of the structures associated with the second phase of folding, F_{2C} , that it can be shown that these F_{1C} folds were developed throughout the region.

The cleavage/bedding intersections associated with the F_{2C} folds (Figure 4.2B) and the axes of small scale F_{2C} structures (Figure 4.2A) are found to lie within the axial surface of this fold phases S_{2C} (Figure 4.2C), but not to be parallel to one another. This indicates that the F_{2C} folds

are non-cylindroidal and must have been formed upon an already deformed surface.

The concentration of these lineations about two closely spaced maxima (Figure 4.2B) indicates that the pre- F_{2C} surface was folded into tight symmetrical folds of a small dihedral angle. Evidence that one of the limbs of the F_{1C} folds was overturned is found at Moulin Plage where about one hundred metres south from the entrance to the beach an antiformal closure within the well bedded Series de Binic may be seen. This closure was developed during F_{2C} . It is tight with a vertical east-west striking axial plane and an axis that plunges steeply to the east. A study of sedimentary features found within the bedding (e.g. graded bedding, cross bedding, flame structures and load casts) indicates that both limbs of this fold are inverted, i.e. they both young towards the axial plane of the fold. This type of fold may only be produced if the bedding was inverted prior to the development of the fold.

One of the features of this first phase of deformation is the lack of associated small scale structures. There are certain localities however such as at Bréhec where small scale F_{1C}/F_{2C} interference structures may be seen. These are basin and dome Ramsay type 1 structures (Ramsay 1962). Such structures are symmetrical, their form suggesting that the trace of the F_{1C} axial plane runs at a high angle to that of the F_{2C} folds. These F_{1C} folds appear to have had steeply inclined north-south trending axial planes with almost horizontal axes.

Examination of Figure 4.1 will show that there are reversals of the dip of the bedding in the Series de Binic along the axis of the F_{2C} Moulin antiform. These reversals are attributed to the F_{1C} phase of folding. It is, however, interesting to note that in the south of the area these reversals are not severe, and it would appear that the dihedral angle of the F_{1C} folds was in the order of 90° as indeed is suggested by the form



Plate 4.1. Small scale F_{2C} folds at Pointe de la Tour. Scale in inches.

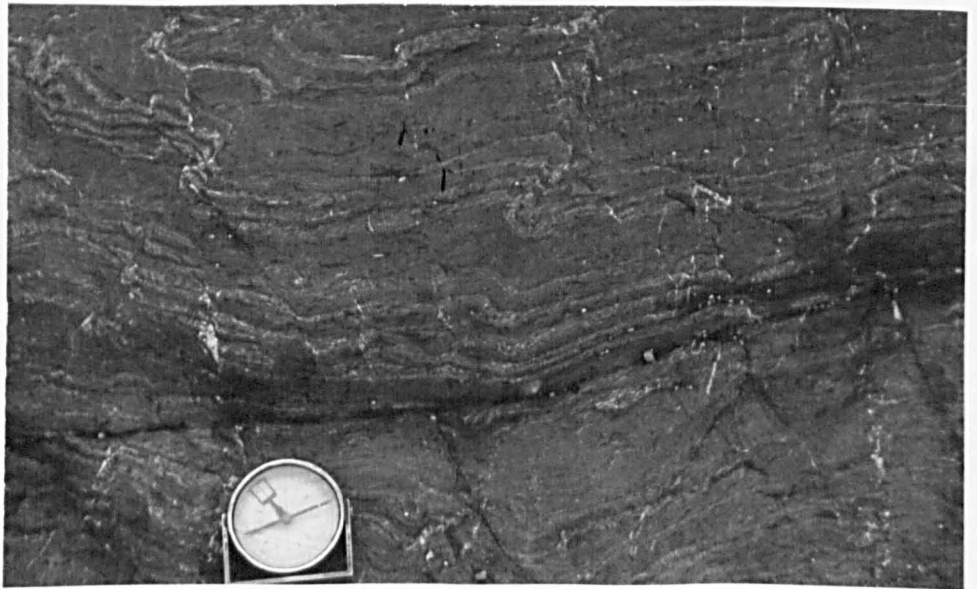


Plate 4.2. Small scale F_{2C} folds at Pointe de la Tour. These are accommodatory folds developed in interbedded siltstones and mudstones that separate thick bands of sandstones. Note that the axial surfaces are not all parallel and that occasional conjugate folds are developed (bottom right).

of the interference structures found at Bréhec. This would seem to contradict the observation that the F_{1C} folds were overturned to the north at Moulin plage. There is probably either a change in style of the folding, the folds being overturned at Moulin plage and not elsewhere, or Moulin plage lies on the limb of a large-scale F_{1C} structure which is overturned and the other regions lie on the hinge region of such a fold. The second alternative is felt to be unlikely as there is no general inversion of bedding at Moulin plage. If there is indeed a change in the style of the F_{1C} folds this may well be associated with the Saint Quay intrusion. The Saint Quay intrusion is cut by shear zones which may have developed during D_{1C} (page 527), the phase of deformation responsible for the F_{1C} . The mineral assemblage in these shear zones is in equilibrium with that of the surrounding rock. This implies that the igneous body had not cooled significantly from its temperature of intrusion although it was rigid enough to be subject to brittle deformation. Thus the rocks in the aureole, i.e. the Brioverian of Moulin plage may well have been hot during the folding and this body may have reacted as a resistant block. Both of these factors could have contributed to the change in style of these folds.

(b) Second phase of folding, F_{2C} .

The folds developed during this phase are the most important in controlling the structures of this region. In the Series de Binic two large scale folds, the Moulin antiform and the Troupelet synform have been developed (Figure 4.1). Elsewhere, although no major folds are recognised, smaller scale folds (Plates 4.1 and 4.2) associated with this event are very common. A penetrative micaceous foliation S_{2C} parallel to the axial surfaces of these folds is present throughout the region but it is best developed in the Series de Binic. (Figure 4.2C) where it is generally vertical and strikes 70° - 250° east of north.

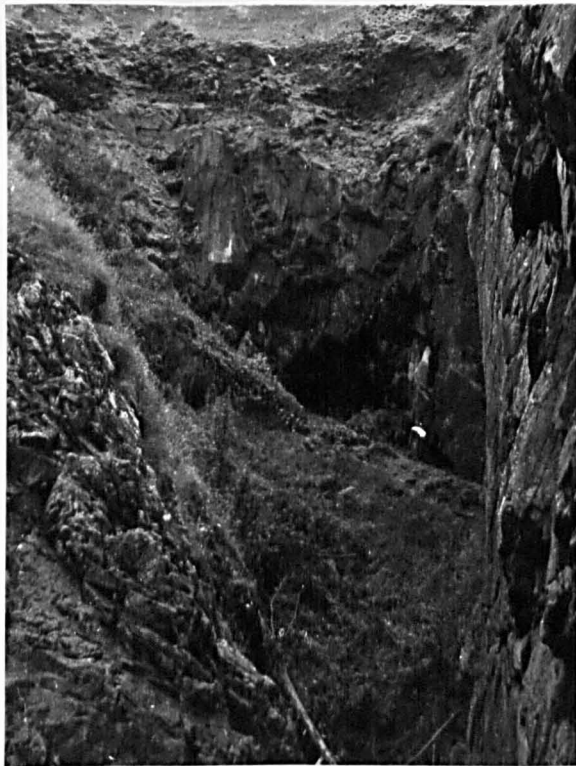


Plate 4.3.

A large scale F_{2C} synform developed on the northern limb of the Moulin antiform. Field of view is approximately 10 m.

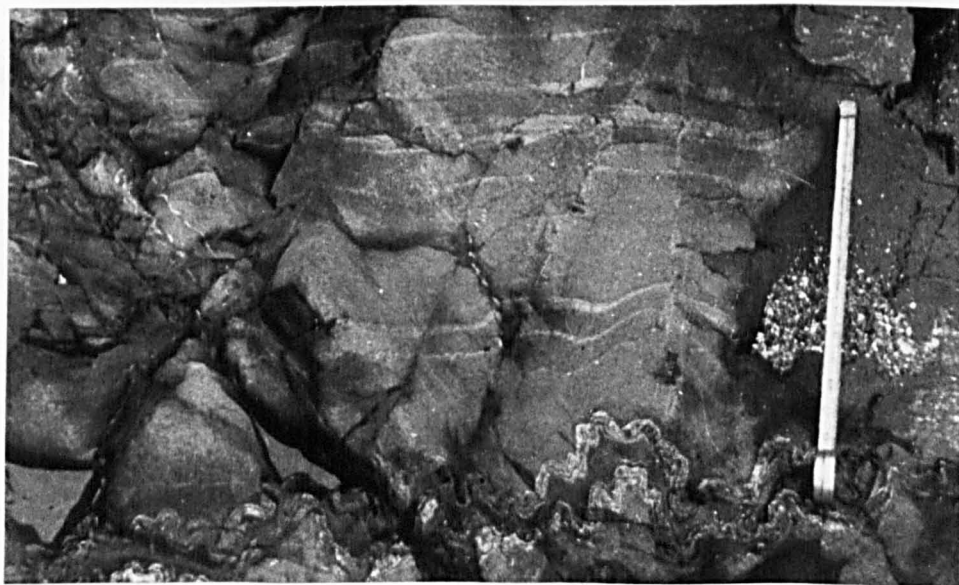


Plate 4.4.

Small scale F_{2C} folds and ptygmatically folded pre- F_{2C} quartz vein, Goudelin plage. Scale in inches.



Plate 4.5.

Boudinaged post F_{2C} quartz vein which is parallel to S_{2C} . This vein^{2C} cuts through the hinge region of an F_{3C} synform (bedding defining this fold is faint^{3C} but can be seen at the top end of the scale and at the 6 inch mark) and is parallel to its axial surface, S_{3C} .

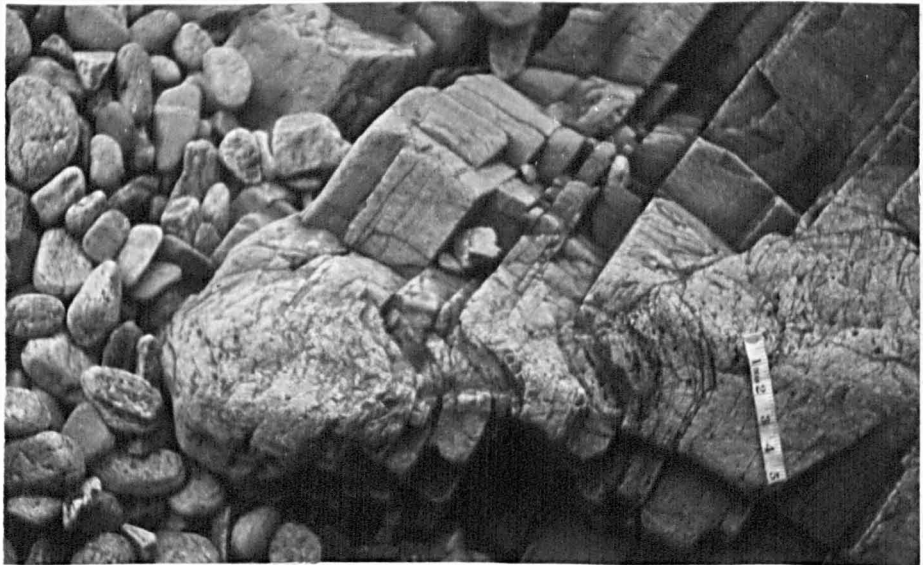


Plate 4.6.

Cadomian kink band in the Plouha Series at Bonaparte plage. Scale in inches.

The Moulin antiform is a complex major fold of wavelength not less than 1.2km and amplitude not less than 0.8km (Figure 4.1). At Moulin plage the statistically defined axis of this fold plunges at 44° towards 85° east of north. The Troupelet synform lies to the south of the Moulin antiform and has a wavelength of not less than 900m. Subsidiary folds (Plate 4.3) developed around these structures have axial planes that are parallel to that of the major folds and S_{2C} , but their axes are not parallel to those of the major folds (Figure 4.2A). Wherever investigated these folds were found to be flattened concentric folds (Class 1c, Ramsay 1967 Chapter 7). Ptygmatic folds (Plate 4.4) of this generation have been formed in quartz veins that were intruded parallel to bedding prior to this event. There is very little change in the thickness of these veins around these folds indicating that they were formed as the result of buckling.

(c) Third Phase of folding F_{3C} .

Quartz veins that cut across the hinge regions of the F_{2C} folds in the Moulin plage area without themselves being folded are often boudinaged. (Plate 4.5). This boudinaging, that is a result of displacement along the S_{2C} cleavage, can be seen to be associated with the formation of small scale folds. These folds, that may be best seen where there are thin beds of silty material interbedded with thick beds of mudstone, have been formed by inhomogenous simple shear that has resulted in differential displacement of the bedding along the cleavage. The thickness parallel to the axial surface of these folds is constant, as would be expected for folds formed by this mechanism. These folds can therefore be classified as Class 2 (Ramsay 1967) or similar type folds. The axial surfaces of these folds are everywhere parallel to the cleavage S_{2C} . As the bedding is not parallel to the cleavage this would suggest that there had been no component of homogenous strain associated with their formation, otherwise this would have resulted in the rotation of their axial planes so that they were no longer parallel

with the shear surfaces along which they were formed , i.e. the cleavage. The plunge of the axes of these folds is variable, although they always lie within the cleavage.

The formation of these folds is not associated with any retrogression of the metamorphic assemblage associated with the development of S_{2C} , and the foliation in their hinge regions is still defined by the alignment of biotite flakes.

This deformation, although closely associated kinetically with F_{2C} , occurred subsequent to the F_{2C} buckling and it has therefore been treated as a separate phase of deformation. Elsewhere in the region studied, the structures and metamorphic assemblages associated with this phase of deformation are very different to those developed in the Binic-Bréhec Series during F_{2C} and the fact that F_{3C} was a distinct and later phase of deformation becomes obvious.

(d) Phase of deformation, D_{4C} , that caused the development of the L_{4C} lineation.

On the southern limb of the Moulin antiform the cleavage S_{2C} is crenulated by microfolds that have resulted in the development of a marked lineation, L_{4C} . This event occurred during the growth of biotite, as flakes of this mineral can be seen to be orientated parallel to the B lineation formed by the axes to the east (Figure 4.2c), no other structures are associated with this deformation. This event was post the development of the S_{2C} cleavage but prior to the phase of kinking which occurred after the end of biotite growth.

(e) The late phases of kinking.

Subsequent to the termination of the major tectonic and metamorphic episodes the region experienced several phases of brittle deformation that have produced kink bands, 'en echelon' quartz veins, quartz veins and epidotized

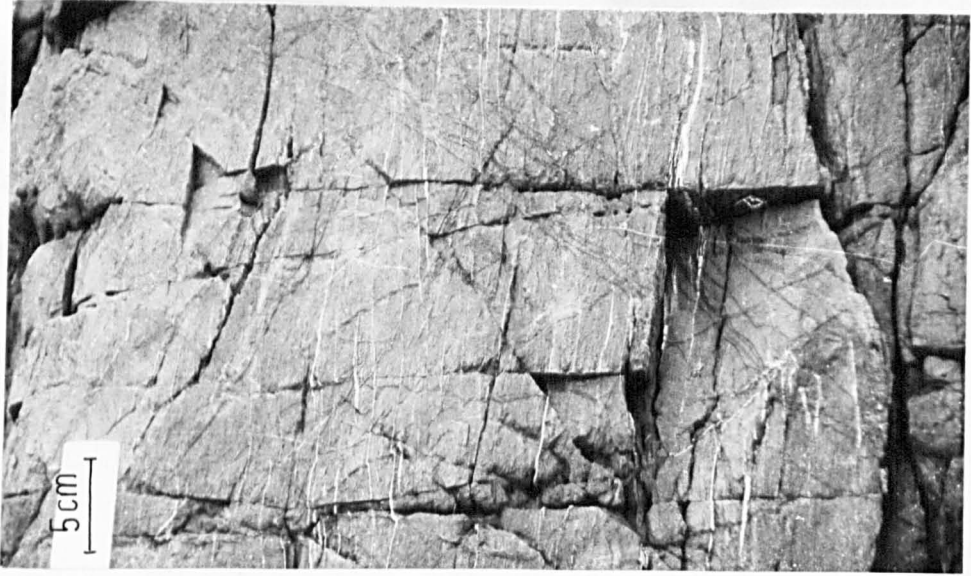


Plate 4.7. En echelon quartz veins at Goudelin plage.

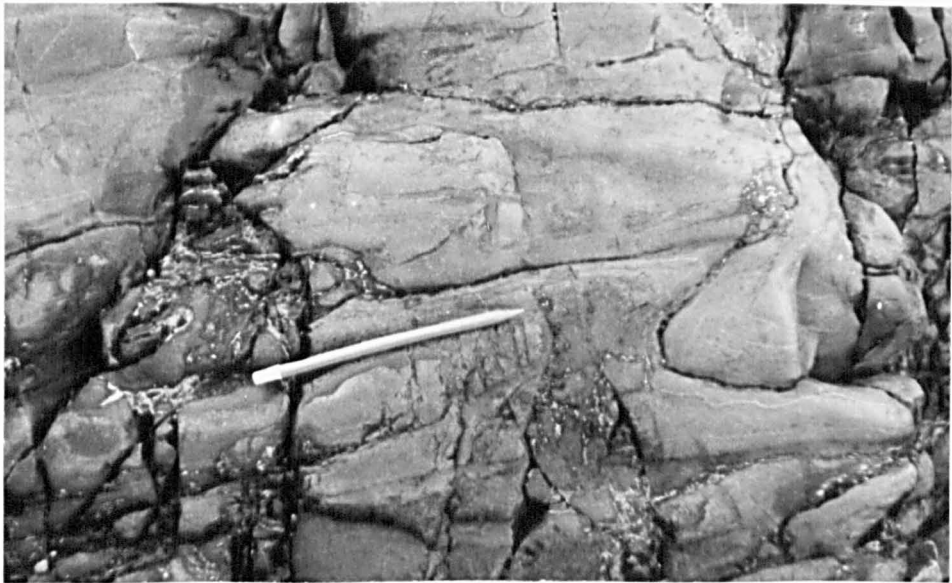
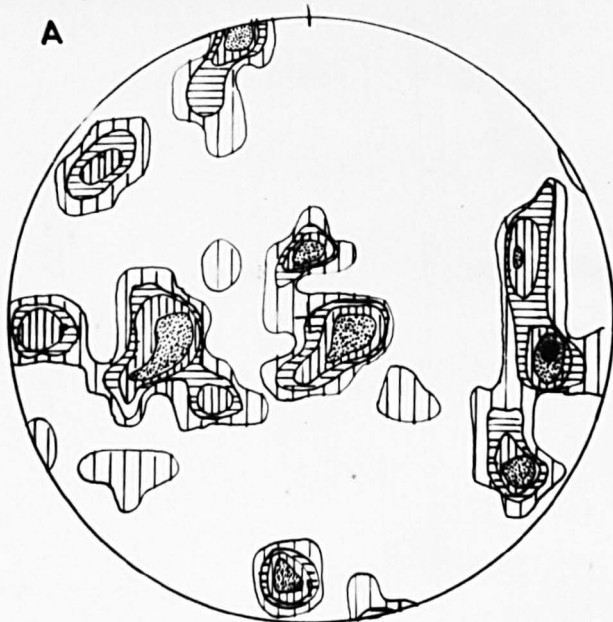
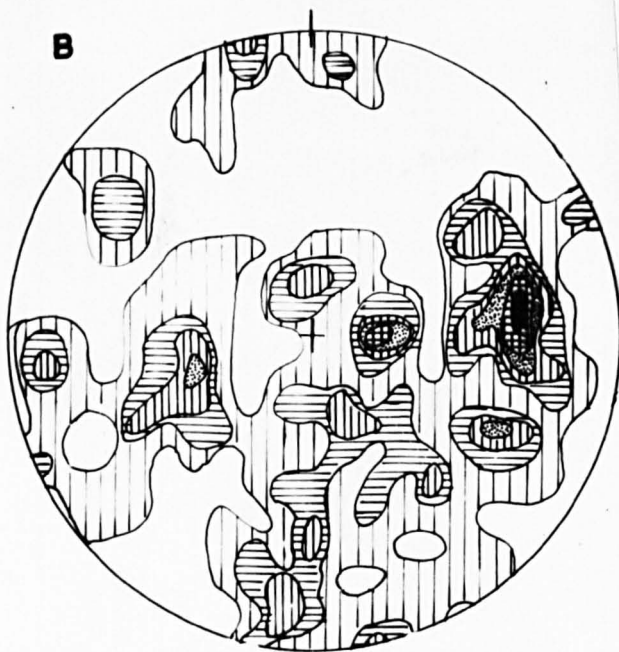


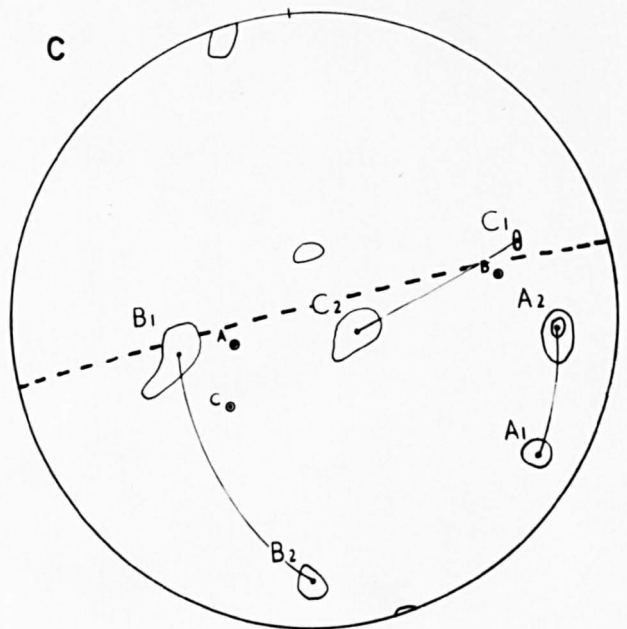
Plate 4.8. Asymmetric 'Z' type F_{1C} folds in the pelites at Palus plage. The pencil is parallel to S_{1C} in the core of a complex antiform.



A
 Poles to axial surfaces 96 kink bands
 [contours at 1,2,3,4,5%]



B
 71 poles to epidotised &
 quartz filled shear zones
 [contours at 0.5,1.5,2.5,4,5,7%]



C
 Maxima from A, indicating 3
 conjugate sets of kinks.

Figure 4.4. Sketch map of Palus plage section showing the location of the various sub-areas referred to in the text. Brioverian sub-areas are preceded by the letter B and Pentevrian sub-areas by the letter P. Contacts between the sub-areas will be denoted by reference to the two notations.

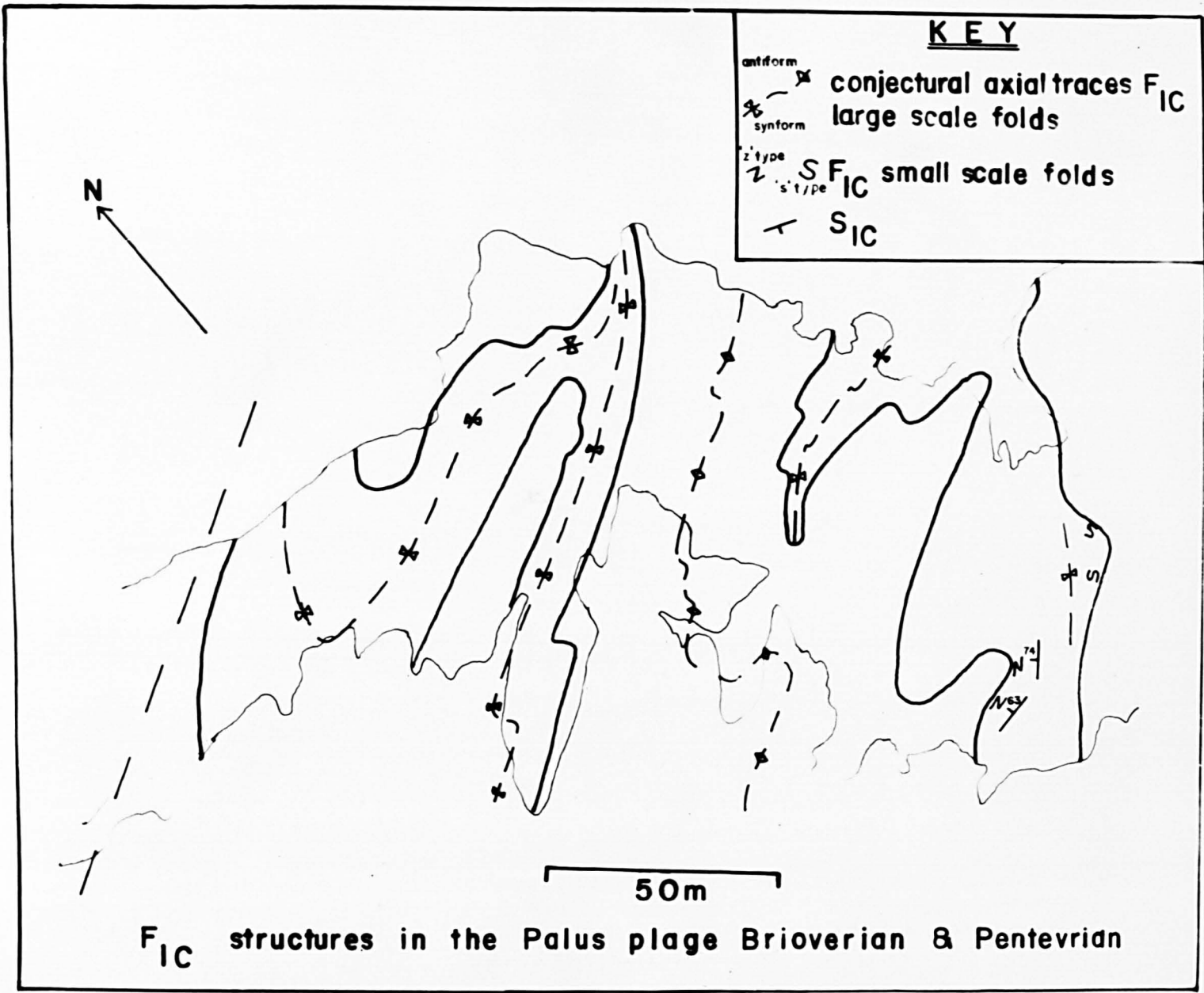


Figure 4.5. Structural sketch map of the centre of the Palus plage section showing the location of the F_{1C} structures. The basement cover contact is represented by a heavy black line.

This area has been divided into nine sub-areas (three within the Brioverian and six within the Pentevrian) for the purposes of structural analysis (Figure 4.4).

(b) First phase of folding F_{1C} .

Deformation during this event has led to the development of tight folds in both basement (sub-areas P1-5) and cover (sub-areas B2 and 3) and tight assymmetric small scale folds in sub area B3 (Figures 4.4 and 4.5). The large scale folds are now isoclinal in form with steeply dipping axial surfaces and inverted north-western limbs (Figure 4.6). Small scale F_{1C} folds are developed in sub-area B3 which is occupied by a sequence of interbedded pelites and semi-pelites (page 3.18 Figure 3.16). These are assymmetric, tight to isoclinal folds which have an axial planar foliation developed in their hinge regions (Figure 4.5, Plate 4.8). The axes of these folds plunge at a moderate to steep angle to the west. The change in symmetry of these folds across sub-area B3 from 'z' type in the west to 's' type in the east indicates that this area is occupied by an F_{1C} synform that closes to the northeast (Figure 4.5). The sedimentological evidence suggests however that the majority of the sediments in sub-area B3 young to the west (page 3.19) and are inverted. This is probably due to the fact that the greater part of eastern limb of the F_{1C} syncline that occupies this sub-area is faulted out along the contact B3/P5 (Figure 4.4). This contact is folded by F_{2C} folds and must therefore have been developed prior to this event and was most probably associated with F_{1C} . These F_{2C} folds are gentle, haveing a small amplitude/wavelength ratio (Figure 4.7), and the trend of this contact, i.e. northeast-southwest may give some indication of its attitude prior to F_{2C} .

The F_{2C} fold axes in sub-area B2 plunge towards the northeast whereas those in sub-area B3 plunge towards the west (Figure 4.6, 4.7 and 4.8B). This discrepancy can only be explained if the axial surfaces of the F_{1C} folds in sub-areas B2 and B3 (Figure 4.5) were not parallel. It is



Plate 4.9. F_{2C} folds in the unconformity at Palus plage, sub area B3. The unconformity is marked by a dashed line. The Pentevrian occupies the foreground and the background and the Brioverian is in the middleground.



Plate 4.10. F_{2C} folds in the unconformity at Palus plage. The Brioverian pelites are in the foreground. Field of view is approximately 2.5 m.

probable that the axial surface of the F_{1C} fold in sub-area B2 dipped to the east or the northeast and that of the F_{1C} fold in sub-area B3 dipped to the west. The scatter of the lineation L_{2C} (Figure 4.8B) may be due to the fact that the F_{1C} folds were not isoclinal prior to F_{2C} . This would mean that the L_{2C} lineations would have different attitudes on different limbs of the F_{1C} folds and that this difference would be maintained even after the limbs were rotated into parallelism. This rotation may have taken place during the later stages of F_{2C} or during D_{3C} .

It is not apparent why there should be such a divergence between the attitudes of the F_{1C} folds. However if these folds were formed as a result of buckling of the contact between a relatively rigid basement and a relatively ductile cover, the resultant folds could be similar to those forms in the external massifs of the French Alps which have variable axial surfaces (Ramsay 1963).

(c) Second phase of folding F_{2C} .

Folds of this generation are developed extensively throughout the area (Plates 4.9 and 4.10). The large scale folds have an amplitude that varies from 30 - 100m and a wavelength from 20 - 70m. The axial surfaces of these folds strike 75° - 255° east of north and dip at 77° to the north-northwest. These folds refold that F_{1C} folds. As in other areas of Brioverian affected by this event the folding has taken place during a phase of regional metamorphism and a foliation S_{2C} is developed parallel to the axial surfaces of these folds. This foliation is only poorly developed in the pelites and the crystal tuffs but is strongly developed within the intermediate tuffs and the agglomerates; the volcanic fragments in the latter are flattened and deformed within the plane of S_{2C} (Plate 3.30 and Figure 4.8A and D).

A lineation L_{2C} is developed in the pelites (Plate 4.11) as a result

Structural Map of the Palus Plage Volcanics

key

- S_B-S_{2C} Lincation
- L_{2C}
- S_{2C}
- S_B

N

0 100m.

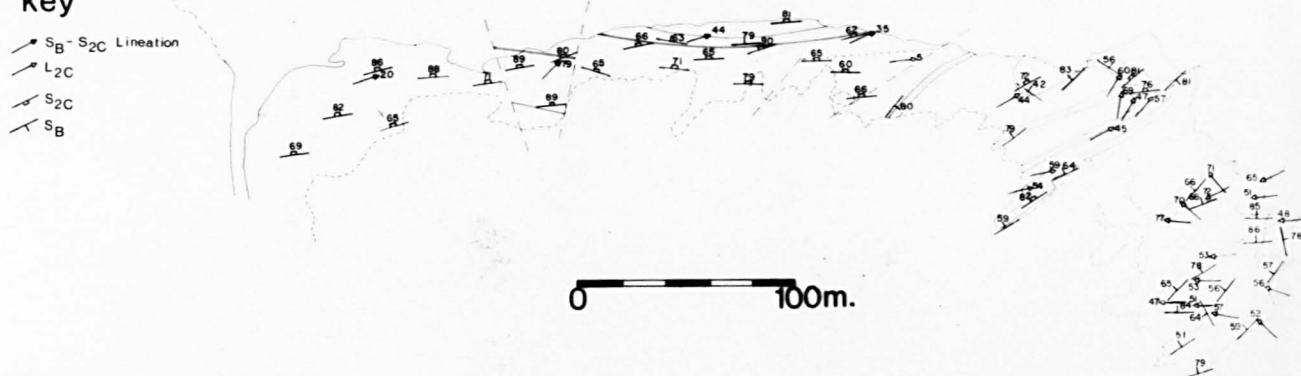
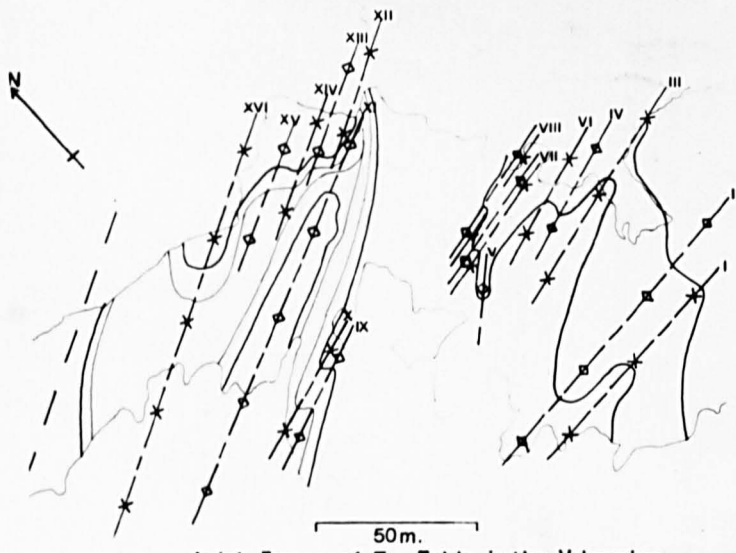


Figure 4.6. Structural map of the Palus plage
Brioverian.



Axial Traces of F_{2C} Folds in the Volcanics.

Poles to the Axial Surfaces (dots) and Axes (crosses) of the above F_{2C} Folds.

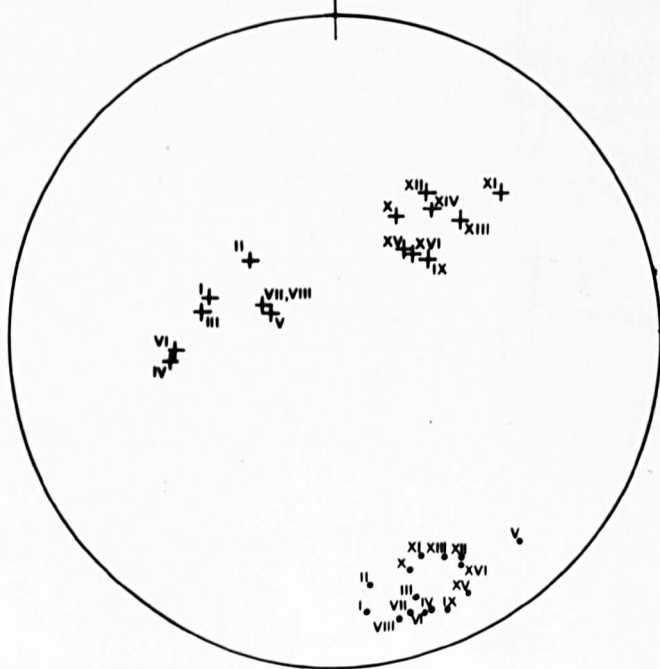
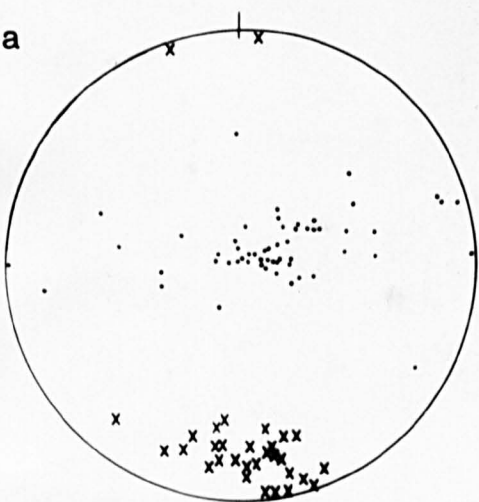


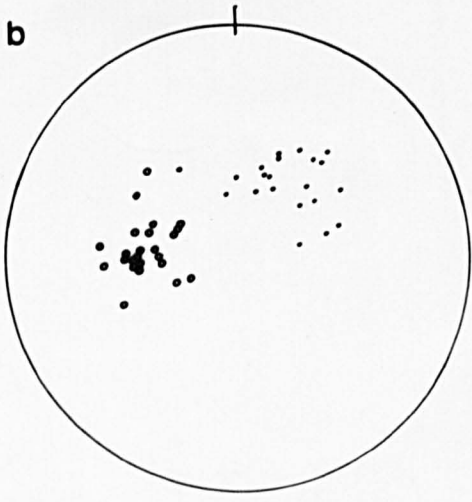
Figure 4.7. Map of the same area as shown in Figure
4.4. showing the location and orientation
of the F_{2C} structures.

a



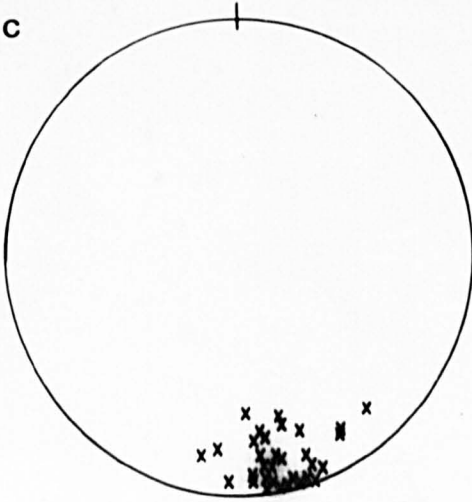
Orientation of the Long Axes of the Pebbles (dots) and the Foliation (crosses) in the Agglomerates.

b



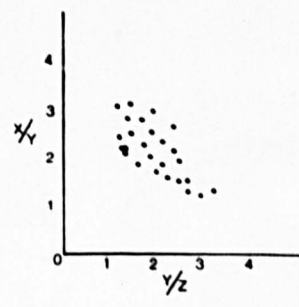
L₂C in the Volcanics, dots=L₂C in West, circles=L₂C in East.

c



S₂C in the Volcanics.

d



Axial Ratios of the Deformed Pebbles of the Agglomerates.

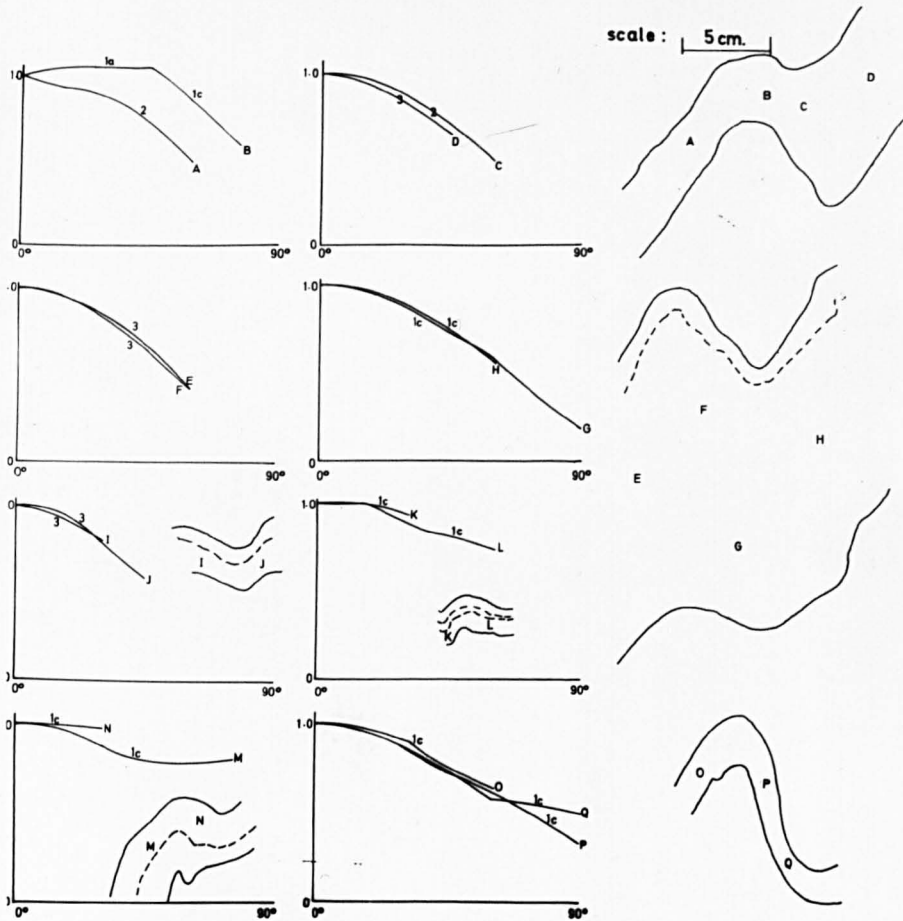
Figure 4.8. Stereographic projections of structures found within the Palus plage Brioverian.

of the formation of microfolds within the more finely bedded bands. This lineation is always parallel to the axes of the F_{2C} folds around which is developed (Figures 4.6, 4.7 and 4.8B). As mentioned above, this lineation which lies within the axial surfaces of the F_{2C} folds is variable in orientation (Figures 4.8B and C), a fact which is explained by the superposition of these folds upon structures developed during the F_{1C} fold phase.

Small scale folds of this generation are found in the pelites in sub-area B3. These are of variable wavelength and amplitude, but their wavelength does not appear to exceed 15cm and their amplitude 8cm. The closures of these folds vary greatly in style and may be from tight to open (Figure 4.9). Their axial planes are parallel or sub-parallel to those of the major folds and their axes are parallel to that of the major fold around which they developed. A study of the variation of the orthogonal thickness of a fold limb (t_a) with the angle it makes with the axial surfaces of the fold (a) has been carried out for several of these structures (Figure 4.9). The resultant diagrams show that many of these folds are asymmetric, with the curve for one limb not being co-incident with that of the other. Whilst these folds may be classified as Type 1c (Ramsay 1967) or Type 3, many of them are in close approximation to the ideal similar folds, Type 2.

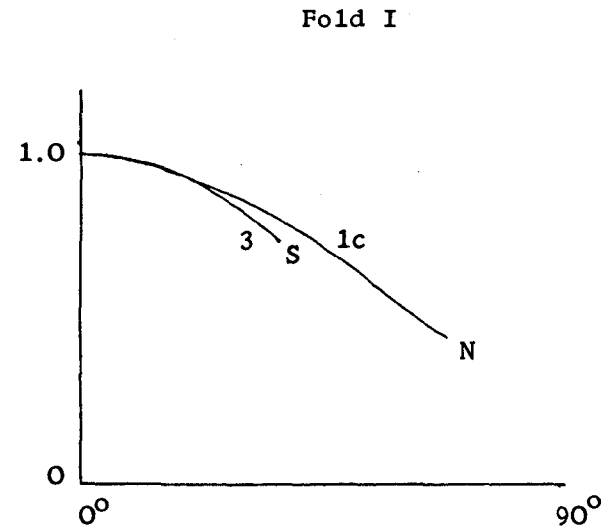
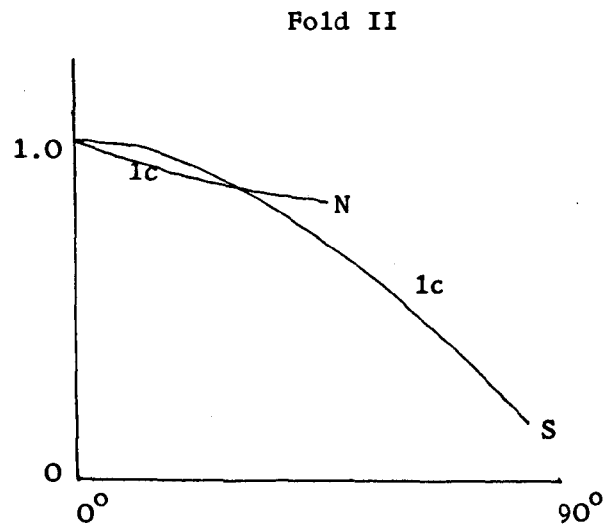
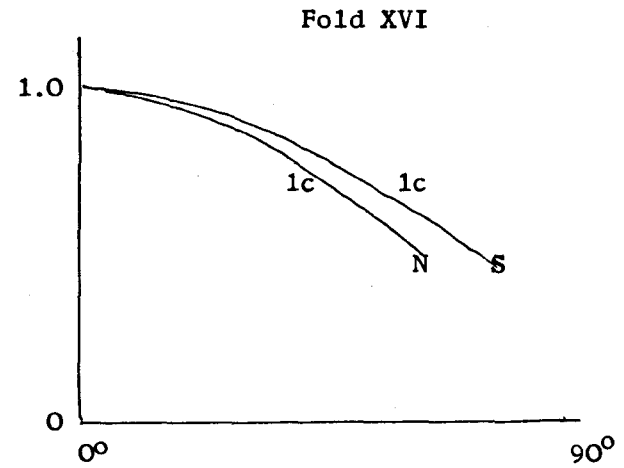
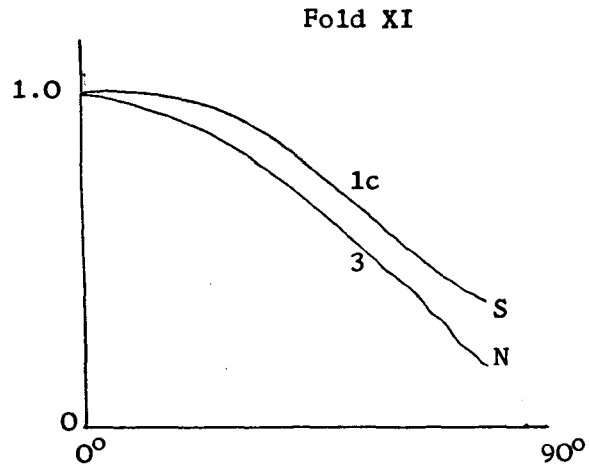
A similar study has been carried out for the F_{2C} major folds (Figures 4.7 and 4.10) which belong to the same classes as the small scale folds. It is interesting to note that these large scale folds are also asymmetric, with the slope of the curves (dt_a/da) being greater for the northern limb than the southern limb.

Folds of this generation are correlated with those developed elsewhere in the Brioverian during F_{2C} on the grounds that these structures are associated with the second phase of Cadomian deformation. Their axial



Plots of d (abscissa) against t_c (ordinate) for small scale F_{2C} folds in Pelites [class of fold written on curve, after Ramsay 1969].

Figure 4.9. Classification of small scale F_{2C} folds
in the pelites (after Ramsay 1967).
Sketches of the folds studied are also shown.
The letters on the individual curves correspond
to those on the fold limbs.



Plots of a' (abscissa) against ta' (ordinate) for large scale F_{2C} folds affecting the unconformity (class of fold written on curve, after Ramsay 1967).

Figure 4.10. Classification of large scale F_{2C} folds affecting the Brioverian Pentevrian contact. The numbers of the folds correspond to those on Figure 4.7.

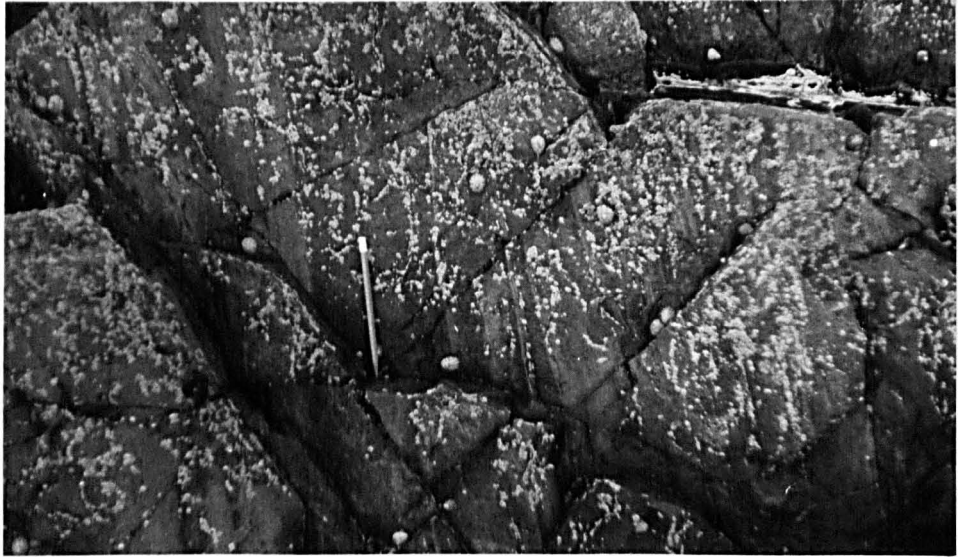


Plate 4.11. L_{2C} lineation (parallel to the pencil) in the pelites at Palus plage.

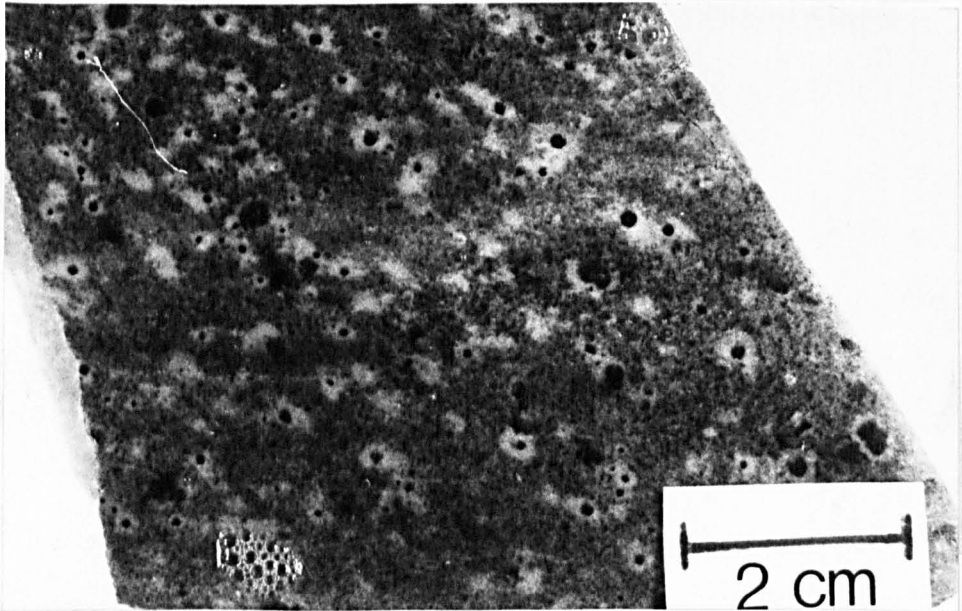


Plate 4.12. Quartz infilled pressure shadows formed during D_{3C} around M_{3C} garnet and magnetite.

surfaces are parallel to those of the F_{2C} folds found elsewhere, while both here and in other areas this folding was associated with a syntectonic metamorphic event (M_{2C} see page 4.17) which led to the development of a penetrative foliation S_{2C} parallel to the axial surface of these folds.

(d) Third phase of deformation D_{3C} .

This event is not truly a phase of folding as no folds associated with it are developed within this area. However, the fabric associated with this event is similar to that of the F_{3C} event within the Brioverian elsewhere, and hence the flattening produced within the Palus Plage Brioverian is believed to be a result of the same stress system as the F_{3C} phase of folding elsewhere in the Brioverian.

During this event both the pre-existing F_{1C} and F_{2C} structures were flattened. Evidence for this flattening is found in the retrogression and considerable deformation of the hornblende and garnet (Plate 4.12) crystals that grew in the closures of the F_{2C} folds during the post- F_{2C} static phase of metamorphism (see M_{3C} , see page 4.21). Further evidence for this flattening is found in the tuffs, where the S_{2C} foliation is seen to be bent around the margins of recrystallised areas that are now made up of an aggregate of large poikiloblastic grains of hornblende and plagioclase that grew after the development of the S_{2C} foliation.

The agglomerates show a great deal of flattening with the long axes of the deformed pebbles within a moderately well-defined plane that is parallel to the S_{2C} foliation within the matrix of the agglomerates. It can be seen that much of the flattening of these agglomerates occurred during this later event as all the pebbles show marked pressure shadows that are filled with epidote and chlorite, minerals developed during the retrogressive phase of metamorphism that accompanied this deformation. A study of the relative lengths of the axes of the

Deformation	Fold phase	Style	Foliation	Lineation	Metamorphism	Mineral assemblages
D _{1C}	F _{1C}	isoclinal folds with NE - SW trending axial surfaces associated with the development of shears in the Palus plage region	?
D _{2C}	F _{2C}	isoclinal folds with 80°-260° striking axial surfaces which are only developed near the contact with the Palus plage Brioverian	S _{2C}	...	M _{2C}	andesine + quartz + biotite + muscovite
...	M _{3C}	andesine + quartz + biotite + garnet (in the Port Goret gneisses at Palus plage); epidote + actinolite + calcite (in the south of the Plouha Series)
D _{3C}	...	shear zones developed throughout the region	S _{3C}	M _{4C} ? ↓ ? ↑ ? M _{5C} 		quartz + albite + chlorite + sericite + epidote + haematite + calcite + sphene + apatite (in shear zones)
D _{5,6,7C}	K _A ,K _B ,K _C	kink bands and conjugate shears	...			muscovite

Table 4.3. Cadomian structural and metamorphic history of the Pentevrian basement.

deformed pebbles show that they correspond to an ellipse of the form $X:Y:Z = 5:2:1$ with Z perpendicular to the S_{2C} foliation (Figure 4.8A). This information may not be used to calculate the form of the strain ellipsoid for D_{3C} as it is necessary either to know the nature of the strain ellipsoid prior to the onset of this phase of deformation (i.e. it would be necessary to be able to estimate the form of the strain ellipsoid after both F_{1C} and F_{2C} , which is not possible), or to be able to assume that these agglomerates had a randomly oriented fabric before they underwent D_{3C} deformation. It is clearly impossible to make the later assumption, as the agglomerates had undergone two phases of deformation prior to this event.

3. Cadomian structures within the Pentevrian basement.

(a) Introduction

Cadomian structures within the Pentevrian basement are not common or easy to recognise except in the region around Palus plage where a definite time plane within the basement, i.e. the surface of unconformity, has been deformed. Here the basement is affected by three Cadomian fold phases as is the Brioverian cover. These are reviewed in Table 4.3.

(b) First phase of folding F_{1C} .

It is obvious from the form of the unconformity (Figure 3.16) that the Pentevrian basement in the Palus plage area (the Port Goret gneisses) was deformed during the Cadomian orogeny. The lack of small scale F_{1C} structures and associated metamorphic textures make it difficult to evaluate the effect of this event upon the basement. Earlier Pentevrian fabrics which may have been used in evaluating the form of the F_{1C} folds have been transposed to some degree by structures associated with the F_{2C} event and F_{1C} folds are only recognised in that they deform the plane of unconformity (Chapter 4, Section 2.b).

(c) Second phase of folding F_{2C} .

These folds are only found in the basement near to the unconformity

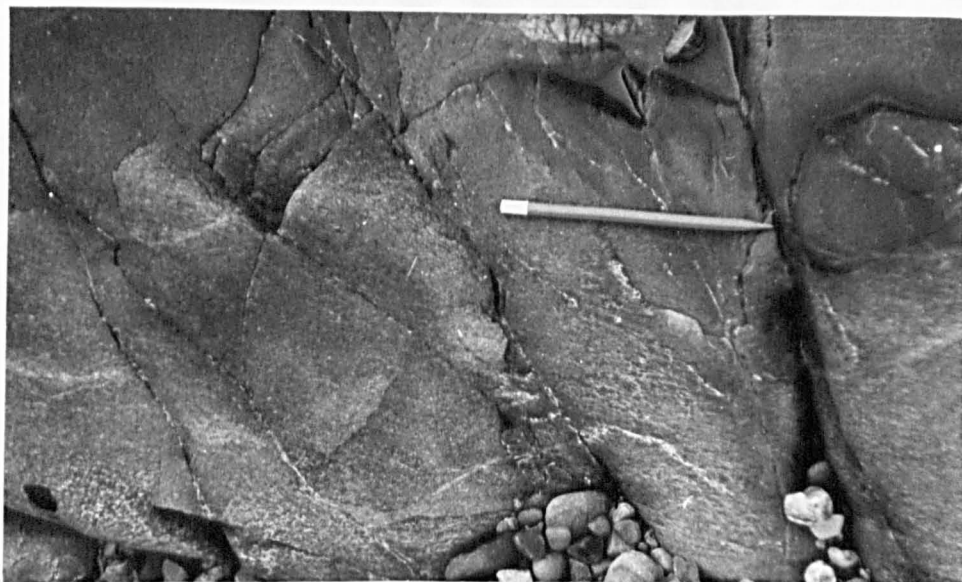


Plate 4.13 S_{2C} (parallel to the pencil) developed in the retrogressed Port Goret gneisses in sub area P3, Palus plage.

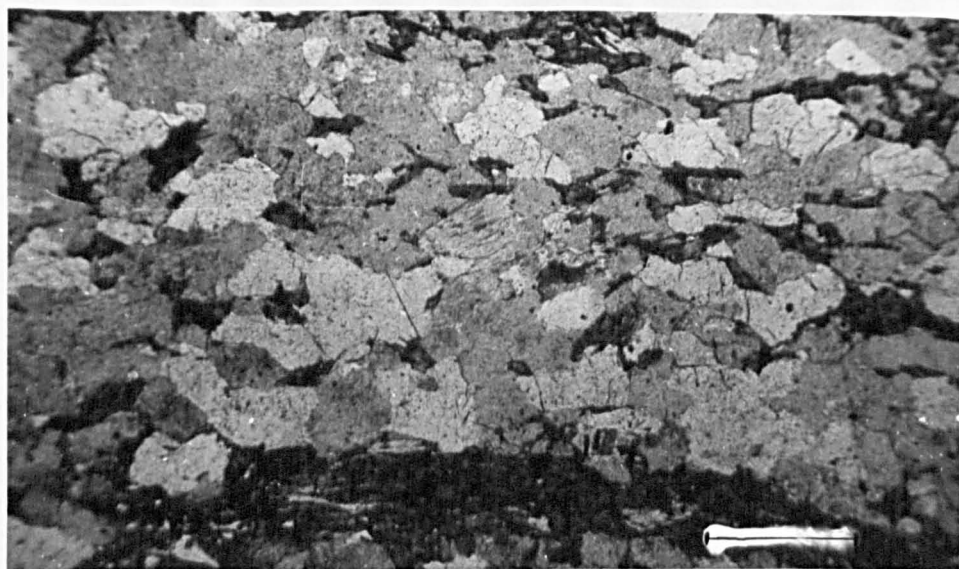


Plate 4.14. Photomicrograph (pp1) of M_{4C} chlorite schist showing the S_{3C} foliation (left to right) developed in the retrogressed Port Goret gneisses, south of Port Goret, sub area P6. Scale 0.69mm.

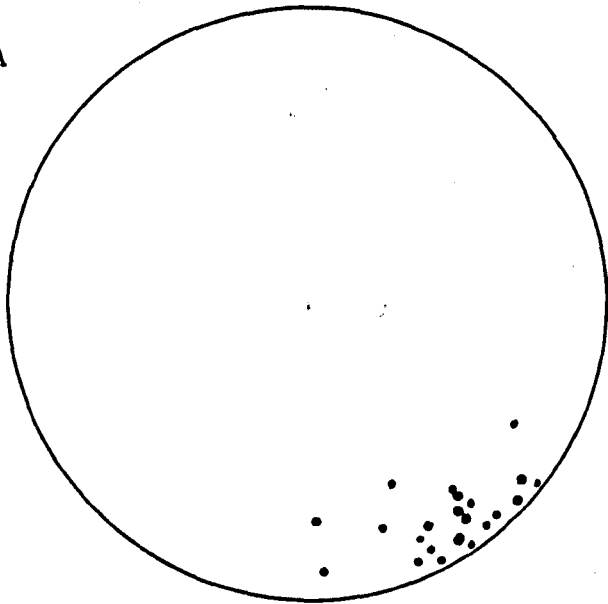
(Plates 4.9 and 4.10). The tightness of these folds and the degree of recrystallisation of the basement during the syn- F_{2C} metamorphic event M_{2C} (see page 4.17) increase in going west from sub-area P5 to sub-area P1. No F_{2C} structures are found in sub-area P6. The basement in sub-areas P1-3 have all their original Pentevrian fabrics transposed by the S_{2C} foliation (Plate 4.13). In sub-areas P4 and 5, although the S_{2C} foliation is developed, the earlier Pentevrian fabrics are still preserved. The S_{2C} foliation dies out in the basement 30m to the east of contact B3/P5.

The F_{2C} folds that are formed in the gneisses to the east of contact B3/P5 have the form of gentle flexures within the gneissic banding. These are only developed where the gneisses have undergone recrystallisation during M_{2C} and they also die out 30m to the east of the B3/P5 contact. In sub-areas P1-4 the F_{2C} folds are isoclinal complex folds that can be identified on account of the outcrop pattern of the unconformity (Figure 4.7). Only one example of small scale F_{2C} folds has been recorded in sub-area P3. The limbs and the axes of these folds are parallel to those found in the cover (page 4.11).

(d) Third phase of deformation D_{3C} .

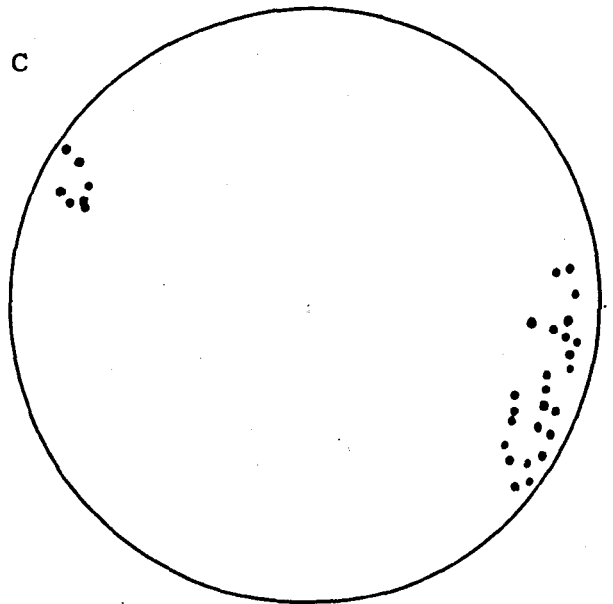
Chloritised shear zones were developed in sub-areas P5 and 6 during this phase. These shear zones are correlated with the D_{3C} structures in the Brioverian as they cut pegmatitic veins of post F_{2C} age that are found in both basement and cover. A major D_{3C} shear zone is developed at the eastern margin of sub-area P6. In this zone, which is 30m wide, many of the pre-existing Pentevrian structures have been transposed and the gneisses recrystallised to a fine grained chlorite schist. The foliation in these schists S_{3C} is parallel or sub-parallel to S_{2C} . The fine grained nature of the recrystallised gneisses is probably due to their being sheared at an early stage during F_{3C} . This cataclasis was followed by an associated metamorphic event (M_{4C} , see page 4.15) that recrystallised the sheared gneisses.

A



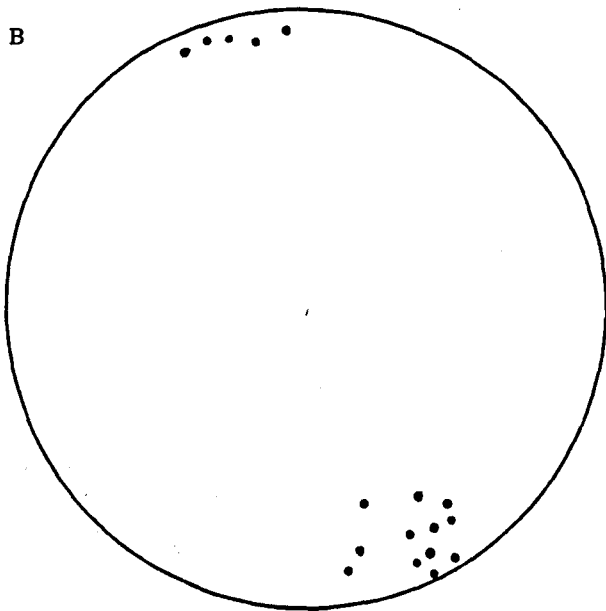
S_{3C} in the west

C



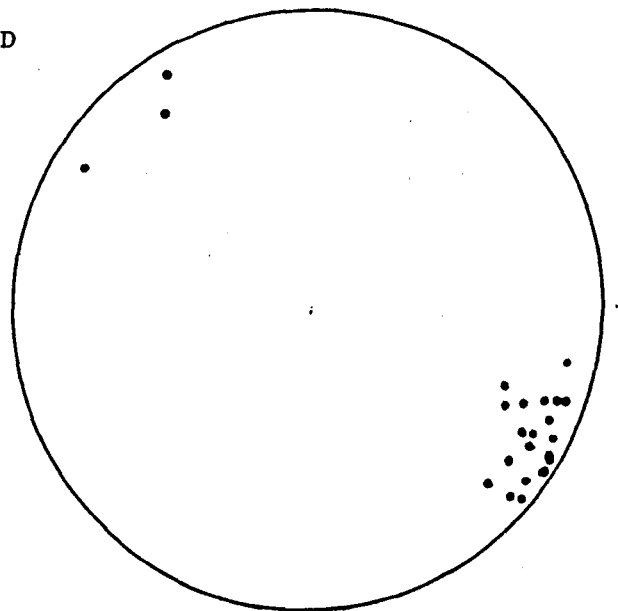
Spg₅ in the east

B



Spg₅ in the west

D



S_{3C} in the east

Figure 4.11. Stereographic projections of D_{3C} shear zones; A) in sub-area P5 and D) in sub-area P6: and of the Spg_5 foliation; B) in sub-area P5 and C) in sub-area P6. S_{3C} and Spg_5 are parallel in the same sub-area.

Deformation	Fold phase	Fold style			Foliation	Lineation	Metamorphism	Metamorphic facies		
		B-B Series	P.p.Brio.	Pent.				B-B Series	P.p.Brio.	Pent.
D _{1C}	F _{1C}	overturned isoclinal	overturned isoclinal+ shearing	overturned isoclinal+ shearing	S _{1C}	...	M _{1C}	middle greenschist	?
D _{2C}	F _{2C}	isoclinal	isoclinal	isoclinal, die out rapidly	S _{2C}	L _{2C}	M _{2C}	middle greenschist	amphibolite (local in Pentevrian)	
...	M _{3C}	middle greenschist	amphibolite (local in Pentevrian)	
D _{3C}	F _{3C}	tight	shears + flattening	shearing	S _{3C}	L _{3C}	M _{4C}	middle greenschist	lower greenschist	
D _{4C}	...	crenulation	L _{4C}
D _{5,6,7C}	K _A ,K _B ,K _C	kinks	kinks + shearing	local low green-schist?
...	shearing?	M _{5C}	metasomatic?		

Table 4.4. Structural and metamorphic history for the Cadomian orogeny in the area studied.

N.B. B-B Series = Binic-Bréhec Series, P.p.Brio. = Palus plage Brioverian and Pent. = Pentevrian.

Elsewhere in sub-areas P5 and 6 narrower chloritised shear zones are developed that are from 10 - 40cm (Plate 4.14) thick but are of indefinite extent. These zones are always parallel to the earlier Pentevrian S_{5P} foliation within the gneisses although this foliation has different attitudes in sub-areas P5 and P6 respectively (Figure 4.11). This is thought to be due to the fact that the orientation of the D_{3C} strain ellipsoid within the Pentevrian gneisses was controlled not only by the orientation of the principal D_{3C} stress axes, which appear to have been parallel to those of F_{2C} (as the foliation produced during this event in the major shear zone to the south of the outcrop of the gneisses is parallel to S_{2C}), but also by the pre-existing fabric within the gneisses. The existence of the S_{5P} penetrative foliation within these gneisses could have meant that it was energetically more favourable to form shear zones that were parallel to this fabric, which is never at a high angle to S_{3C} , rather than to form shears that were discordant to this fabric. A similar occurrence, where the orientation of later structures are thought to have been influenced by a pre-existing fabric, is described by Tobisch (1969).

(e) Conclusions

It may be concluded that in this region both basement and cover have been affected by the Cadomian orogeny. Deformation during this orogeny has led to the development of an early, possibly north-south fold phase F_{1C} , with a locally developed axial planar foliation S_{1C} . This was followed by a second east-west fold phase with an associated axial planar foliation S_{2C} . A third phase of deformation D_{3C} gave rise to folding, flattening and associated shearing with the local development of an associated foliation S_{3C} . These events were followed by the development of a crenulation lineation L_{4C} in the Series de Binic and then several subsequent conjugate sets of kink bands were formed. The structural history of the Brioverian in the area studied is reviewed in Table 4.4

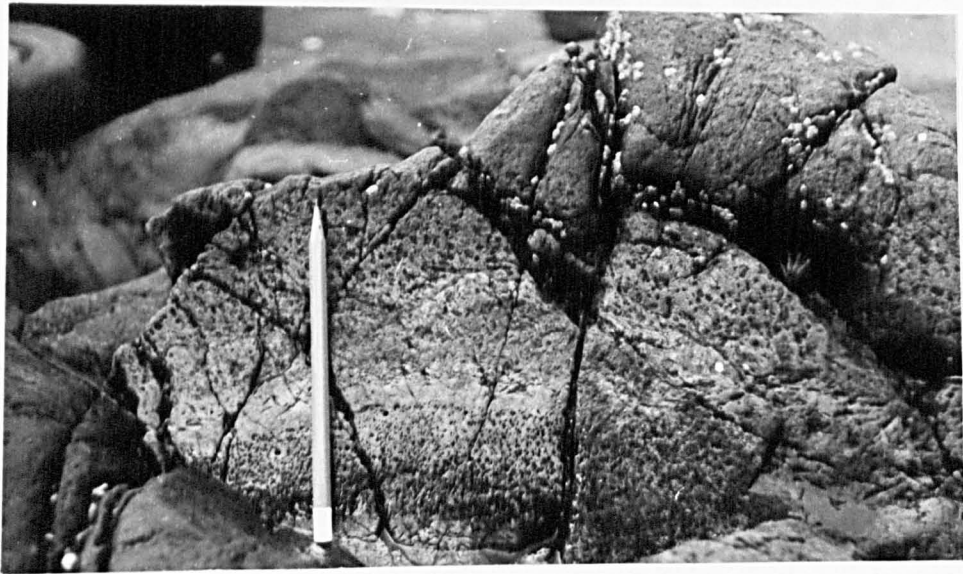


Plate 4.15. M_{1C} actinolites in the pelites (near the base of the pencil) that have been transposed by S_{2C} ; and M_{3C} garnets and anthophyllites (near the pencil point).

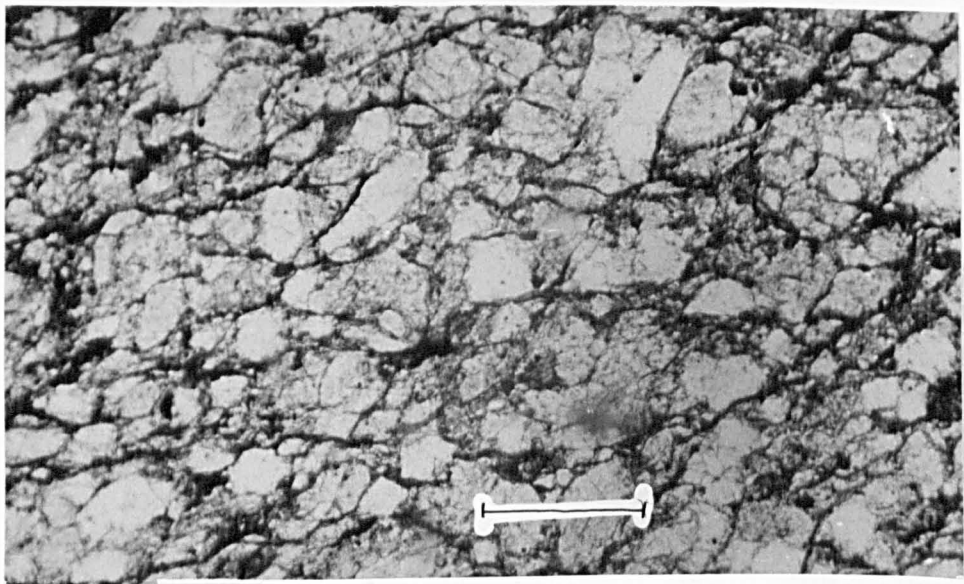


Plate 4.16. Photomicrograph (pp1) of a metasandstone in the Binic-Bréhec Series that shows flattening of the original clastic grains and the development of biotite in the matrix to define the S_{2C} foliation. Scale 0.32mm.

C. Cadomian Metamorphic Events

1. Introduction

Five separate metamorphic events have operated within the region during the Cadomian orogeny (Table 4.4). These are:

1. Syntectonic prograde metamorphism, M_{1C} ;
2. Syntectonic prograde metamorphism, M_{2C} ;
3. Static prograde metamorphism, M_{3C} ;
4. Syntectonic retrograde metamorphism, M_{4C} ;
5. Potassium metasomatism? M_{5C} .

These events are not developed equally throughout the region.

In some localities one or more of these events may be absent, while in other the metamorphic assemblage associated with an individual event may represent a different grade of metamorphism to that found elsewhere.

2. Syntectonic prograde metamorphism, M_{1C} .

Textures associated with this event are only found in the pelites of the Palus plage Brioverian in sub-area B3 (Figure 3.16 and 4.4). Here, in the hinge regions of the F_{1C} folds a biotite foliation is developed. In some tuffaceous bands at the top of the pelites in the east of sub-area B2 (Figure 4.4) subidioblastic actinolites (Plate 4.15) have been developed. These actinolites have been recrystallised and transposed by the S_{2C} foliation (Plate 4.15) which was developed during the second phase of Cadomian metamorphism (see below) and were thus probably developed during M_{1C} . The extant mineral assemblages suggest that metamorphism during this event was within the middle greenschist facies.

3. Syntectonic prograde metamorphism, M_{2C} .

(a) Introduction

This event was developed during the F_{2C} phase of folding and has produced a marked planar fabric throughout the Brioverian in the region studied that is everywhere parallel to the axial surfaces of these F_{2C} folds. The mineral assemblages within the Binic-Bréhec series indicate that this

metamorphism only reached the biotite zone of the greenschist facies whereas the assemblages developed within the Palus plage Brioverian and the recrystallised Pentevrian of the Palus plage section are typical of the amphibolite facies.

(b) M_{2C} in the Binic-Bréhec Series.

The metamorphic assemblages developed during this event in both the pelitic and the psammitic portions of this sequence are identical, the typical assemblage being quartz+albite+biotite with accessory white mica, haematite, sphene and epidote.

The rocks appear to be only partly recrystallised and the clastic texture of the coarser grained sediments is still evident. The clastic fragments retain their original form (Plate 4.16) although they are often embayed around the margins. Quartz grains often have sutured margins, show strained extinction, become partially recrystallised at the margins to a granular sutured aggregate of greatly reduced grain size, and have overgrowths of quartz in such a way as to form an elongate granular aggregate whose long axis within the plane of the foliation. Clastic grains of plagioclase are often embayed by quartz at the margins. They are albitic in composition and often show very finely developed polysynthetic twinning. The matrix is recrystallised to a microcrystalline mesh of quartz+albite and very small irregular biotite laths. The biotite laths are oriented to form the S_{2C} foliation and appear to be particularly concentrated along micro-shears that run through the matrix.

There is a marked change in the textures of these metasediments in the area between Moulin plage to the south of the outcrop of Port Goret gneisses and the cliffs on the north side of Goudelin plage. Here, the form of the original clastic grains has not been lost, as they are still considerably larger than the grains of the matrix. The clastic grains are flattened and are granoblastic in form with much more regular, less sutured margins. The

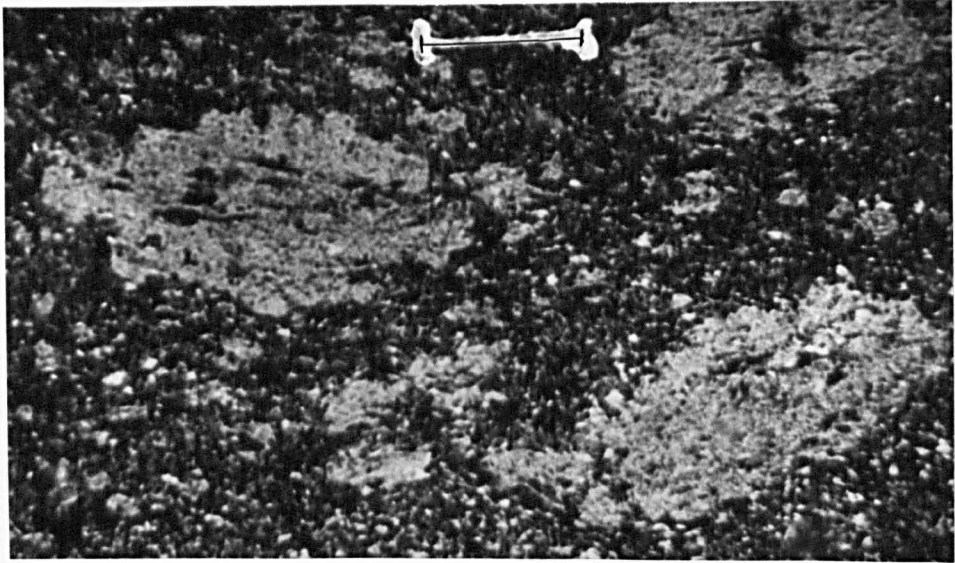


Plate 4.17. Photomicrograph (pp1) of retrogressed cordierite porphyroblasts in the metamorphic aureole of the Saint Quay intrusion. They are flattened and are replaced by biotites that define the S_{2C} foliation. Moulin plage. Scale 0.69mm.

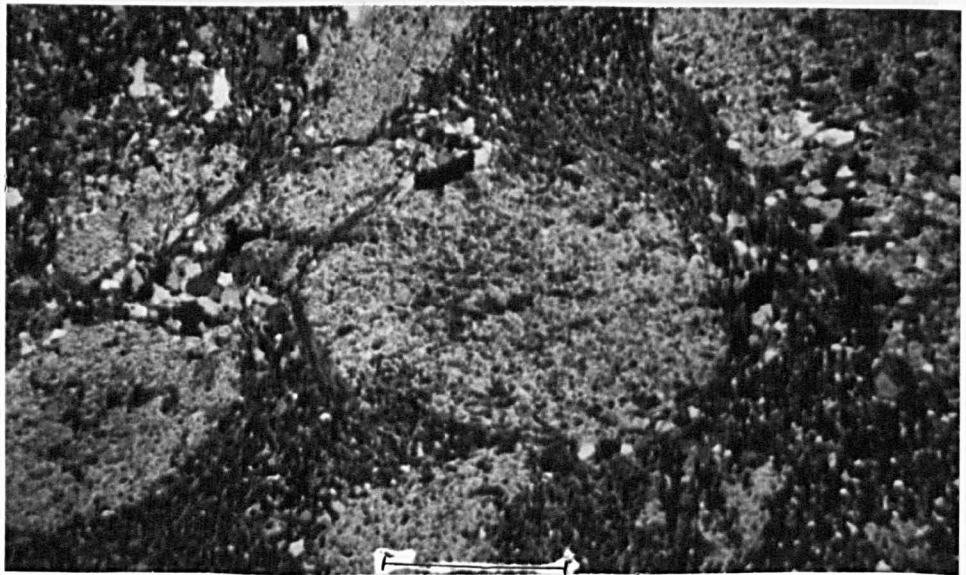


Plate 4.18. Photomicrograph of retrogressed cordierites (cn) in the metamorphic aureole of the Saint Quay intrusion, Moulin plage. The S_{2C} foliation, defined by biotite, is deflected by these porphyroblasts. Scale 0.68mm.

grains of albite and quartz within the matrix are granoblastic polygonal in form and other show rational boundaries with one another. The biotite laths are elongate, larger and much more regular in form and the S_{2C} foliation is strongly developed.

The mineralogical assemblages developed during M_{2C} indicate that this event attained the same grade of metamorphism throughout the Binic-Brehec Series. However, the granoblastic polygonal texture, which is only found in the Moulin plage section, suggests that equilibrium was more closely approached during M_{2C} in this section than elsewhere in the Binic-Brehec Series. Two hypotheses may be put forward to explain this effect: firstly there could have been an increased rate of reaction, which was possibly caused by an increase in the fluid phase and/or by the presence of catalysts; secondly M_{2C} was superimposed on sediments that had already been contact metamorphosed by the Saint Quay intrusion. It is believed that the second hypothesis is the most important, since the textures described above coincide exactly with the area in which porphyroblasts of cordierite and/or andalusite were developed during the contact metamorphism of the Brioverian of the Moulin plage section by the Saint Quay intrusion. These poikiloblastic porphyroblasts were retrogressed during M_{2C} and are replaced by white mica + biotite + quartz. Some of these relict porphyroblasts are flattened and their long axes lie within S_{2C} (Plate 4.17), whilst others maintain more of their original form and the S_{2C} foliation is flattened around them (Plate 4.18). Those porphyroblasts that occur in the pelites tend to be more flattened than those which occur in the psammites.

The calcareous siltstones and sandstones that occur in the turbidite facies of the Brioverian show markedly different metamorphic assemblages to those of the surrounding pelites and psammites, however, the grade of

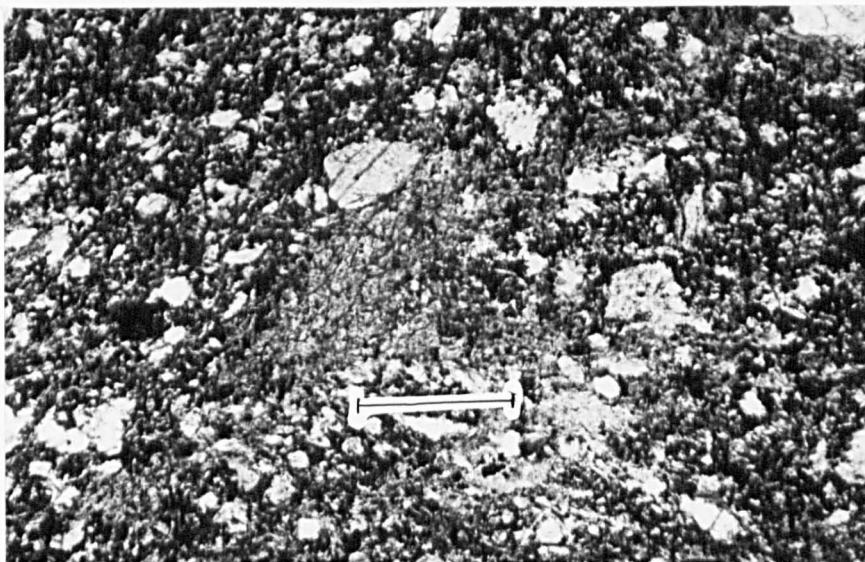


Plate 4.19. Photomicrograph (pp1) of the calc-siltstones in the Binic - Bréhec Series at Pointe de la Rognouse which were metamorphosed during M_{2C} to a quartz + zoisite assemblage. Scale $0.32mm$.

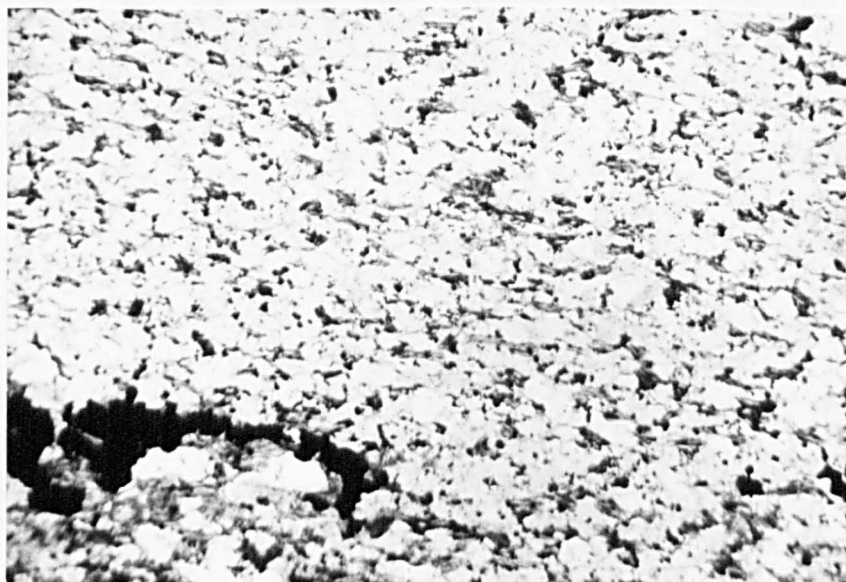


Plate 4.20. Photomicrograph (pp1) of the pelites at Palus plage showing the development of M_{2C} biotites to define the S_{2C} foliation. $20\times$ normal size.

metamorphism and the associated textures are similar to those in the rest of this sequence. An assemblage of quartz, clinozoisite, calcite and muscovite with accessory sphene, haematite and garnet is found in the calc-siltstones at Pointe de la Troupelet (Plate 4.19). Here, the clastic grains are only partially recrystallised, quartz shows strained extinction, sutured margins and very slight replacement by calcite at the margins. There are no overgrowths of metamorphic quartz upon these grains, plagioclase also shows sutured margins, partial replacement by muscovite and/or calcite, and in some cases the grains of plagioclase are completely pseudomorphed by a microcrystalline aggregate of clinozoisite. The matrix consists of a very fine aggregate of quartz, calcite, clinozoisite and muscovite, with all grains showing irregular sutured boundaries with one another. The muscovite grains, although of irregular form, are aligned to define a foliation in those areas of the matrix that are free of many large clastic grains. This foliation is parallel to that of the biotite in the surrounding metasediments.

The calc-siltstone bands and the calcareous nodules that are found in the area between Goudelin plage and Moulin plage, like the surrounding sediments, show a similar mineralogical assemblage but markedly different textures from those of similar rock types that are found elsewhere in the area. Here, there are no longer any recognisable clastic grains and the matrix is made up of interlocking poikiloblastic grains of clinozoisite with varying amounts of polygonal granoblastic quartz. The clinozoisite has inclusions of muscovite, calcite or sphene. Large fibrous aggregates of tremolite that have a random orientation are developed.

(c) M_{2C} in the Palus plage Brioverian

The assemblages developed within the volcanic and sedimentary rocks at Palus plage indicate that the amphibolite facies grade of metamorphism was attained during this event, which is a higher grade than is found elsewhere in the region for this event. The mineralogical assemblages

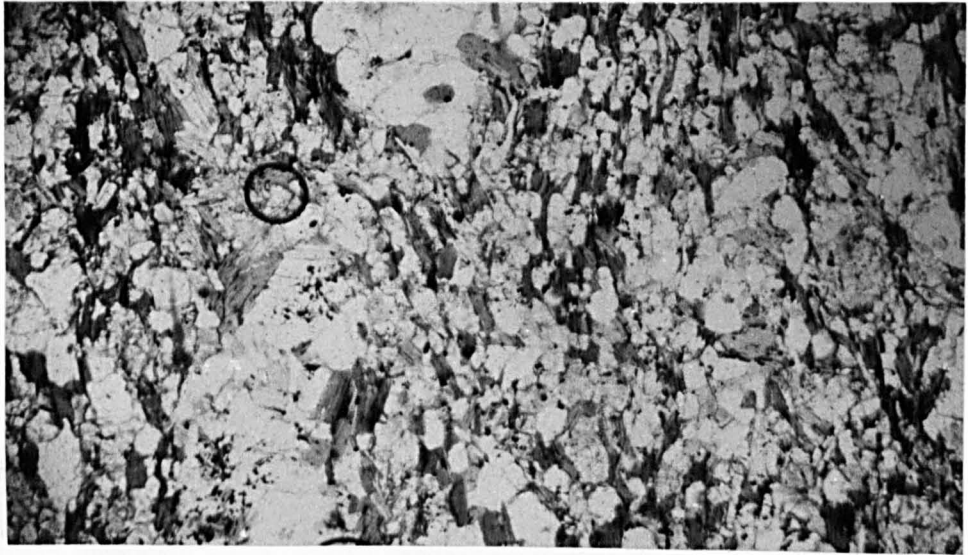


Plate 4.21. Photomicrograph (pp1) of M_{2C} biotites in the retrogressed Port Goret gneisses at Palus plage. 20x normal size.



Plate 4.22. Static M_{3C} hornblendes developed in the intermediate tuffs at Palus plage. Scale in inches.

developed are quartz + andesine + biotite in the metasediments and quartz + andesine + hornblende + biotite in the metavolcanics. The Pelites in sub-area B3 have been recrystallised to a fine grained irregular matrix of quartz + andesine which enclose biotite laths that are aligned to define the S_{2C} foliation. In sub-areas B1 and B2 the S_{2C} foliation is defined by hornblende and/or biotite which are enclosed in a granoblastic polygonal matrix of quartz + andesine. A similar texture is developed in the matrix of the metavolcanics where M_{3C} prophyroblasts are developed. It is possible, therefore, that this granoblastic polygonal texture of the matrix was partly or wholly developed during M_{3C} .

(d) M_{2C} in the Pentevrian basement

The only area of Pentevrian basement to have undergone significant recrystallisation during this event is that comprising the Port Goret gneisses in the Palus plage area. The gneisses in Sub-areas P1-4 and in the eastermost 30m of P5 have been recrystallised. An assemblage of andesine + quartz + biotite + white mica is developed within the recrystallised gneisses (Plate 4.21). The andesine and quartz are irregular in form and they show sutured margins against one another. White mica intergrown with quartz replaces the staurolite porphyroblasts. The biotite is in the form of elongate laths that are orientated to define a marked foliation that is parallel to S_{2C} and transposes all pre-existing Pentevrian structures.

4. Static prograde metamorphism M_{3C}

(a) Introduction

Recrystallisation and the growth of distinctive mineral assemblages during this event, which occurred post- F_{2C} but pre- F_{3C} , has only taken place in the Brioverian and the Pentevrian in the Palus plage area. Although there is evidence that the Brioverian in other parts of this region was subject to a greenschist facies metamorphism at this time, no distinctive

Table 4.5. Mineral assemblages developed in the Palus plage Brioverian during M_{3C}.

ROCK TYPE	MINERAL ASSEMBLAGE							
	Quartz	Andesine	Hornblende	Biotite	Garnet	Cordierite	Anthophyllite	Magnetite
Quartzo-felspathic	X	X		X	X			X
Tuffaceous sandstone	X	X		X	X	X		X
Intermediate tuffs	X	X	X	X	X	X		X
Dark tuffs	X	X		X				X
Agglomerates	X	X	X	X				X
Crystal tuffs	X	X		X	X			
Pelites	X	X		X	X		X	X
Psammites	X	X		X	X			X

textures are developed in these rocks to allow it to be distinguished as a separate phase of metamorphism.

(b) M_{3C} in the Binic-Bréhec Series

Within the Brioverian turbidites the metamorphic foliation S_{2C} that is developed is parallel to the axial surfaces of folds developed during both F_{2C} and F_{3C} . This foliation, which was an active structural element throughout both of these phases of deformation, is everywhere defined by biotite that is associated with quartz and albite. This would make it probable that these two closely associated phases of deformation took place during the same metamorphic event that maintained the rocks of this area at greenschist facies temperatures throughout F_{2C} and F_{3C} . The duration of this metamorphic event in the Binic-Bréhec series would therefore be equivalent to that of M_{2C} , M_{3C} and M_{4C} in other parts of the region studied.

At several localities within the Series de Binic large poikiloblastic plates of biotite are grown within the matrix of the metasediments. These porphyroblasts which are equidimensional, as opposed to the elongate biotites that define the foliation, are often kinked, show decussate texture and occur in both pressure shadows of the clastic grains and in the matrix. It is thought that these biotite plates were grown in the period of metamorphism that affected this area between F_{2C} and F_{3C} and are equivalent to minerals grown during M_{3C} at Palus plage.

(c) M_{3C} in the Palus plage Brioverian

This event was marked by the recrystallisation of earlier metamorphic textures and the growth of poikiloblasts of new minerals. The mineralogical assemblages developed in the various rock types are summarised in Table 4.5 and are a great deal more varied than those formed during M_{2C} but show that M_{3C} also attained the amphibolite facies. Thus, although the temperatures reached during the two metamorphic events M_{2C} and M_{3C} were

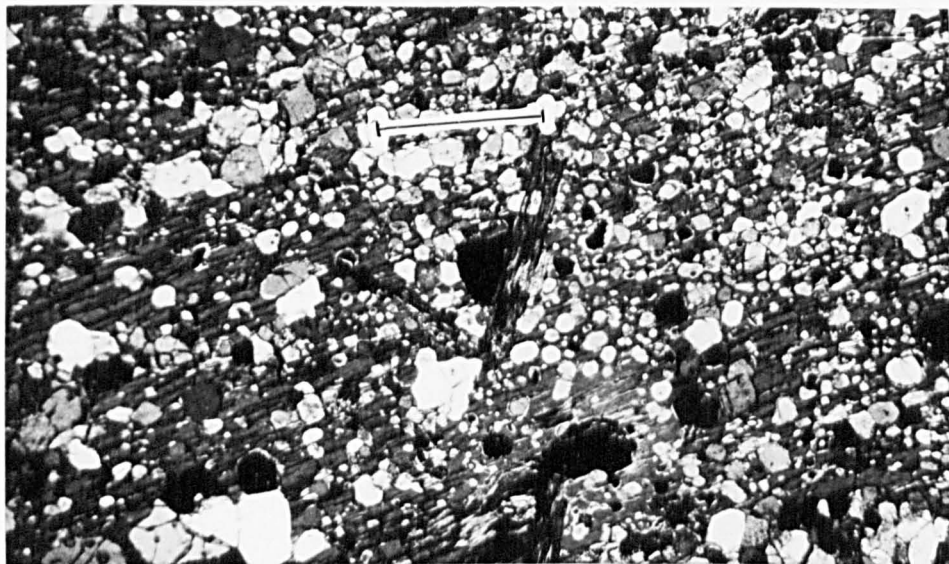


Plate 4.23. Photomicrograph (pp1) taken from the locality shown in Plate 4.22. of an M_{3C} hornblende porphyroblast that is poikilitic to quartz. Scale 0.32mm.



Plate 2.24. Photomicrograph (cn) of an M_{3C} quartz porphyroblast that is poikilitic to quartz. This section was taken from the locality shown in Plate 2.22. Scale 0.32mm.

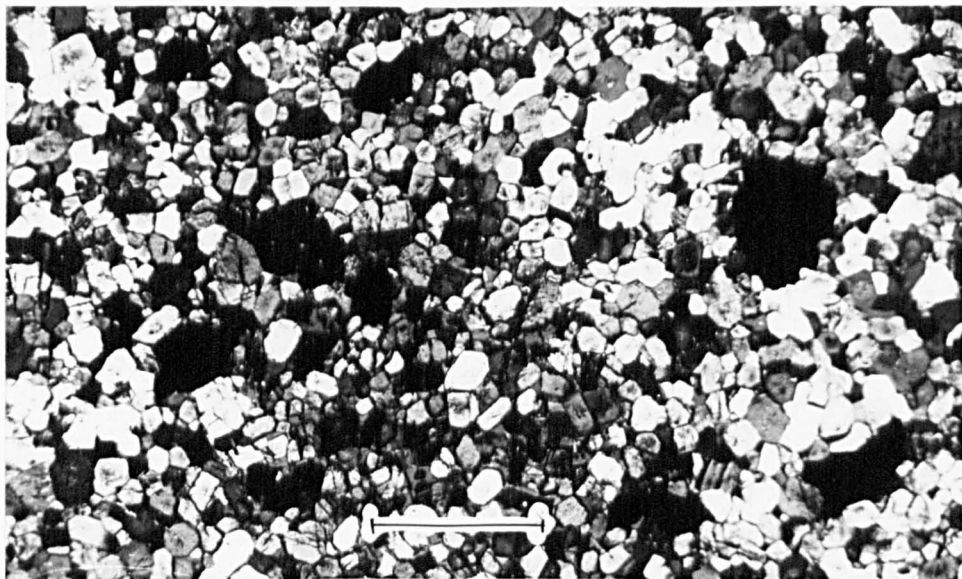


Plate 4.25. Photomicrograph (cn) of the granoblastic polygonal texture developed in the matrix of the agglomerates at Palus plage during M_{3C} . Scale 0.32mm.

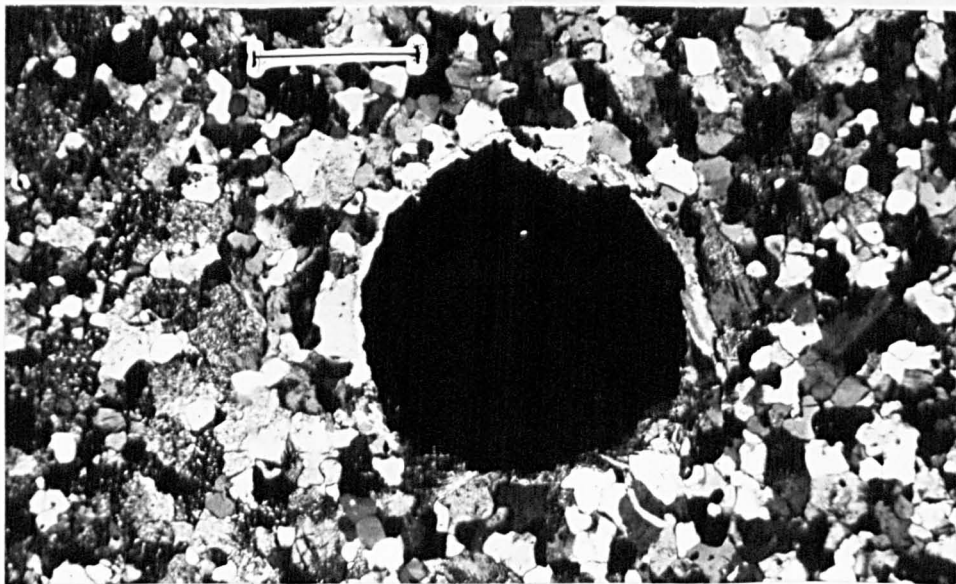


Plate 4.26. Photomicrograph (cn) of a static M_{3C} magnetite grown in the acid dyke that cuts the agglomerates at Palus plage. The grain is rimmed by chlorite and epidote that grew during M_{4C} . Scale 0.69mm.

very similar, there was a marked decrease in deviatoric stresses during M_{3C} .

This event has, in many places, caused the wholesale recrystallisation of the quartz+andesine matrix to an equidimensional granoblastic polygonal aggregate of quartz and andesine (Plate 4.22), in which each of the grains show rational unilateral boundaries with one another. The elongate laths of biotite and hornblende retained their dimensional orientated texture that defines the foliation S_{2C} and do not appear to have undergone recrystallisation. However, new growths of these two minerals, which tend to be poikiloblastic, may either replace mimetically the biotite or hornblende grown during M_{2C} , or develop as large porphyroblasts of irregular orientation.

Within the intermediate tuffs a spectacular texture has developed during this event. There are irregular patches, up to 30cm across, in which the rock is of a much coarser grain size than elsewhere. Here, set in a fine-grained matrix of granoblastic polygonal quartz and andesine lie idioblastic poikilitic porphyroblasts of hornblende (Plates 4.23 and 4.24) up to 5cm in length, together with biotite, quartz (Plate 4.25) and smaller idioblastic porphyroblasts of magnetite. The hornblende and biotite are intergrown. The sizes of the quartz and andesine inclusions within the centres of the hornblendes are much larger than those at the margins or those within the biotites, a relationship which would indicate that the hornblende was the first mineral to have begun crystallisation. The magnetite occurs as small inclusions in the outer regions of the hornblende porphyroblasts, but the larger idioblastic grains, which occur outside the hornblende, are themselves surrounded by biotite. This would indicate that the order of appearance of the porphyroblasts was hornblende, magnetite and then biotite. Porphyroblasts of garnet and magnetite (Plate 4.26) are developed in a quartzo-felspathic dyke that cuts the agglomerates (Figure 3.16).

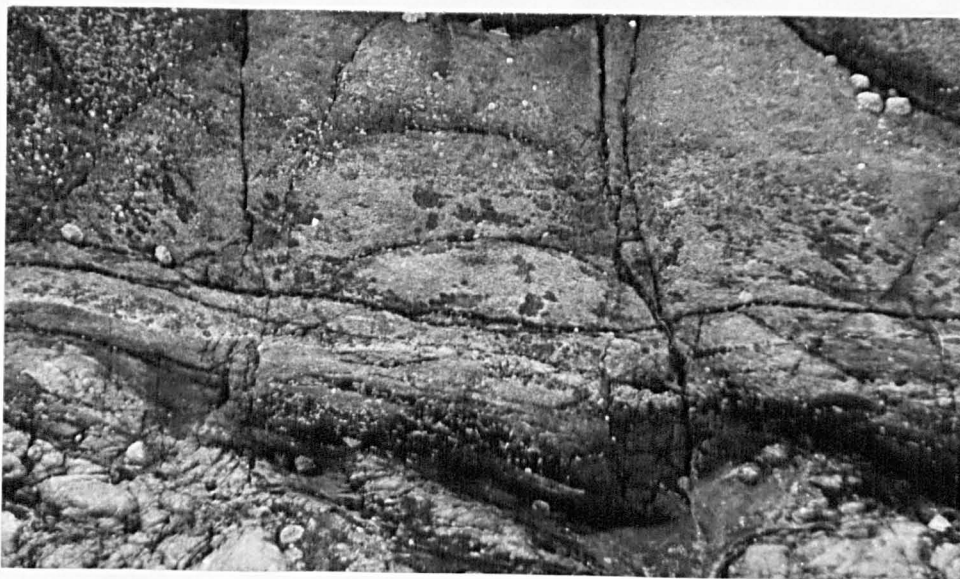


Plate 4.27. Static M_{3C} biotites developed in the retrogressed Port Goret gneisses at Palus plage (sub area P1). Field of view approximately 1m.



Plate 4.28. Photomicrograph (cn) of an M_{2C} garnet in the retrogressed Port Goret gneisses at Palus plage (sub area P3). Scale 0.32mm.

Other minerals that grow as porphyroblasts are garnet, cordierite and anthophyllite. Garnets are usually small, not greater than 5mm, idioblastic and only slightly poikiloblastic. They grow throughout all rock types except the pelites, in which they are only found in the hinge regions of the F_{2C} folds. Anthophyllite is only found in association with these garnets in the hinge regions of the folds. It occurs as randomly orientated sub-idioblastic elongate needles that are occasionally grouped into radial aggregates. These crystals may attain a length of up to 2.5cm and have diamond shaped cross sections. The cordierite which occurs as irregular poikilitic porphyroblasts within the tuffaceous sandstones and the intermediate tuffs shows sector twinning and a $2V_z$ of $42^\circ - 80^\circ$.

(d) M_{3C} in the Pentevrian

The Pentevrian basement has been recrystallised by this event in the area around Palus plage. Here, small static biotites of irregular orientation are developed throughout the pelitic gneisses. In places, pegmatitic patches are developed where large decussate poikiloblastic laths of biotite (Plate 4.27) are set in a matrix of zoned andesine porphyroblasts that show well developed albite twinning and large irregular strained quartz grains.

In the areas of Pentevrian that were severely recrystallised during the M_{2C} events, porphyroblasts of garnet (Plate 4.28) are developed in the now completely recrystallised staurolite porphyroblasts. These garnets are irregular in form and are poikiloblastic, being so full of quartz inclusions that they are almost spongy. Where garnets are grown in the matrix they are idioblastic and very much smaller in size. The textures of the larger garnets is probably inherited from the staurolite porphyroblasts that they eventually replaced. In the Plouha Series the hornblende and plagioclase of the matrix of the meta-basalts is replaced by epidote. The garnets in the amygdalae are also replaced by epidote + calcite (Plate 2.36).

These textures are only developed close to the amygdales, the intervening matrix not being greatly affected. This is thought to be due to the fact that amygdales acted as centres of nucleation for these minerals which then grew outwards. In the same areas that these textures are developed radial aggregates of actinolite have grown in the meta-rhyolites

This event is thought to have taken place during the Cadomian as it is only in evidence in those rocks which occur near the Brioverian. As the textures associated with this event are typical of a static phase of metamorphism it is correlated with the M_{3C} event. If this correlation is correct, the mineral assemblages in the Plouha Series represent a lower grade of metamorphism than that which developed during M_{3C} at Palus plage, but are approximately of the same grade as that found in the Binic-Bréhec Series.

(4) Syntectonic retrograde metamorphism, M_{4C}

(a) Introduction

This event was synchronous with F_{3C} and has caused local retrogression of the assemblages associated with the three preceding metamorphic events in the Palus plage Brioverian and the Pentevrian. However the grade of metamorphism attained in the Binic-Bréhec Series during M_{4C} was the same as that of the previous two events, M_{2C} and M_{3C} .

(b) M_{4C} in the Binic-Bréhec Series

In areas where the F_{3C} structures are formed, the associated S_{3C} foliation is defined by biotite that is associated with quartz and albite. In these areas this event was of the same grade as M_{2C} and M_{3C} and, as mentioned above, it is thought that the Binic-Bréhec Series was subjected to only one phase of greenschist facies metamorphism that occupied the same period of time as the M_{2C} , M_{3C} and M_{4C} events at Palus plage.

(c) M_{4C} in the Palus plage Brioverian

This event is marked by the replacement of pre-existing mineral



Plate 4.29. Photomicrograph (cn) of M_{4C} chlorites replacing hornblende and biotite in the matrix of the agglomerates at Palus plage. The plagioclase is also retrogressed. Scale 0.69mm.

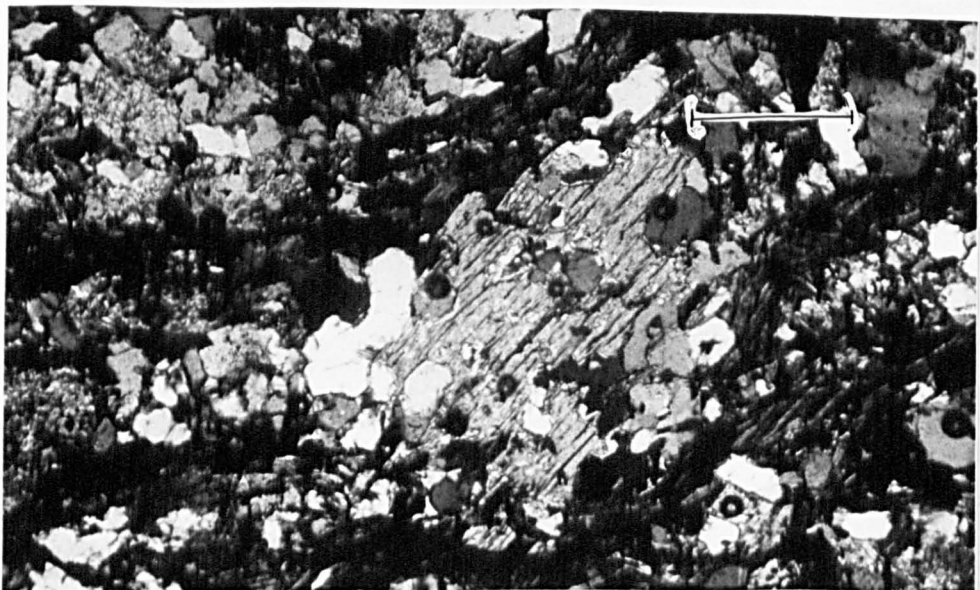


Plate 4.30. Photomicrograph of an M_{5C} muscovite porphyroblast (cn) grown in a retrogressed portion of the Port Goret gneisses at Palus plage (sub area P4). Scale 0.69mm.

phases by epidote, chlorite, sericite and serpentine, and has resulted in the recrystallisation of the quartz+andesine matrix to an irregular mesh of quartz and albite. These effects are usually only seen where the rocks have undergone shearing or flattening during the D_{3C} phase of deformation and are particularly marked in the pelites that are immediately adjacent to the unconformity in the southern part of this area. Here, as indicated earlier, the D_{3C} flattening has caused tightening of the F_{2C} folds and this has been accommodated by flexural slip along the gneiss-pelites contact which has resulted in the severe retrogression of the pelites in this area.

Elsewhere, the amount of retrogression is controlled by the amount of shearing that is present in the individual rock types. Generally, this event has had little effect other than in, or around shear zones. In the agglomerates the pressure shadow zones of the flattened pebbles are filled with epidote that replaces andesine, hornblende and biotite, but the growth of chlorite, sericite (Plate 4.29) and serpentine is mainly restricted to shear zones. Where this retrogression does take place the hornblendes first become a darker green in colour and then are replaced by chlorite. Biotite is also progressively replaced by chlorite, which first grows along the cleavage and then replaces the whole grain. In addition the garnets are often broken up to some extent and are progressively replaced by serpentine pseudomorphs, magnetite is replaced by haematite, and both plagioclase and cordierite are sericitised. The sericitic aggregate that replaces the cordierite is of a marked yellow colour. In some of the larger shear zones complete recrystallisation has taken place. A matrix of irregular elongate sutured grains of quartz and albite, that show a dimensionally oriented texture, enclose elongate laths of chlorite that are oriented to form a foliation that is parallel to the margins of the shear zone.

(d) M_{4C} in the Pentevrian

As in the Palus plage Brioverian the effects of this event are best developed in D_{3C} shear zones, although it has led to the chloritisation of biotite and the sericitisation of plagioclase throughout the Pentevrian.

In the Port Goret gneisses garnets are also retrogressed where the rock is cut by D_{3C} shears. The clots of white mica that replaced the staurolites are still preserved but are more streaked out and less well defined towards the north. In the area to the south of Port Goret, where the gneisses are in contact with the Saint Quay intrusion, they have been subjected to extensive D_{3C} shearing and many shear zones are developed. The matrix of these zones is formed of a quartz+albite+chlorite schist whose foliation is parallel to the margins of the shear zone (Plate 4.14). Within these zones all previous textures are transposed and the rock becomes homogenous.

This event has resulted in the replacement of all the plagioclase by sericite in the matrix of the meta-basalts of the Plouha series. Hornblende, garnet, magnetite and epidote have all been replaced by varying degrees of chlorite. This is particularly marked in the areas where epidotisation had taken place during the previous metamorphic event. Magnetite has been rimmed or replaced by haematite. Quartz has been recrystallised and shows irrational sutured margins. The effects of this event are less marked in the other lithologies of this series although most plagioclases show some degree of sericitisation. Hornblende and biotite are replaced by chlorite and staurolite and cordierite are replaced by an aggregate of white mica and minute granules of ore.

The Port Moguer tonalite was affected by this phase of retrograde metamorphism which was associated with the development of brittle fractures and recrystallised shear zones. The mineral assemblage developed during this event is chlorite + sericite + albite + quartz with accessory calcite, sphene and allanite.

The chlorite nearly always grows at the expense of the M_{5P} biotites and it usually mimics their decussate texture. However, where the growth of chlorite is associated with the development of shears, it is orientated to define a foliation that is sub-parallel to the shear zone. In the sheared specimens all stages of alteration from biotite to chlorite are seen. The chlorite is apparently iron rich since it shows a markedly green pleochroism. Sericitisation of the igneous plagioclase occurred at this time and those plagioclases that are within or adjacent to a shear zone are very heavily sericitised.

Both quartz and albite have been recrystallised to a very fine interlocking mesh within these shear zones. An interesting texture is developed where pre-existing plagioclase grains are cut by a shear zone. The albite that crystallised in the shear zone can be seen to have grown in optical continuity with the original crystal of plagioclase, the result being that only one grain of albite grows in the space between the two halves of the original crystal and this cements these two halves together.

Shear zones that occur towards the margin of the intrusion are sometimes filled with calcite, sphene and occasionally a little allanite. It is not clear whether these minerals were formed by the alteration of the tonalite or by the metasomatic introduction of these minerals from outside of the body.

This event did not result in a whole scale recrystallisation of the body. Generally new microfabrics were only developed where the rock had undergone D_{3C} shearing. Although many of the granoblastic quartz grains now show strained extinction and the development of fritted and sutured margins, the microfabrics in the non-sheared regions do not appear to have been altered by this event and it is probable that any recrystallisation of quartz that did occur was in optical continuity with the pre-existing grains.

KEY
sample
○ with muscovite
● without muscovite

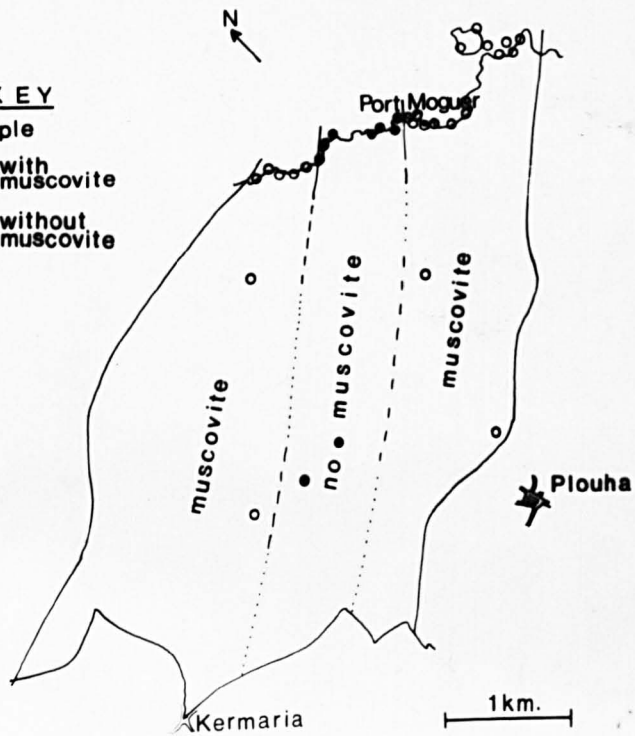


Figure 4.12. Sketch map of the Port Moguer tonalite showing the regions where M_{5C} muscovites are being developed. Comparison with Figure 2.13. will show that the muscovite is developed in the more sheared parts of the tonalite.

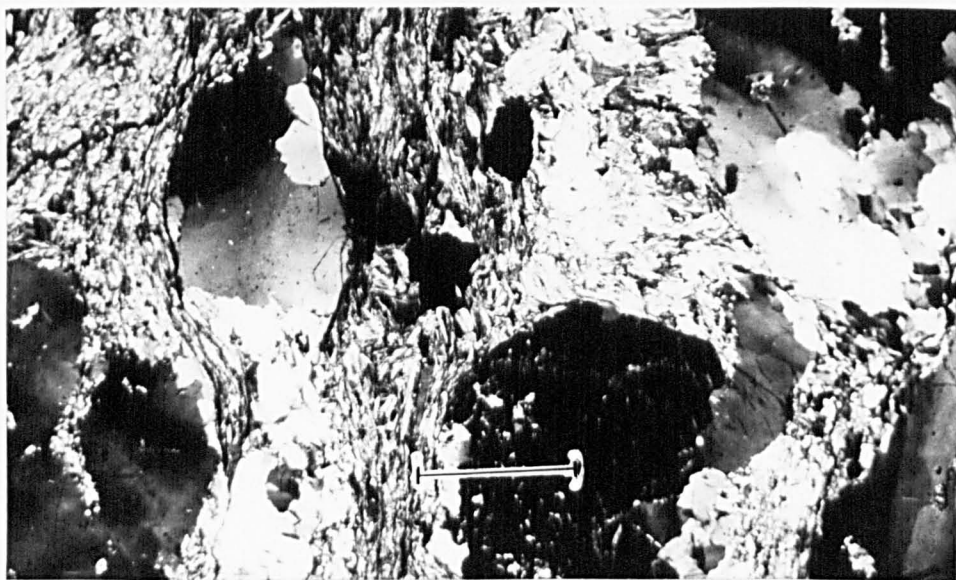


Plate 4.31. Photomicrograph (cn) of a garnet-muscovite filled shear zone developed during M_{5C} in the Port Moguer tonalite 600m north of the harbour at Port Moguer. Scale 0.69mm.

6. M_{5C} , a late phase of muscovite growth

This event has resulted in the growth of muscovite porphyroblasts throughout the region (Plate 4.30). Muscovite either grows as large poikilitic porphyroblasts that replace any pre-existing mineral, particularly plagioclase, or as non-poikilitic memetic laths that grow along the cleavage of biotite or chlorite and gradually replace the whole grain. Although these plates of muscovite may be found throughout the whole area they are particularly well developed in regions that have undergone pre- M_{5C} shearing. They are, for example, well developed in the Port Moguer tonalite at its margins but die out inwards and become restricted to late shear zones. They do not occur in the less sheared central third of the body (Figure 4.12). Where muscovites are developed in these shear zones they occasionally define a foliation that is parallel to the margins of these zones (Plate 4.31). Zoned, euhedral garnets that deflect the foliation are developed in the pressure shadows of these shear zones and also in the crushed tonalite immediately adjacent to the shear zone. These textures suggest that these shear zones were still active during M_{5C} .

The distribution of the muscovite would suggest that the tonalite was partially impervious to the metasomatising fluids. These fluids did not penetrate the central third of the body and they could only penetrate past the outer third along shear zones. The plates of muscovite grown during this event may often be seen to be kinked. This would suggest that, although this event was post D_{3C} , as the muscovite is always seen to cross cut D_{3C} fabrics, it was prior to one or more of the phases of kinking that operated towards the end of the Cadomian orogeny in this area.

The intermediate tuffs within the Palus plagioclase Brioverian are cut by several irregular veins within which calcite, haematite, sphene and large porphyroblasts of garnet, up to 4cm across, are found. These veins

also occur on a microscopic scale in the Pentevrian basement in the region of the unconformity. The relationship of these veins to the M_{5C} metasomatic event is not clear. Although they are not as widespread as the muscovite they were developed during D_{3C} , as they can be seen to be intruded along D_{3C} shears in some places, and to cut D_{3C} shears discordantly in others.

D. Summary of the tectonic and metamorphic history of the Cadomian orogeny in the region studied.

A detailed study of the metamorphic and structural history of the Cadomian orogeny in this area has shown that it was a good deal more complex than a study of the French literature would suggest. In place of the predicted two phases of deformation and one phase of metamorphism at least six phases of deformation and five phases of metamorphism are recorded:

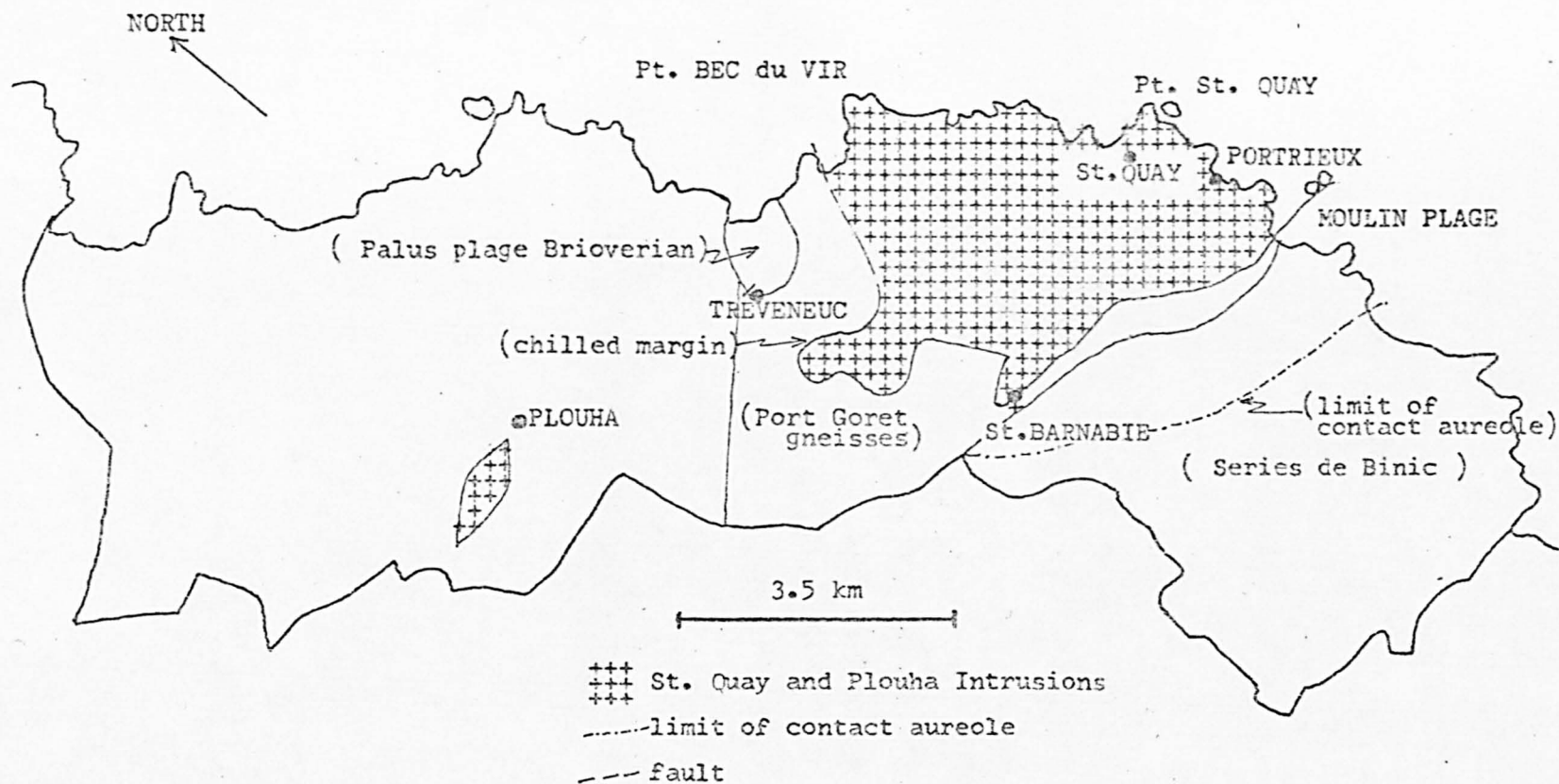
- F_{1C} . A phase of folding that was developed throughout the region. This event produced large scale close to isoclinal-overtured folds in the Binic-Br  hec series and both large and small scale isoclinal folds with an associated axial planar foliation S_{1C} , developed during the greenschist facies M_{1C} metamorphic event, in the Palus plage Brioverian. The axial surfaces of these folds probably had a steep dip and a north-south to northeast-southwest strike. Northeast-southwest shear zones may have been developed in the Palus plage area during this event.
- F_{2C} . Tight to isoclinal structures with steeply dipping east-west to east-northeast-west-southwest striking axial surfaces were developed throughout the region in association with the second Cadomian metamorphism M_{2C} . This metamorphic event, which varies in grade from greenschist facies in the Binic-Br  hec series to amphibolite facies in the Palus plage Brioverian and the Port Goret gneisses, has resulted in the formation

of a foliation S_{2C} that is everywhere parallel to the axial surfaces of the F_{2C} folds. In the region of Palus plage a lineation L_{2C} is developed as a result of the formation of microfolds upon the limbs of mesoscopic F_{2C} folds.

- M_{3C} . A static amphibolite facies metamorphism that is only well developed in the Palus plage area.
- F_{3C} . A phase of deformation that caused the formation of shear zones in the Palus plage area and the tightening of previous structures, and the formation of small scale folds by movement along the cleavage S_{2C} in the rest of the area. This event was associated with a regional metamorphic event M_{4C} that resulted in chlorite grade metamorphism elsewhere. The structures formed during this event are of the same orientation as those formed during F_{2C} . A lineation L_{3C} is developed at Palus plage as a result of the orientation of the long axes of deformed pebbles.
- L_{4C} . A phase of crinkling that is found in the Brioverian at Moulin plage. This occurred after the F_{3C} event but during the crystallisation of M_{4C} biotites.
- M_{5C} . A phase of metasomatism that has resulted in the growth of muscovite throughout the region. This event occurred post- F_{3C} , but pre-or syn-the late kinking.
- K_A, K_B, K_C . Several late phases of brittle deformation that gave rise to the development of at least three conjugate sets of kink bands and conjugate shear folds.

CHAPTER V

THE SAINT QUAY INTRUSION



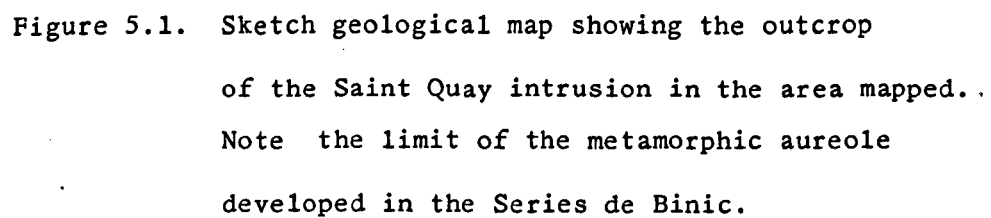


Figure 5.1. Sketch geological map showing the outcrop
of the Saint Quay intrusion in the area mapped..
Note the limit of the metamorphic aureole
developed in the Series de Binic.

A. Introduction

The Saint Quay intrusion is a body of basic igneous rocks that is exposed for a distance of 5km along the coast between Pointe Bec du Vir and Mbulin plage. The part of the body that is exposed on the mainland has the form of a trapezium with the longer side extending for 5km along the coast while the shorter side, of 2km length runs between Froidville and Kerihouet. The height of this trapezium is in the order of 2.6km. There are two small apophyses to this intrusion, one being located at Kerlan and the other at Saint Barnabie (Figure 5.1). The surface area of that part of the body exposed on the mainland is 9.2sq.km. On Sheet Number 59 of the French Geological 1:80,000 map the intrusion is shown as outcropping to the east of the Rade de Portrieux on the Roches de Saint Quay. This suggests that the body has a minimum length of 10km. and a minimum surface area of 40sq.km. A study of the geology of the Roches de Saint Quay has not been carried out.

The coastline along which the body is exposed is very irregular with many small bays and indentations. The cliffs are usually gently sloping and not more than 20m in altitude. Inland the body occupies a platform that is approximately 60m in altitude, rising to 80m at its western margin. On the coast it can be seen that above the high water mark there is a zone of spheroidal weathering that may be up to 5m in depth. The outcrop pattern of this body is

not greatly affected by topographic changes, which suggests that it has steeply dipping contacts.

A small stock, similar in nature to the Saint Quay intrusion, outcrops to the west of Plouha. This body, which is termed the Plouha intrusion, is poorly exposed. The primary igneous minerals have been retrogressed to a chlorite+actinolite+sericite assemblage during the Cadomian orogeny.

B. History of Previous Research

The intrusion was originally mapped by Barrois in 1898, this map was revised by Barrois in 1932 and again in 1938 in conjunction with Pruvost and Waterlot. They describe the intrusion as being a hornblende diorite and believed that it had been formed by the reaction at depth between the Variscan granites and the gneissose basement.

The hypothesis that the various diorite stocks in Brittany are not of a Variscan age was put forward by Cogné (1962). He believed that they were in fact due to the assimilation of the Brioverian ophiolite sequence (Étage d'Erquy) by the granitising fluids that were associated with a period of uplift that occurred post-Middle Brioverian but pre-Upper Brioverian, i.e. the Constantian phase of uplift (Graindor 1962). The contact metamorphic aureole of this intrusion is discussed by Jeanette and Cogné (1968), who state that this event has alone been responsible for the metamorphic assemblage (cordierite+biotite) developed in the Series de Binic.



Plate 5.1. Photomicrograph (cn) of the Saint Quay intrusion/Port Goret gneiss contact at Moulin plage. The gneiss is on the left. Scale 0.69mm.

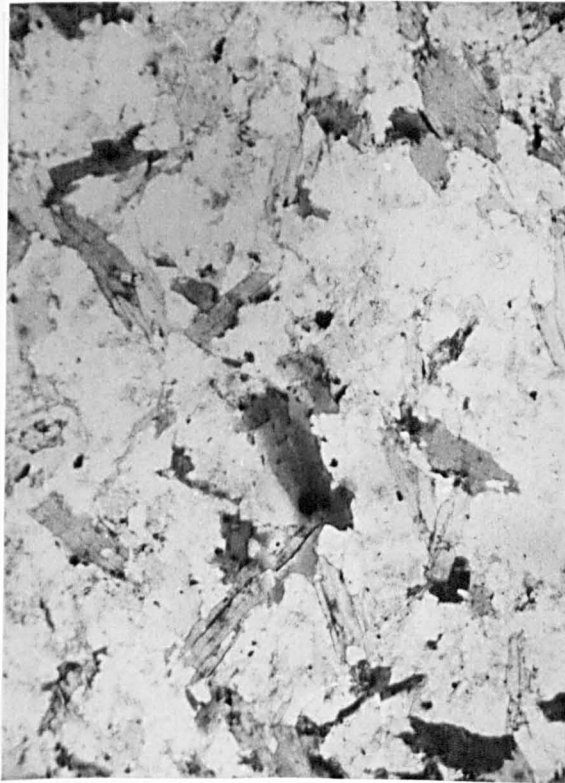


Plate 5.2. Photomicrograph (pp1) of contact metamorphosed Port Goret gneiss at Moulin plage. Note the static biotites. Scale 0.69mm.

C. The Metamorphic Aureole

The body is intruded into the Pentevrian Port Goret gneisses. To the south of the body these form a thin shield of 200-300m in thickness between the intrusion itself and the Brioverian Series de Binic. In the north and the west the outcrop of the gneisses surrounding the body is much thicker. These gneisses pass northwards into the Plouha Series, except for a small area around Palus plage where Brioverian metasediments and metavolcanics are found (Figure 5.1).

A recognisable contact metamorphic aureole in the Port Goret gneisses is only seen at Moulin plage. Here, immediately adjacent to the intrusion, there is a zone of several metres in thickness in which biotite within the gneisses has been recrystallised (Plate 5.1). The new biotites are mimetic and preserve the earlier Pentevrian fabrics, they have a weaker pleochroism and are not kinked (a feature that is common in Pentevrian biotites found elsewhere). At the actual contact of the gneisses with the intrusion large labradorite porphyroblasts are grown in the gneisses up to 5cm away from the contact (Plate 5.2). The contact between the intrusion and the gneisses at Moulin plage is not simple and several large blocks of gneiss rest within the intrusion (Map 2). In the most northerly of these a strange texture is observed. There is a zone of about 50cm in width in which blocks of gneiss 5-10cm across are irregularly oriented in a matrix of quartz+albite+biotite schist, the foliation in which is parallel to that in the neighbouring Series de Binic. The relationships between this block and the rest of the gneisses is poorly exposed and the

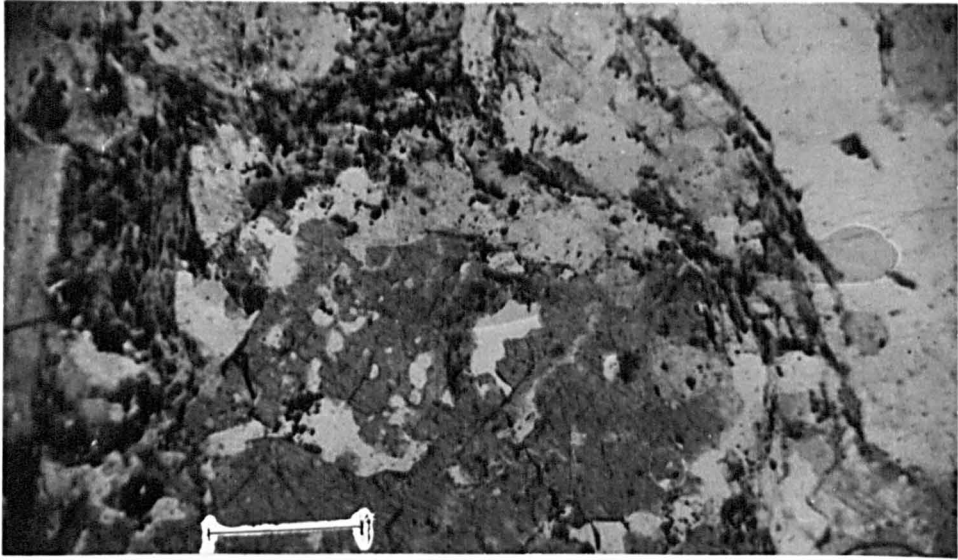


Plate 5.3. Photomicrograph (pp1) of tourmaline developed in the Port Goret gneiss adjacent to the Saint Quay intrusion at Moulin plage. Scale 0.69mm.



Plate 5.4. Retrogressed cordierite/andalusite porphyroblasts in the aureole of the Saint Quay intrusion in the Series de Binic. Some porphyroblasts are streaked out parallel to the cleavage S_{2C} (parallel with the ruler). Moulin plage.

origin of this texture is unknown, although it is possible that this may be a small wedge of Brioverian basal conglomerate. Thin veins of pegmatite are found in the gneisses. These contain quartz, orthoclase and tourmaline (Plate 5.3).

The gneisses to the north of the intrusion show no contact metamorphic effects. The actual gneiss intrusion contact is faulted, there being a zone of cataclasis and later retrogression that extends some 50m to 100m to either side of the fault. The fault dies out inland after 1.2km. (Map 1). The cataclasis and retrogression associated with this fault has overprinted any of the previous metamorphic textures in the gneiss and there is no evidence for contact metamorphism of the gneisses. Although the intrusion does not appear to have effected the Brioverian metavolcanics and metasediments at Palus plage, it has been responsible for the development of a substantial metamorphic aureole in the Brioverian sediments of Moulin plage to the south, where now retrogressed cordierite and/or andalusite porphyroblasts are developed up to 1200m from the intrusion (Map 1 and Plate 5.4). This metamorphic aureole may be traced inland for 7km with its outer limit lying parallel to the margins of the intrusion (Figure 5.1, Map 1). The cordierite and/or andalusite prophyroblasts are found in both the pelitic and the psammitic bands, although they are more frequent in the former. They increase in size and frequency as the intrusion is approached and near the contact they make up some 30% by volume of the pelitic bands. They were retrogressed (Plates 4.17 and 4.18) by the main Cadomian metamorphism in this area, M_{2C} , to a muscovite sericite felt and are often streaked out in the plane of the S_{2C} foliation (Plate 5.5). Thus

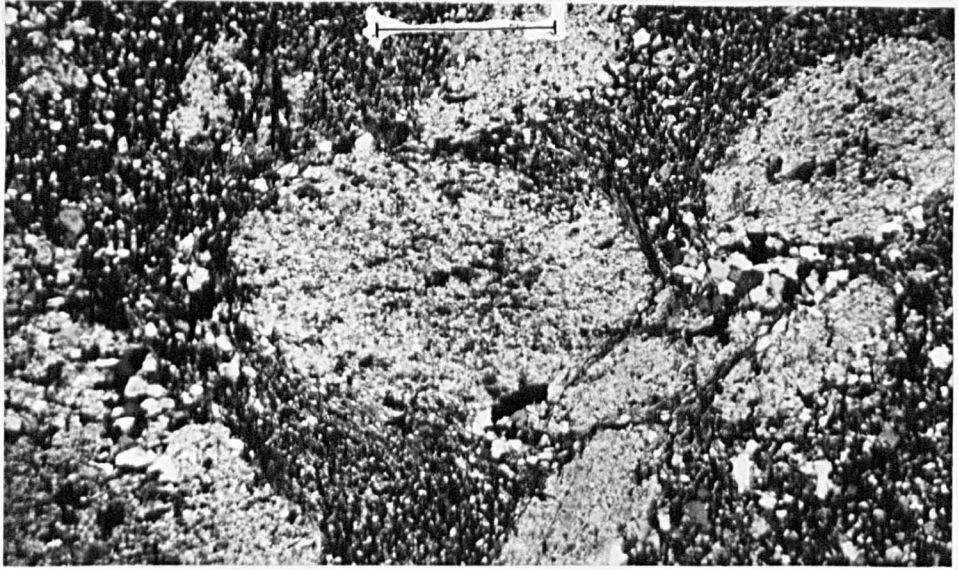


Plate 5.5. Photomicrograph (pp1) of retrogressed, pre S_{2c} , contact metamorphic aureole of the Saint Quay intrusion in the Series de Binic at Moulin plage. Scale 0.69 mm.



Plate 5.6. Photomicrograph (cn) of central norite showing alignment of elongate plagioclase grains to define fluxion structure (parallel to line). 5 x actual size.

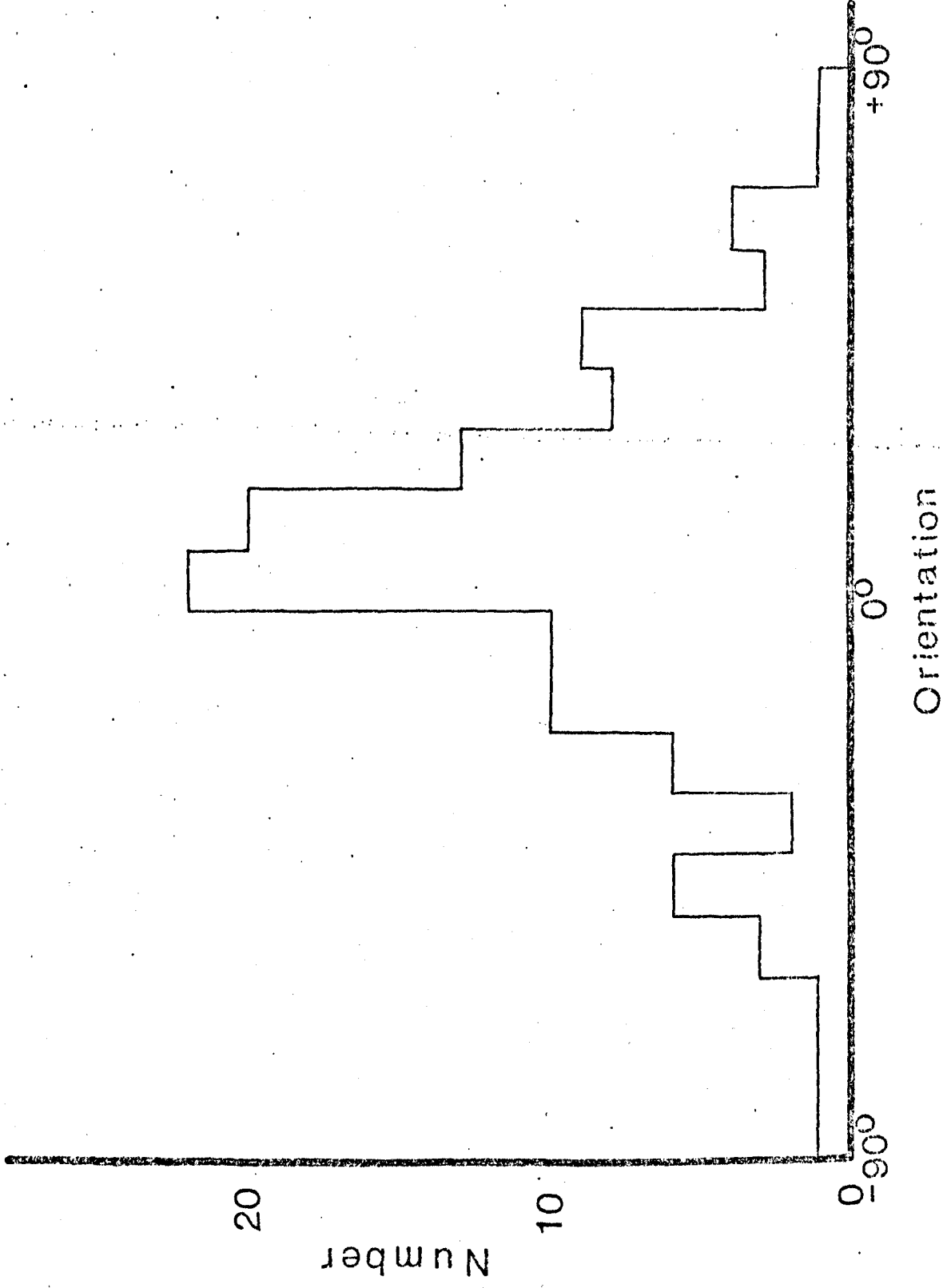


Figure 5.2. Histogram showing the orientation of 100 longest axes of plagioclase laths in a thin section of the central norite cut perpendicular to the igneous lamination. Note there is a strong preferred orientation of these laths which has a maximum at $+5^{\circ}$ (i.e. clockwise) to the long axis of the slide.

the emplacement of the intrusion and the development of the associated metamorphic aureole occurred prior to the F_{2C} folding and the syn- F_{2C} regional metamorphism, M_{2C} .

D. Field Relationships within the Intrusion

1. Introduction

There are essentially two main rock types within the intrusion: (1) norite and (2) quartz-hornblende gabbro. The norite is a melanocratic, medium grained holocrystalline rock which exhibits a poor foliation owing to the alignment of the long axes of plagioclase feldspars and pyroxenes (Plate 5.6). The quartz-hornblende gabbro is a mesotype medium grained holocrystalline rock in which the plagioclases appear white as a result of alteration. It shows particularly well developed igneous lamination in which the amphibole prisms and plagioclase laths exhibit a planar preferred orientation but no linear alignment (Figure 5.2). This lamination must be a primary igneous feature and not a post-magmatic deformational feature because the latter would only have developed in those portions of the intrusion that were subjected to Cadomian metamorphism and deformation, i.e. the northern margin. This structure appears to lie parallel to the margins of the intrusion (Map 1) and is thought to be due to the circulation of partially crystalline magma within the chamber. Along the coast the norite occupies a zone about 1.5km. in length from St. Marc in the north to place St. Quay in the South. This central zone of norite is bordered on both sides by a transitional zone, approximately 600m in width, comprised of a hornblende-ferrohypersthene-

gabbro intermediate in nature to the other two rock types, (Map 2). Irregular bands of anorthositic gabbro, 1m in thickness occur in this zone. The outer part of the intrusion is comprised of quartz-hornblende gabbro which extends 1.2km to the north, where it is cut off by a fault at Port Goret, and 2.5km to the south, where it is in contact with the Port Goret gneisses at Moulin plage (Map 2). It is difficult to trace these rock types inland as they are poorly exposed, but it appears that the majority of the outcrop is occupied by norite (Map 1) with the quartz-hornblende gabbro occupying belts to the north and the south that die out inland (Map 1). Pyroxene hornfels enclaves are found throughout the intrusion. These enclaves are 5-50 cm across, comprise up to 20% by volume of the rock and occur in zones that are up to 50cm wide that are parallel to the igneous lamination (Map 2). The rock enclosing the enclaves contains more pyroxene and less hornblende and biotite than the neighbouring rock which is enclave free.

At Moulin plage the quartz-hornblende-gabbro shows no chilled margin. At the contact there is a zone of about 30cm in width in which small stoned blocks of gneiss and mica schist lie with their long axes in the plane of igneous lamination. This is then followed by a zone about 80m in width where large blocks (up to 3m across) and irregular stringers (up to 10m in length) of gneiss and mica schist occur within the gabbro. These show little alteration except for the development of plagioclase porphyroblasts up to 1cm in length within the mica schists. Inland where the norite is seen to be in contact with the Port



Plate 5.7. Photomicrograph (cn) of unretrogressed shear zone in central norite. 5 x actual size.

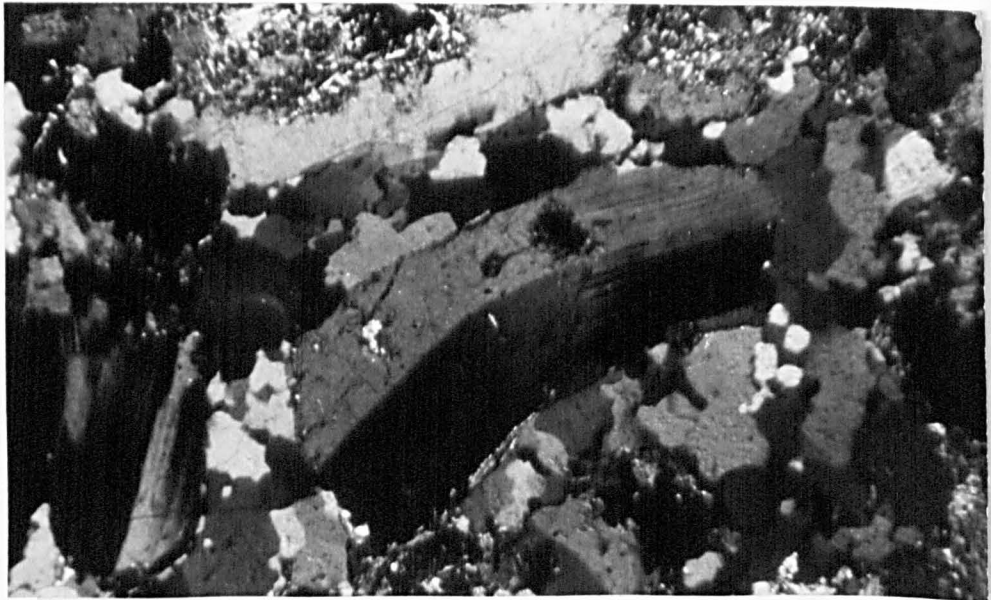


Plate 5.8. Photomicrograph (cn) of bent plagioclase grain in the quartz hornblende gabbro. 2 x actual size.

Goret gneisses there is a marked chilled margin of about 1m thickness. The rocks of this chilled margin are identical in mineralogical composition to those of the central norites. At place St. Quay large angular unaltered blocks of medium grained norite are found to be completely enclosed within the quartz-hornblende gabbro. These are associated with a belt of large blocks of pyroxene hornfels and appear to have been stoped from the central norite by the later intrusion of gabbro. Here also, it is possible to see evidence of reaction between the gabbro and norite enclaves. A plagioclase rich zone of about 1cm across surrounds the enclave, and this is then surrounded by a zone of coarse hornblende (0.5-1cm) again about 1cm in width. This, coupled with the lack of chilled margin associated with this rock type, would suggest that it was intruded as a crystalline mush after the solidification of the norite.

The intrusion is cut by shear zones that were developed whilst the intrusion was still hot (there being no retrogression associated with these shears (Plate 5.7) but sufficiently solid to accept shearing stresses. There is also evidence of disruption of the crystal mush in that anorthosite bands, believed to be formed by crystal settling in the magma chamber, are now of irregular form. Crystals of all the primary magmatic minerals show some degree of bending, again with no associated retrogression (Plate 5.8).

There is a zone, approximately 500m in width, at the northern contact where the gabbro has been retrogressed during the Cadomian orogeny. The plagioclase is heavily sericitized and biotite shows alteration to chlorite. The northern contact is

comprised of mylonitized gabbro formed as a result of cataclasis during faulting. In the south it appears that the plagioclases become slightly more altered as one approaches the contact but no other effects of alteration are seen.

In the gabbro around Port Goret and Isle de la Comtesse there are pegmatite veins that have cut the solid gabbro and can be seen to stope small blocks of gabbro. These are made up of graphic feldspars with quartz rich centres. The body is cut by late titanium-rich dolerite dykes that can be seen at Port St. Quay, and between plage St. Quay and St. Marc. These are chilled against the intrusion. In thin section they are porphyritic. About 5% of the mode consists of altered, zoned euhedral labradorite phenocrysts up to 1cm. across, and the groundmass shows a good ophitic texture with elongate plagioclase (An_{60}), 1mm in length (60% of mode), pink pleochroic titanium augite (20% of mode) and 1mm long needles of ilmenite (5% of mode), plus a few grains of quartz.

E. Petrology

1. Introduction

The map of the intrusion was constructed using two criteria. The first was the actual distribution of rock types as recognised in the field. The second was the mineralogical composition of the rock types as studied in thin section. This was necessary because it was extremely difficult to recognize all the distinctions between the rock types in the field. On this basis

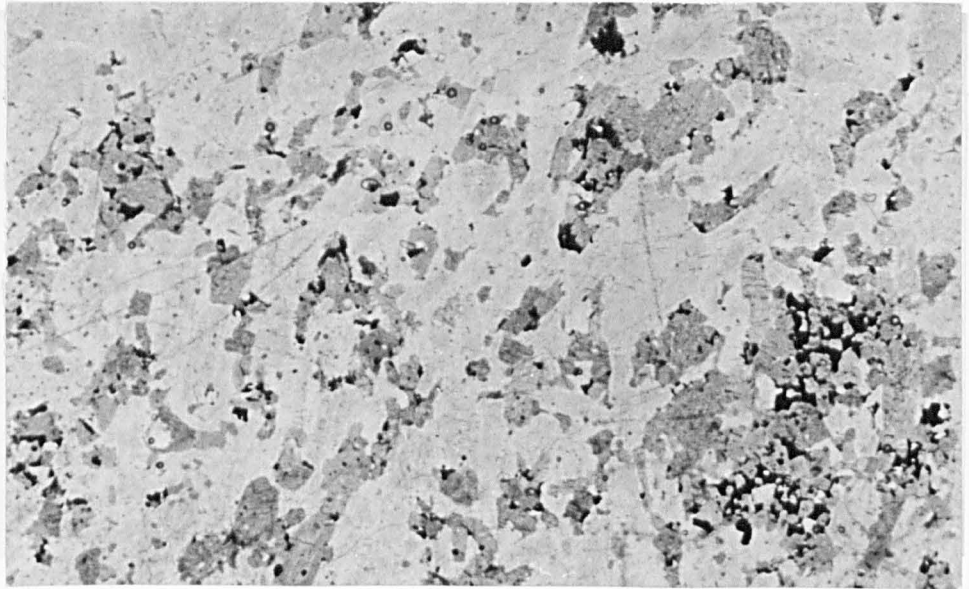


Plate 5.9. Photomicrograph (pp1) of the central norite. Note the low mafic index and the cumulate of ore and pyroxene grains at the bottom right corner. 5^x normal size.

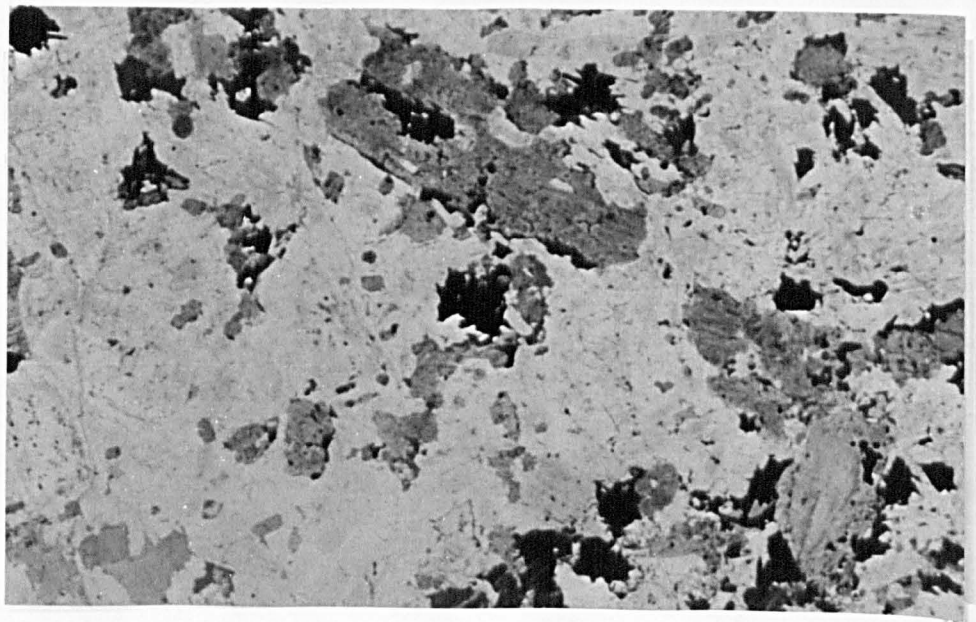


Plate 5.10. Photomicrograph (pp1) of the marginal facies of the central norite. Note that the pyroxene grains are rimmed by biotite. 5^x normal size.

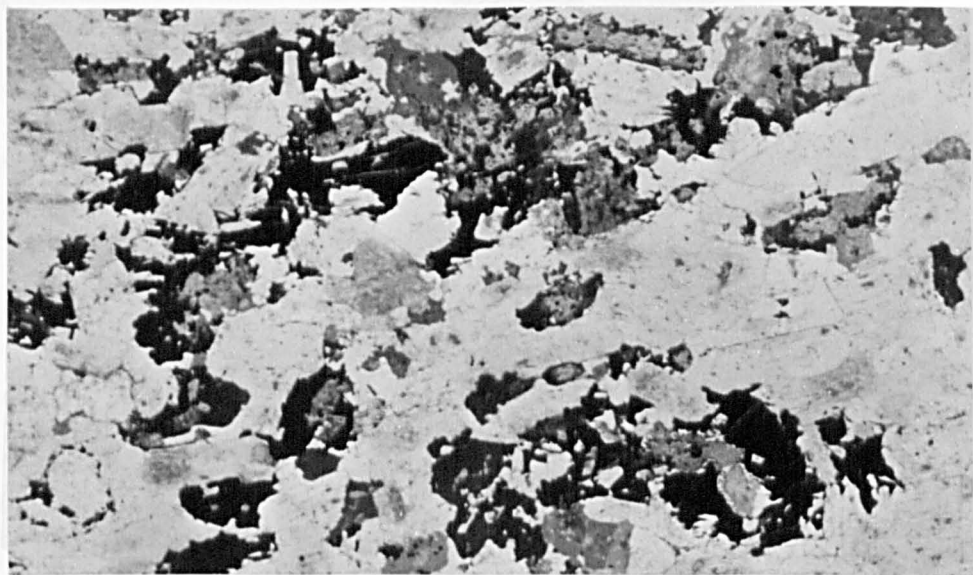


Plate 5.11. Photomicrograph (pp1) of the hornblende-ferrohypersthene gabbro of the transition zone. The pyroxenes are rimmed and partially replaced by hornblende (dark-grey) and biotite (black). 5^x normal size.

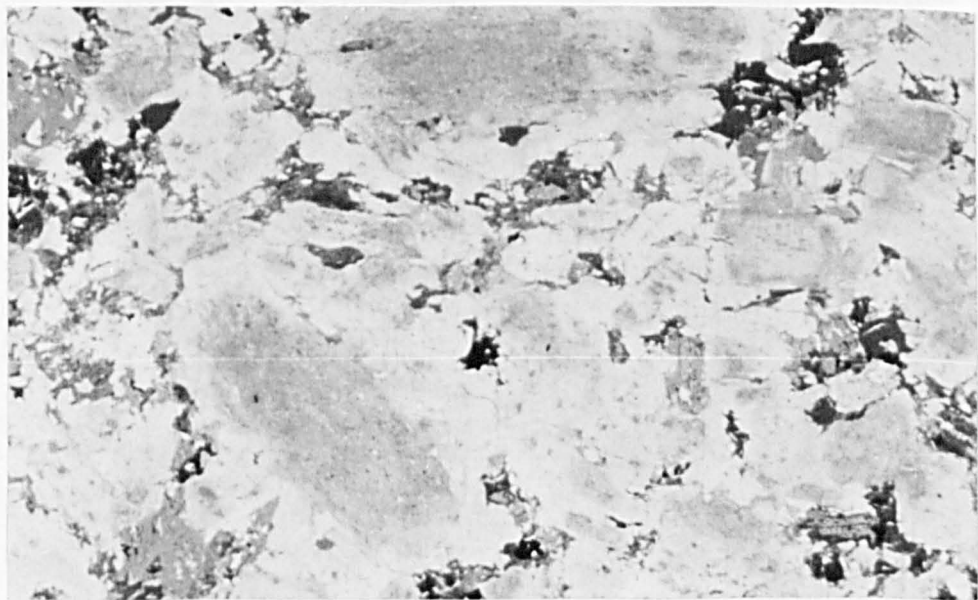


Plate 5.12. Photomicrograph (pp1) of the quartz-hornblende gabbro. Pyroxenes are almost completely replaced by hornblende (dark-grey) and biotite (black) and the plagioclase grains are sericitised. A relict orthopyroxene is seen in the bottom right hand corner. 5 normal size.



Plate 5.13. Photomicrograph (cn) of zoned plagioclase in the norite. 10^x normal size.

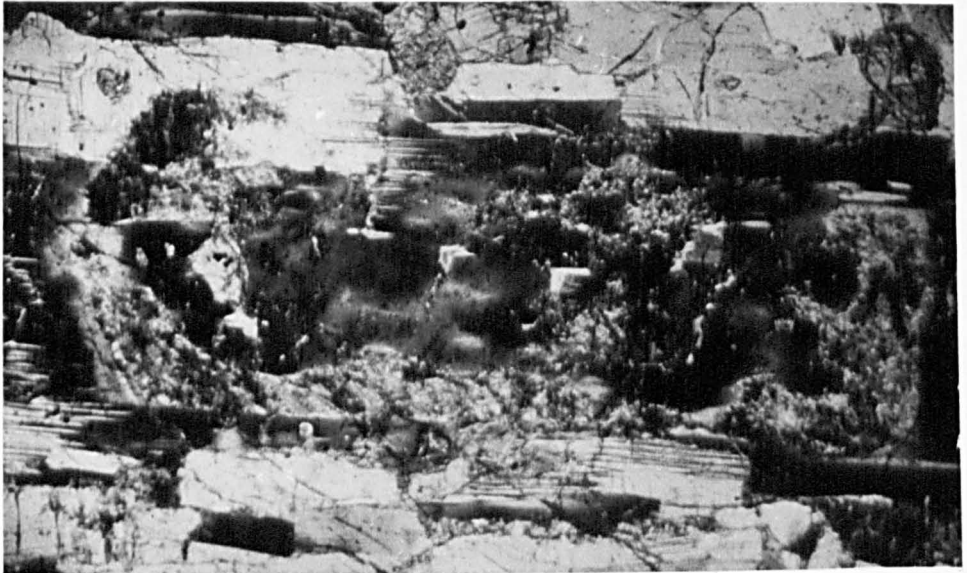


Plate 5.14. Photomicrograph (cn) of plagioclase in the norite which exhibits patchy zoning. 10^x normal size.

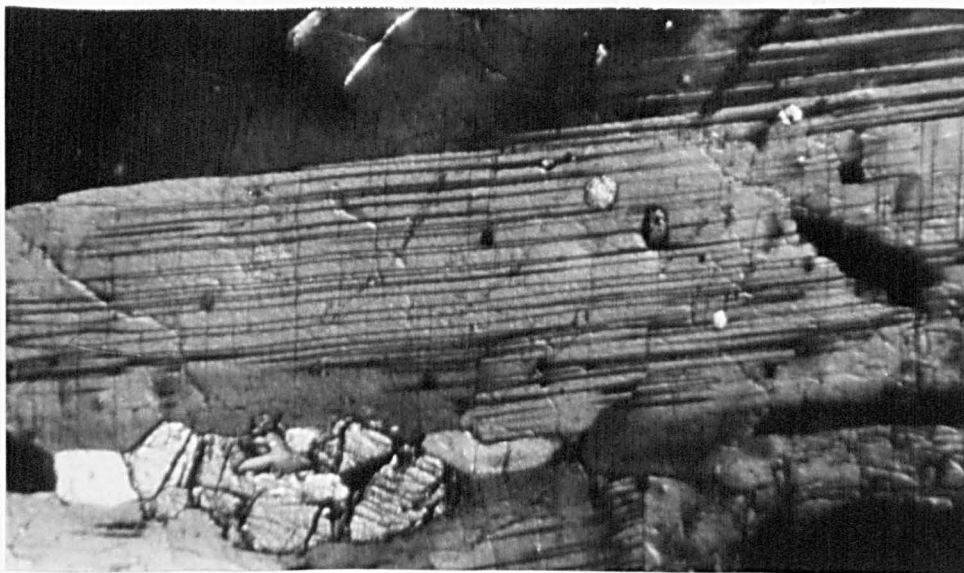


Plate 5.15. Photomicrograph (cn) of plagioclase that poikilitically encloses small grains of orthopyroxene. 20^{\times} normal size.

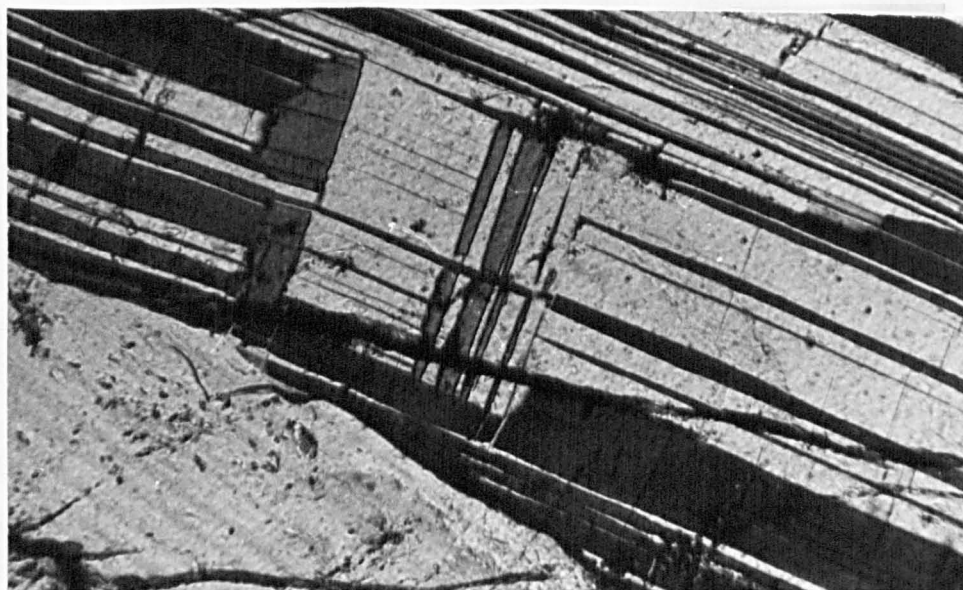


Plate 5.16. Photomicrograph (cn) of albite twins in plagioclase that are displaced by pericline twins. 80^{\times} normal size.

the intrusion has been divided into three rock types, although almost continuous variation between the two end members (i.e. norite and quartz-hornblende gabbro) exists.

- (a) The central zone is made up of fresh unaltered norite in which the modal percentage of pyroxene is greater than biotite and hornblende. Quartz is absent. (Plates 5.9, 5.10).
- (b) The transitional zone consists of hornblende-ferrohypersthene gabbro where the modal percentage of pyroxene is approximately equal to that of hornblende and biotite. (Plate 5.11).
- (c) The outer zone is made up of quartz-hornblende gabbro where nearly all the pyroxene has been replaced by either hornblende or biotite, and the modal percentage hornblende and biotite is much greater than that of pyroxene. (Plate 5.12).

2. The norite of the central zone

This is a dark coloured, medium grained holocrystalline rock, with hypidiomorphic to allotriomorphic texture, made up of plagioclase, orthopyroxene, clinopyroxene, ore and apatite. Plagioclase comprises between 66-78% of the mode. There are both large porphyritic grains that make up to 30% of the mode, and smaller grains 2-3cm in length within the groundmass. The grains are generally anhedral, except where two adjacent grains have their C axes parallel and here they will show a face in common. The composition of these groundmass plagioclases are in the range An_{60-69} with an average of An_{63} .

The larger crystals are commonly zoned, showing good oscillatory euhedral zones with a normal trend. Up to sixteen zones have been counted in any one individual ranging from An_{40} in the centre to An_{45} near the margin (Plate 5.13). The outer zones of the grains are wider than the zones of the interior and are of andesine An_{35-40} . The more central zones of the larger plagioclases show patchy zoning with irregular more sodic areas An_{56} , that are surrounded by more calcic areas, An_{61} , (Plate 5.14). Often associated with the patchy zoning are trails of rounded clinopyroxenes and euhedral ore crystals (0.02mm). These trails are sometimes parallel to the euhedral outlines of the zones. Orthopyroxenes, about 0.5-1mm in size, are occasionally poikilolitically enclosed in the outer half of the larger plagioclase grains (Plate 5.15).

The plagioclase show irregularly developed carlsbad twins that cause euhedral zones to show re-entrant angles (Plate 5.30). There are also well developed albite and carlsbad-albite twins. The lamellae are of constant thickness of about 0.1-0.05mm. The plagioclase laths show bending of up to 40° , which appears to be associated with the development of pericline and wedge-shaped albite twins. The pericline twins are seen to displace the regular albite twin and are therefore later. (Plate 5.16). Vance (1961) showed that such carlsbad twins are probably growth twins whereas the regular albite twins may be due to the inversion of the plagioclase, while the wedge shaped albite and pericline twins are developed during deformation. Many of the large grains show fine exsolution needles of ore about 30-60 μ long and 1 μ in diameter. They appear to lie in the four cleavage directions



Plate 5.17. Photomicrograph (pp1) of ore needles in plagioclase which lie within cleavage planes. 300^x normal size.



Plate 5.18. Photomicrograph (pp1) of subidiomorphic grain of ferrohypersthene showing exsolution of ore along 100. 10^x normal size.

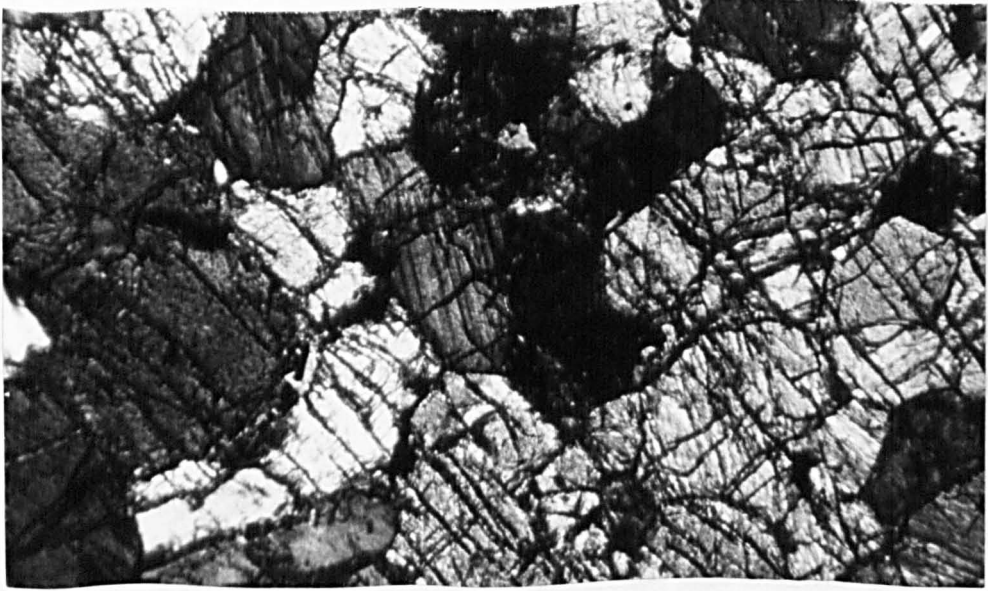


Plate 5.19. Photomicrograph (cn) of ferrohypersthene cumulate in norite. 40^x normal size.

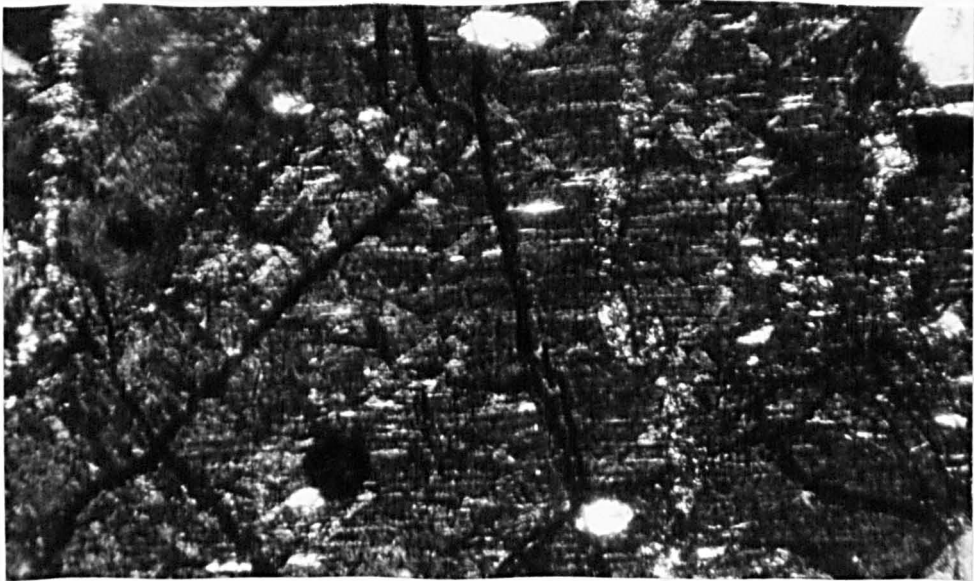


Plate 5.20. Photomicrograph (cn) of ferrohypersthene showing exsolution lamellae of clinopyroxene along 010. 80^x normal size.

$\{001\}$, $\{010\}$ and $\{110\}$ (Plate 5.17).

Orthopyroxene comprises between 6-20% of the mode.

It tends to occur in two forms: (1) subhedral elongate laths up to 6mm in length (Plate 5.18); (2) small rounded individuals (1mm) that occur packed together in clots of about 2cm across that are thought to represent relics of a cumulative phase disrupted during intrusion to the present level. (Plate 5.19). These may have interstitial plagioclase or ore. The mineral is mildly pleochroic α -pink, β -colourless, γ - colourless with $2V=58^{\circ}-62$ which gives the composition ferrohypersthene $En_{36}Fe_{64}$ to $En_{32}Fe_{68}$. The birefringence is high ($\alpha-\gamma = 0.0165$) giving interference colours up to a second order mauve. These are orthopyroxenes of the Bushveld type with fine exsolution lamellae of clinopyroxene parallel to $\{010\}$ (Plate 5.20) which cause anomalous extinction on $\{100\}$. Exsolved ore occurs parallel to $\{100\}$. (Plate 5.18).

Small ferrohypersthene grains are poikilitically enclosed by plagioclase, ore and clinopyroxene (Plate 5.21). The larger subhedral grains enclose small plagioclase crystals towards their margins although they themselves are included subpoikilitically in the plagioclase.

All degrees of serpentization are seen, the pyroxene being replaced by a brown fibrous bastite and a fine mat of ore (10u). The serpentine pseudomorphs appear to be replaced by

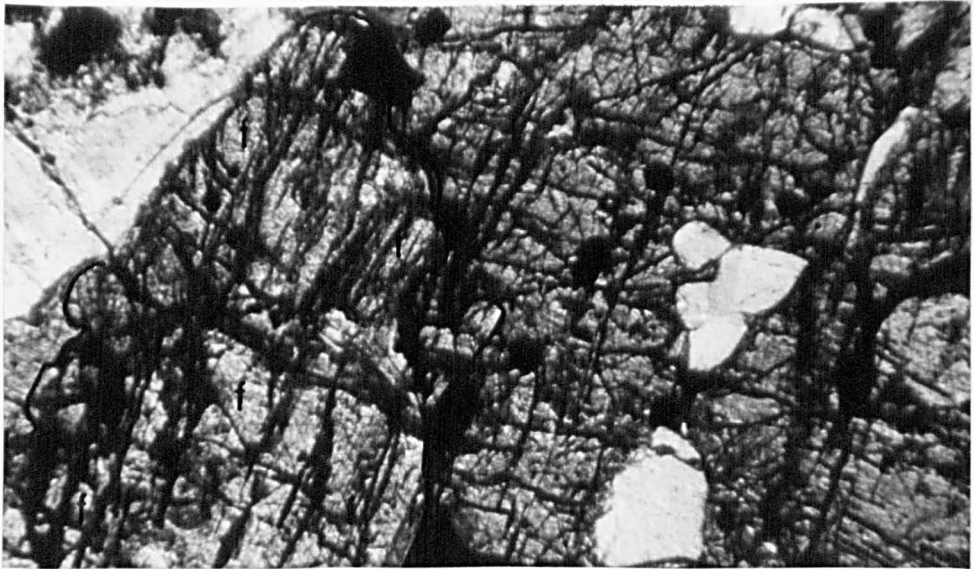


Plate 5.21. Photomicrograph (pp1) of a ferrohypersthene grain (f) that is enclosed subpoikilitically by hedenbergite. 40^{\times} normal size.



Plate 5.22. Photomicrograph (cn) of the central norite showing a grain of ferrohypersthene (left centre) rimmed with hornblende. 10^{\times} normal size.

both anthophyllite, $2V_z = 62^\circ$, which occurs in the form of colourless fibres, and actinolite which has a $2V_x = 74^\circ$, $Z \wedge C = 14^\circ$ and occurs as larger elongate crystals that are about 0.3mm in length. There does not seem to be any special relationship between the types of amphibole which replace the pyroxene. Both these amphiboles are replaced by hornblende (Plate 5.22) which develops on the outside of the replaced pyroxene and grows inwards, resorbing the ore that is exsolved in the original breakdown of the pyroxene.

Undeformed serpentized grains of pyroxene are found in specimens in which many fresh pyroxene grains are deformed. If serpentization had taken place before the deformation it would seem likely that the less competent serpentized grains would be effected, thus the serpentization probably took place after the deformation.

Clinopyroxene comprises between 7-8% of the mode. It occurs as large euhedral poikilitic plates that include plagioclase, ore and orthopyroxene (Plate 5.21) and have a grain size between 7mm and 1mm, the average being 2.5mm. The mineral is colourless, $2V_z = 57^\circ - 59^\circ$ and $Z \wedge C = 45^\circ$, this would give it a composition of $Wo_{45}En_{25}Fe_{30}$ or Hedenbergite. Normal twinning about 100 is common and this may be simple or repeated. Exsolution of ore occurs along 100 and in the cores of some of the grains along the two cleavage directions. The 100 parting is well developed. A few of the larger grains show zoning with a slight decrease in $2V$ and a slight increase in birefringence towards the margins of the grain, suggesting that the cores are poorer in the ferrosilite molecule than the margins.

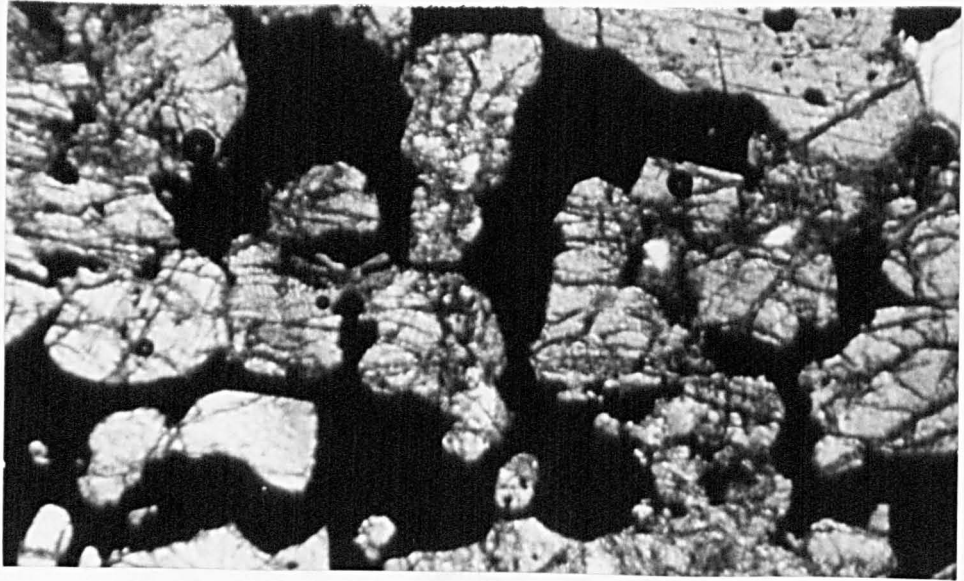


Plate 5.23. Photomicrograph (pp1) of ferrohypersthene/
magnetite cumulate. 40^{\times} normal size.

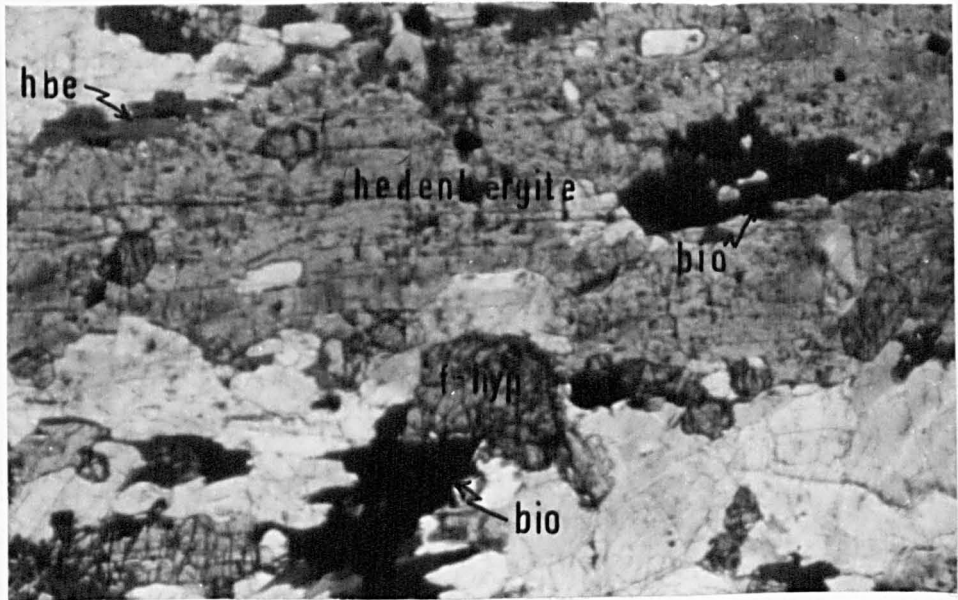


Plate 5.24. Photomicrograph (pp1) of ferrohypersthene (high
relief) being replaced by biotite (black) and
of hedenbergite (centre) being rimmed by hornblende
(dark grey) and biotite (black). 10^{\times} actual
size.

The pyroxenes may be rimmed by a green hornblende.

Ore comprises 2-3% of the mode. It has the form of anhedral interstitial magnetite grains usually 1-2mm in size. These poikilitically enclose orthopyroxene (Plate 5.23) which in contact with plagioclase are rimmed with biotite. Apatite is an ubiquitous accessory. The grains are euhedral, 0.3mm in length and comprise 0.1-0.4% of the mode. It is enclosed by all minerals except orthopyroxene.

3. The hornblende-ferrohypersthene gabbro of the transition zone

This is a medium grained mesotype allotriomorphic granular rock with plagioclase, pyroxenes, hornblende and biotite. Plagioclase comprises between 65-75% of the mode and a composition of An_{60-65} . It shows similar features to the plagioclases of the norite except that the grains show an increased amount of bending, internal disruption and intergrain cataclasis (Plate 5.28). Occasionally the more calcic cores may be slightly sericitised.

The orthopyroxene is a ferrohypersthene which comprises 2-12% of the mode and is similar in both composition and texture to that of the norite. It is often rimmed by biotite (Plate 5.24). Between the two minerals there is always a fine rim of quartz that is 0.03mm in thickness. It is quite common for the orthopyroxene to remain unaltered while the clinopyroxene is replaced by hornblende. The clinopyroxene is similar in composition to that encountered in the norite and comprises 2-10% of the mode. It is rimmed or partially replaced by a green hornblende (Plate 5.25).

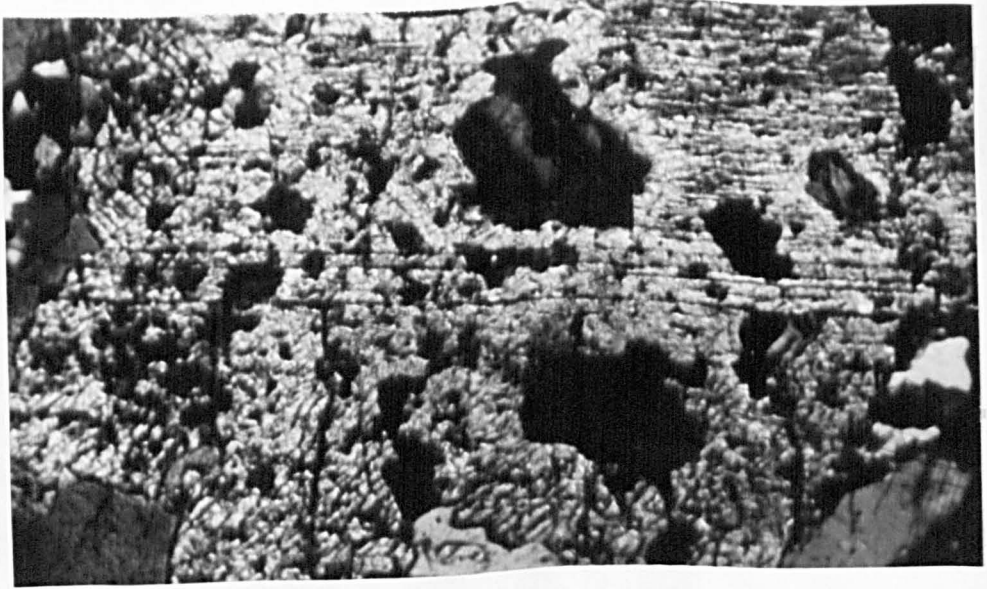


Plate 5.25. Photomicrograph (cn) of twinned hedenbergite grain sieved with hornblende (black). 20^{\times} normal size.



Plate 5.26. Photomicrograph (pp1) of hornblende grain cored with hedenbergite and exsolved ore. Note the relatively unaltered ferrohypersthene grain to the right. 20^{\times} actual size.

Hornblende makes up 3-10% of the mode and has a $2v_x = 69^\circ - 79^\circ$ with an average $\hat{Z} C = 19^\circ$ and it shows simple twinning on 100. The pleochroic formula shows variation between (a-greenish yellow, β -green, γ -blueish green) and (a-buff, β -brownish green, γ -olive brown). It occurs in plates up to 1cm in length that replaces both clinopyroxene and orthopyroxene. Many of the hornblende grains may be seen to be cored by fresh grains of pyroxene that show sutured, irregular contacts with the hornblende (Plate 5.26). The hornblende also always shows sutured margins with the plagioclase.

The brown variety tends to have a slightly higher $2V$ than the green and is more commonly found at the core of a grain, whereas the green variety occurs at grain margins, where it is involved in a reaction with the plagioclase. For example is one grain the brown hornblende at the centre has a $2V_x = 73^\circ$, whereas the green hornblende at the margin has a $2V_x = 69^\circ$.

The breakdown of pyroxene to hornblende seems to be preceded by a heavy exsolution of ore from the pyroxene along $\{100\}$, after which a sieve texture is developed in which the hornblende is seen to grow along the $\{100\}$ parting (Plate 5.25). Gradually, the hornblende grows inwards at the expense of the pyroxene (Plate 5.26 and 5.27). The hornblende replaces the pyroxene in such a way that it has the b axis and one optic axis parallel to those of the pyroxene it replaces. When a pyroxene twin is replaced the hornblende undergoes a rotation about the b axis of approximately 20° to still keep one optic axis parallel



Plate 5.27. Photomicrograph (cn) of a hornblende grain that has completely replaced hedenbergite, relicts of which are found in the centre of the grain. Note the poikilitically enclosed plagioclase and ore, a texture inherited from the pyroxene. 40^{\times} normal size.

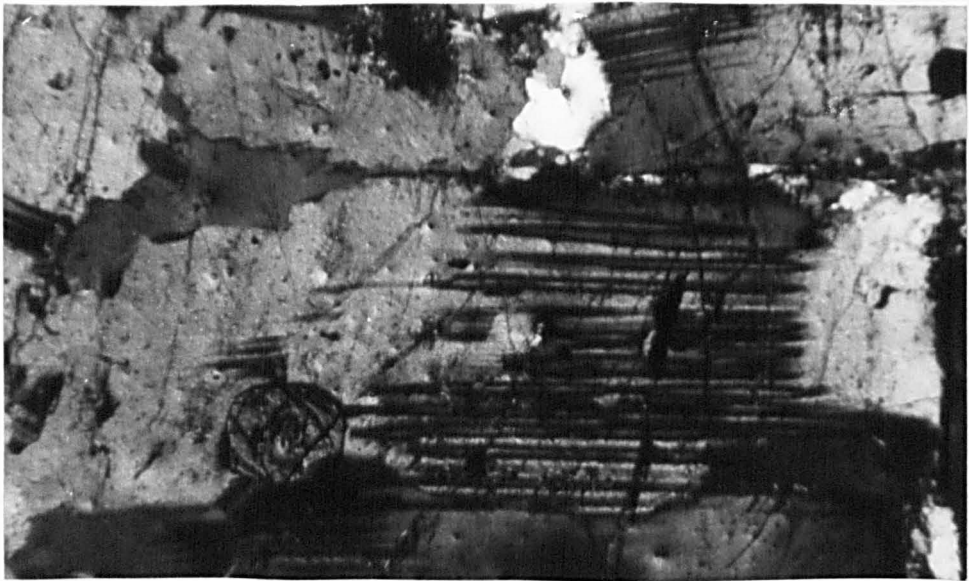
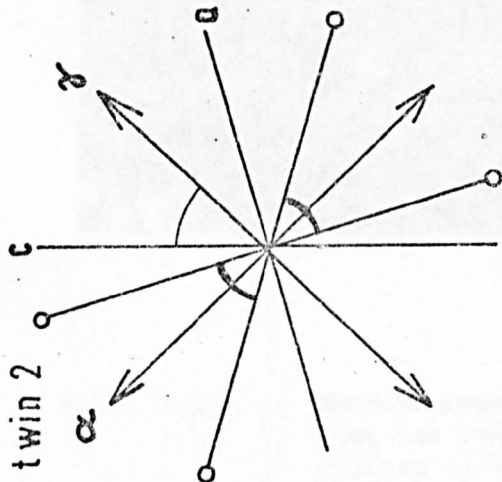
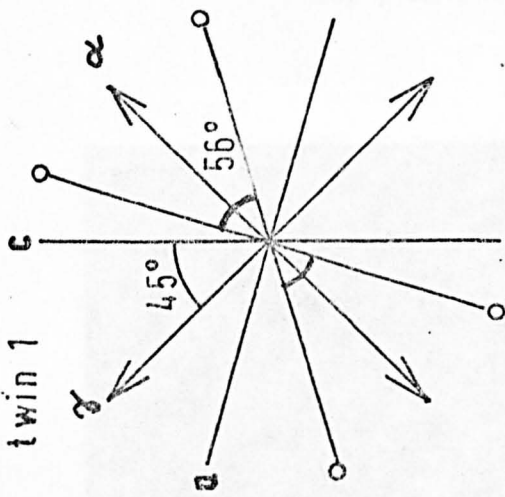


Plate 5.28. Photomicrograph (cn) of a shattered plagioclase with fractures filled with quartz. Quartz hornblende gabbro. 40^{\times} normal size.

PYROXENE
twin 1



HORNBLende

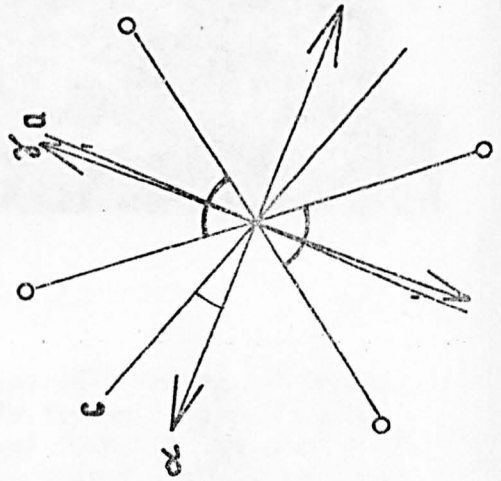
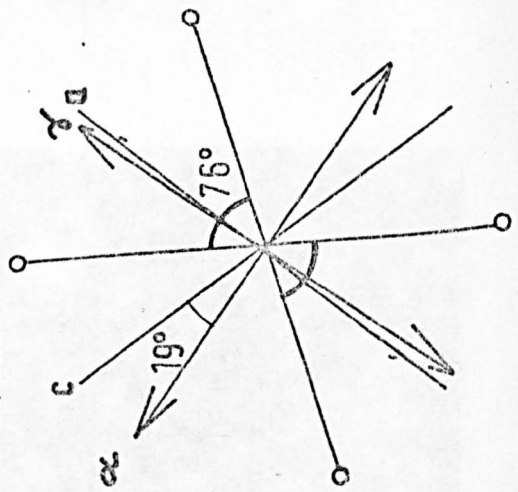


Figure 5.3. Crystallographic and optic axes of the two twinned individuals in a hedenbergite grain. Similar axes are shown for the hornblende grains beneath those of the twin which they replace. Note that in each case an optic axis is common to both the hedenbergite and the hornblende.

to that of the other pyroxene individual (Figure 5.3). Where an aggregate of pyroxene grains is replaced the hornblende is always seen to show these relationships with at least one grain of the aggregate, which is assumed to be the grain at which the nucleation of the hornblende was initiated.

Where the pyroxenes are partially replaced patches of quartz occur that often show intergrowths with the hornblende. This is due to the exsolution of quartz by the relatively silica-rich pyroxene as it is altered to hornblende. The hornblende can show undulose extinction.

Biotite comprises 5-12% of the mode, shows chestnut brown to yellow pleochroism and has a $2V_z = 10^\circ - 13^\circ$, which may be anomalous. It occurs as large plates, up to 1cm across, that rim both orthopyroxene and ore, and shows reaction rims with plagioclase. These grains are frequently bent or kinked. The plates of biotite that replace the plagioclase appears to have thin streamers of prehnite, approximately 5μ wide, that lie along the cleavage. These probably represent the regions where the concentration of the Ca^{++} ions left from the breakdown of the plagioclase was sufficiently high to allow the crystallisation of prehnite.

Quartz comprising 2-5% of the mode is generally interstitial (Plate 5.28), shows strained extinction and is intergrown with hornblende or biotite. Ore comprises less than 1% of the mode and occurs as cores in biotite, and as an alteration

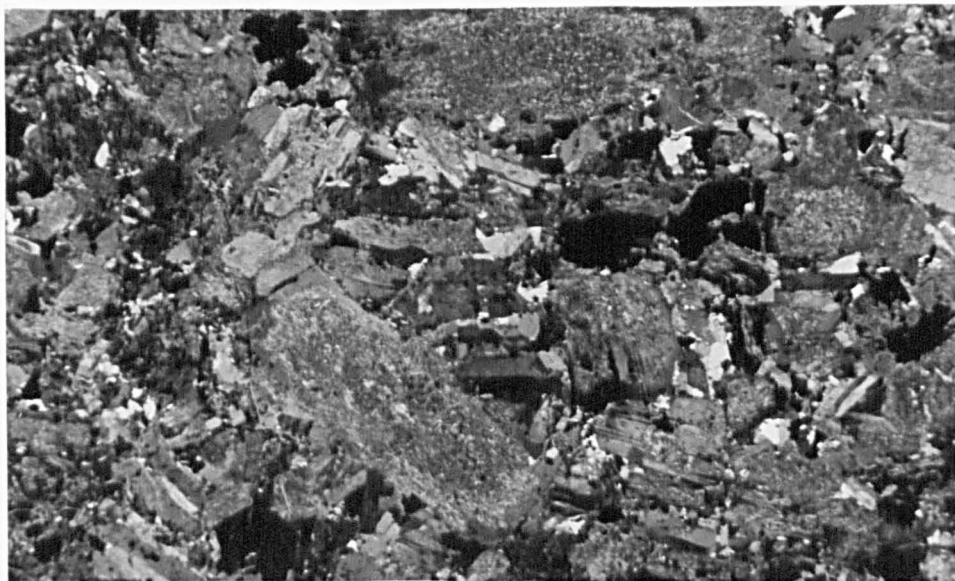


Plate 5.29. Photomicrograph (cn) of the quartz-hornblende gabbro. Note sericitisation of plagioclase and the quartz (clear white) grains in the matrix. 5^x actual size.



Plate 5.30. Photomicrograph (cn) of the quartz hornblende gabbro. Note the twinned hornblende (left centre) and zoned plagioclase with re-entrant angle at the Carlsbad twin plane (right centre). 10^x actual size.

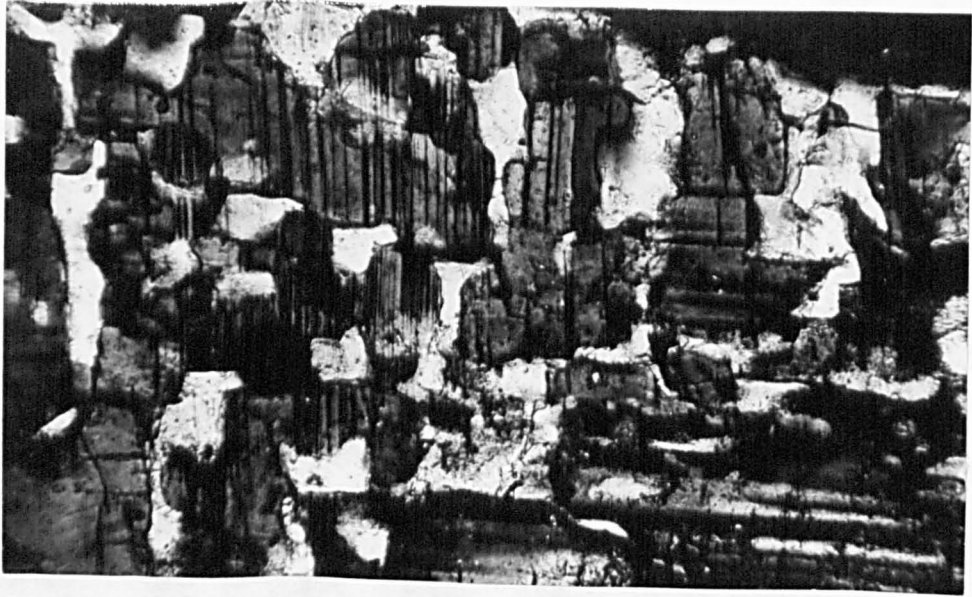


Plate 5.31. Photomicrograph (cn) of graphic quartz-plagioclase intergrowths in the quartz-hornblende gabbro. 40^x normal size.

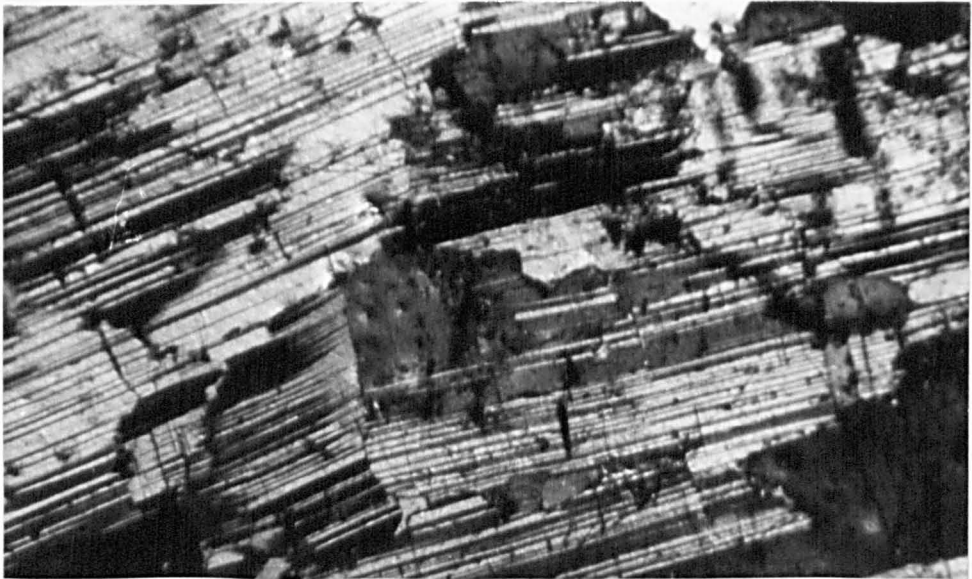


Plate 5.32. Photomicrograph (cn) of disrupted plagioclase in the quartz-hornblende gabbro. 40^x normal size.

product of orthopyroxene. Apatite occurs as small euhedral grains that are enclosed in plagioclase, hornblende and clinopyroxene.

4. The quartz-hornblende gabbro of the outer zone

This is a mesocratic medium grained allotriomorphic granular rock with plagioclase, hornblende, biotite and quartz (Plate 5.29 and 5.30). Towards the northern contact the rock becomes completely altered, the plagioclase being heavily sericitised and replaced by epidote while the biotite is altered to chlorite. The hornblende is first altered to actinolite and this is later replaced by chlorite.

Plagioclase comprises 57-63% of the mode and has a composition of An_{60-65} . It is very similar in nature to that of the other two rock types. Calcic cores are altered to sericite while the more sodic margins (An_{35-40}) often show myrmekitic and graphic intergrowths with quartz (Plate 5.31). The grains show a slight increase in the degree of cataclasis and disruption over those in the other rock types (Plate 5.32). Shearing appears in places to have taken place along Carlsbad twin planes.

Hornblende comprises from 13-34% of the mode, has an average grain size of 4mm, and is generally a greenish variety. Many of the grains show relicts of hedenburgite in their centres (Plate 5.26) and also contain small grains of plagioclase (0.2mm) that were originally enclosed within the pyroxene that has been replaced. (Plate 5.27). These plagioclase grains always show evidence

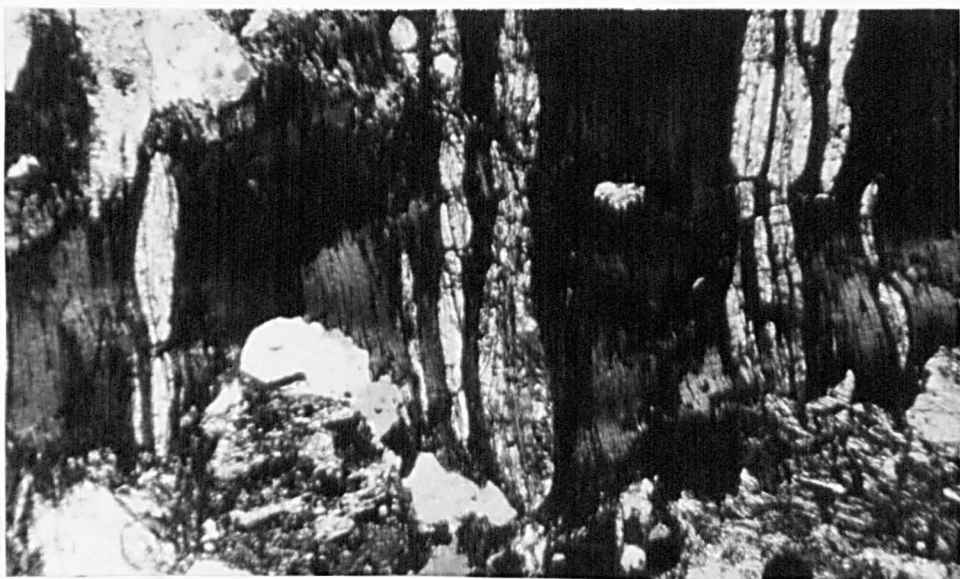


Plate 5.33. Photomicrograph (pp1) of biotite with lenses of prehnite along the cleavage. $20\times$ normal size.

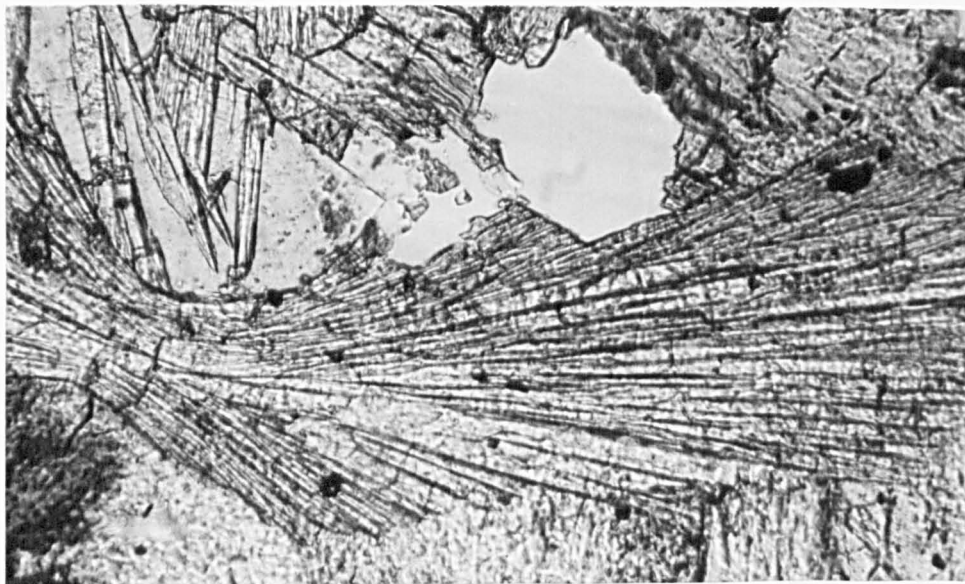


Plate 5.34. Photomicrograph (pp1) of sheaf like aggregate of prehnite in vein. $40\times$ normal size.

of reaction with the enclosing hornblende.

Biotite comprising 3-18% of the mode occurs as plates of up to 1cm in length that show deep chestnut to brown pleochroism. Large ellipsoidal lenses of prehnite lie along the cleavage within the plates (Plate 5.33). There is a definite association between the alteration of the plagioclases and the size and frequency of the prehnite lenses. These are probably formed as a result of the fixation along the {001} biotite cleavage of the Ca^{++} ions released during the alteration of the plagioclase. This means that there must have been considerable short range migration of Ca^{++} ions along the biotite cleavages. Prehnite also occurs as a vein mineral where it exhibits the typical sheaf like aggregates (Plates 5.34). It has a $2V_z = 65^\circ$ Quartz comprises between 2-6% of the mode. It is interstitial and grains are extremely strained. It shows graphic and myrmekitic intergrowths with plagioclase (Plate 5.31) and symplectic intergrowths with biotite and hornblende. Apatite occurs as small euhedral grains that are enclosed in both plagioclase and hornblende.

5. The anorthosites

These are leucocratic rocks that are made up mainly of plagioclase that comprises between 78-85% of the mode (Plate 5.35). They contain variable amounts of pyroxenes, hornblende, biotite and ore which are similar in both texture and composition to those found in the surrounding rock type. They occur as variably orientated irregular bands within all rock types, but are best developed in the transitional zone. Generally they do not appear to

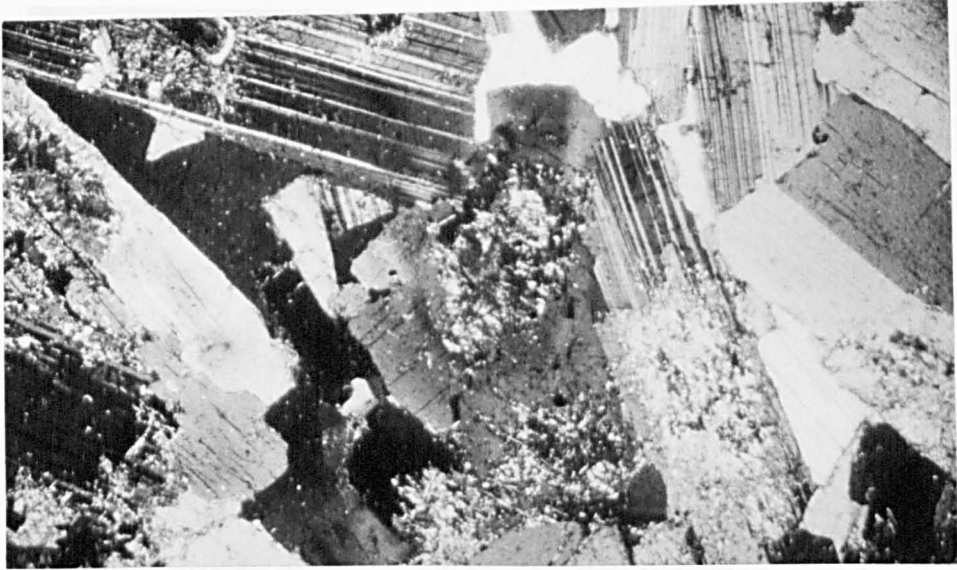


Plate 5.35. Photomicrograph (pp1) of the anorthosites.
10^x actual size.



Plate 5.36. Photomicrograph (cn) of a pyroxene hornfels enclave. Note that the ferrohypersthene is rimmed by hedenbergite (centre). 5^x normal size.

persist for more than a few metres and do not exceed 1m in thickness. They often show one sharp and one gradational contact with the surrounding rock, either of these contacts may be at the base of the band. The existence of such leucocratic bands, coupled with the occurrence of disrupted clots of pyroxene/ore cumulates, would indicate that crystal settling had taken place within the magma in some lower chamber and that intrusion to the present level resulted in the disruption of the resultant layers.

6. The pyroxene hornfels

These are of similar composition to the norites. They are melanocratic and fine grained in the field, showing a saccharoidal texture with rare subidiomorphic megacrysts of plagioclase, orthopyroxene or clinopyroxene (Plates 5.36). No matter what rock type they are enclosed within the larger enclaves show relatively little alteration of the pyroxenes although smaller enclaves show all degrees of digestion by the surrounding rock. It is felt that their smaller grain size and the fact that they were solid during intrusion has been responsible for the lack of alteration. The pyroxene hornfels enclaves are composed of plagioclase (An_{65}) forming 69% of the mode, ferrohypersthene (20%), hedenbergite (7%) hornblende (1%), biotite (0.5%) and apatite. In the centre of the intrusion they are homogenous whereas at the margins some of the enclaves are banded and show some resemblance of the surrounding gneisses.

F. The Alteration of the Norite to the Quartz-Hornblende Gabbro

The mineralogical and textural changes that occur in the alteration of the norite to the quartz-hornblende gabbro may be summarised as follows:

1. While the plagioclases of all three rock types are of the same composition, the degree of sericitisation increases with the degree of alteration of the parent norite. Also, such features as the nylonitisation of grain margins, the internal disruption and bending of grains, and the development of pericline twinning increase with the alteration of the norite.
2. There is a slight increase in the average colour index in going from the norite (C.I. 28%) to the hornblende-ferrohypersthene gabbro (C.I. 31%) then to the quartz-hornblende gabbro (C.I. 35.5%).
3. The composition of the orthopyroxene does not change although its modal value decreases as the norite becomes altered. It is fresh in the norite but becomes gradually serpentinised and then replaced by anthophyllite or actionlite and finally by hornblende in the other rock types.
4. The composition of the clinopyroxene does not vary, but whereas it is only rimmed with hornblende in the norite, it is rimmed with green hornblende and sieved with brown hornblende in the hornblende-ferrohypersthene gabbros and completely replaced by green hornblende in the quartz-hornblende gabbro.
5. The amount of biotite in the mode progressively increases from 2% to 18%, it replaces plagioclase, pyroxenes and ore. The size and the frequency of

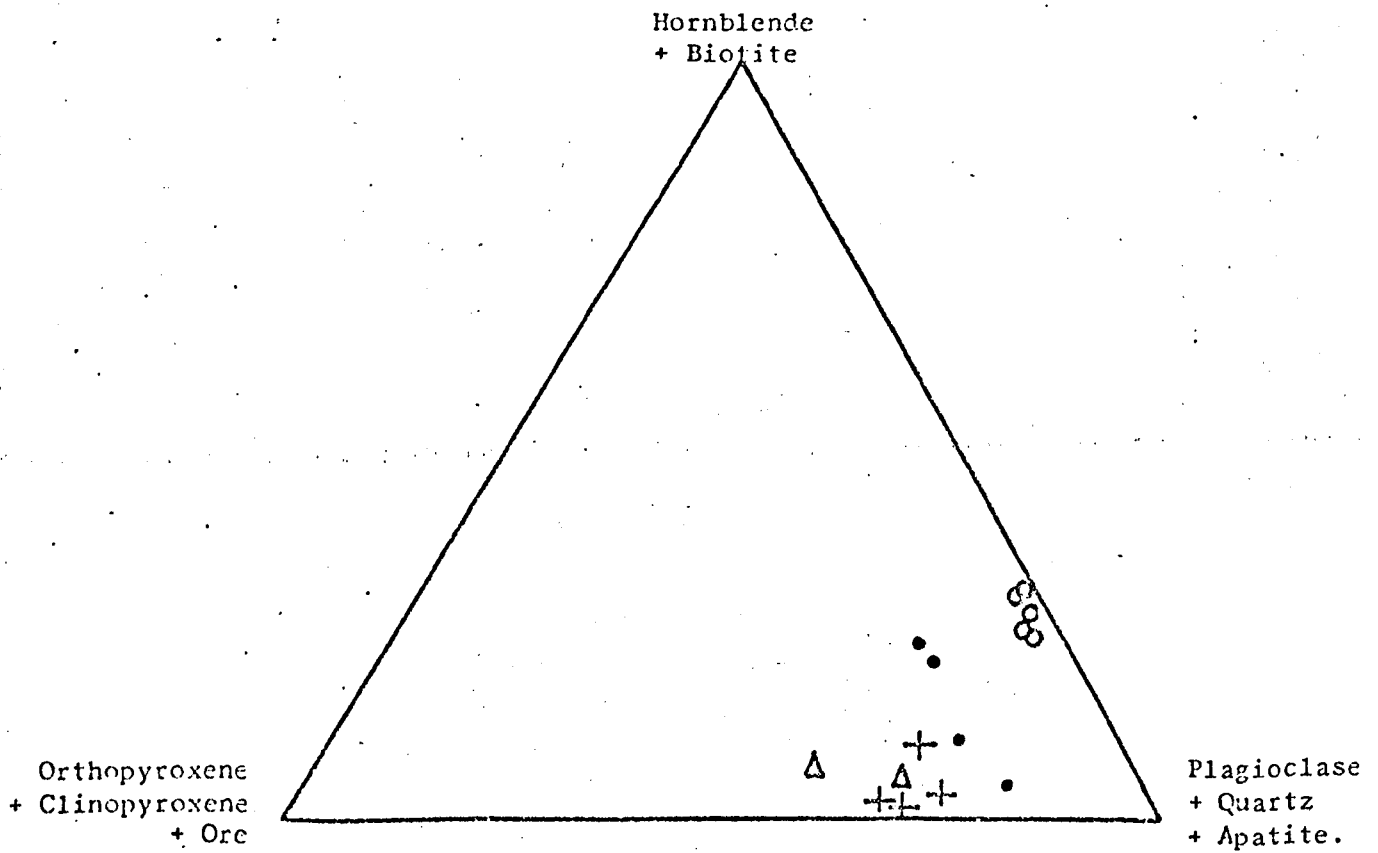


Diagram to show the mineralogical variation within the rock types of the Saint Quay Intrusion.

Crosses=norite, dots=hornblende-ferrohypersthene gabbro, open circles=quartz-hornblende gabbro and open triangles=pyroxene hornfels.

Figure 5.4. Ternary diagram showing the variation in mineral composition in the rock types of the Saint Quay intrusion. Crosses= norite, dots =hornblende-ferrohpersthene gabbro, open circles = quartz-hornblende gabbro and open triangles = pyroxene hornfels.

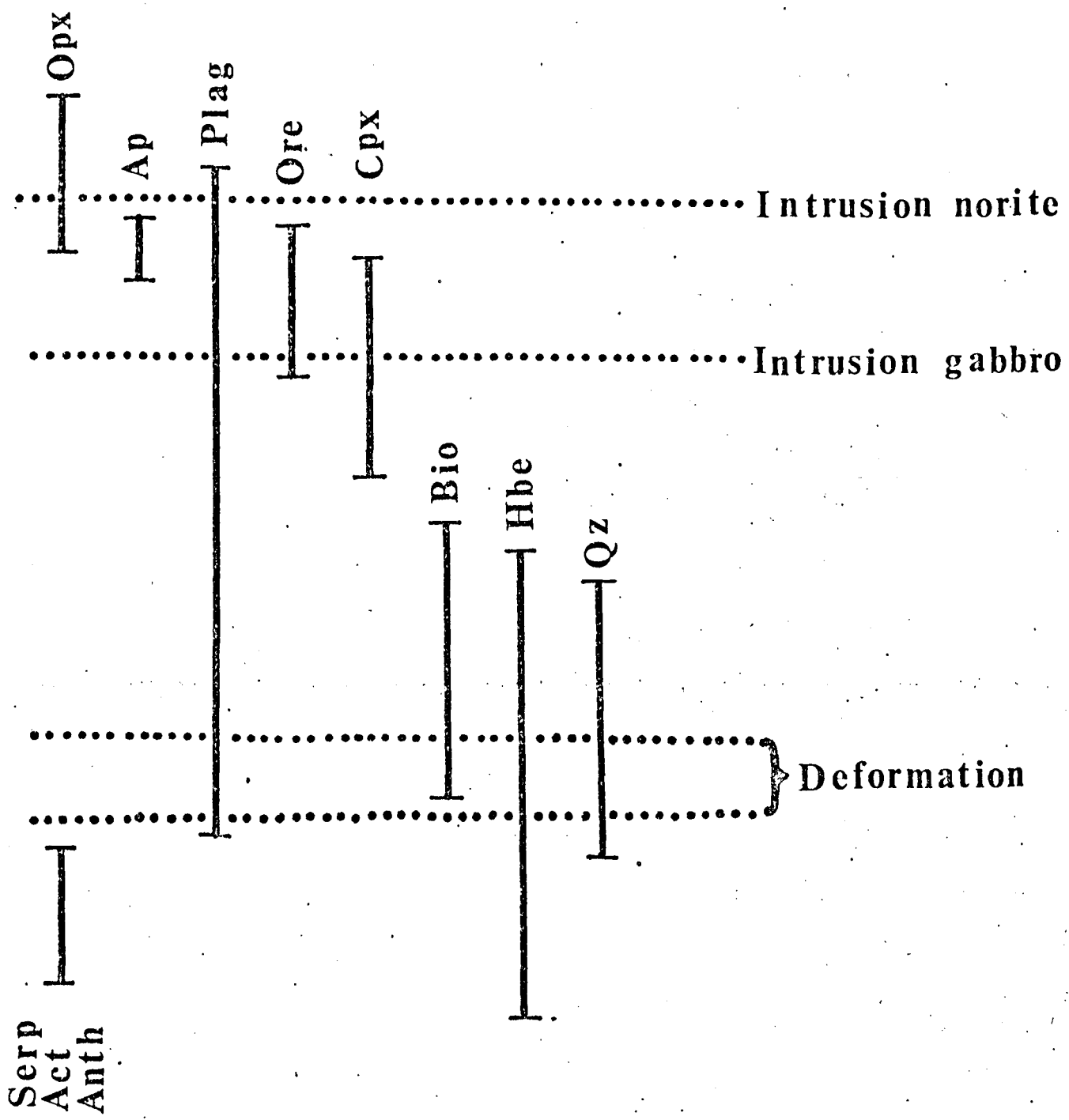


Figure 5.5. Diagram showing the order of appearance of solid mineral phases within the magma chamber which was the source of the Saint Quay intrusion. The intrusive and deformational events are also shown. Opx = ferrohypersthene. Ap = apatite. Plag. = labradorite. Ore = opaque minerals. Cpx = hedenbergite. Bio = biotite. Hbe = hornblende. Qz = quartz. Serp = serpentine. Act = actinolite. Anth = anthophyllite.

the prehnite inclusions in the biotite also increase.

6. Quartz increases in the mode from 0% to 6%. The above mineralogical changes are summarized in Figure 5.4.
7. All the rock types contain pyroxene hornfels enclaves of similar composition.
8. The norite shows chilled margins, whereas the quartz-hornblende gabbro does not.

G. The Sequence of Crystallization

This is summarised in Figure 5.5. The orthopyroxene was the first of the primary magmatic minerals to crystallize, closely followed by plagioclase, apatite, ore and clinopyroxene in that order. A certain amount of crystal settling took place in the early stages before intrusion. The norite was intruded during or following the labile stage of the crystallisation of the orthopyroxene but, before any of the other minerals had undergone significant crystallisation. The quartz-hornblende gabbro was intruded as a crystal mush with most of the primary magmatic mineral phases well into their crystallisation history.

Biotite, hornblende, quartz and plagioclase of a more sodic nature crystallised in the late magmatic phase after intrusion of both bodies, when they were solid but not cool. This may be inferred from the fact that the body underwent deformation and the development of shear zones prior to or at the time of the

Major element analyses

	S4	S11	S12	S13	S9	S15b	S151	S1	S6	S7	S10	S20	S22	S19	S26
SiO ₂	51.36	50.76	51.08	51.51	52.29	54.78	54.83	56.49	56.46	54.28	56.05	53.45	54.33	45.80	50.88
TiO ₂	0.59	0.81	0.64	0.73	0.71	0.80	0.50	0.61	0.86	1.05	0.81	0.77	0.76	0.90	0.57
Al ₂ O ₃	19.05	19.44	18.80	18.87	18.56	17.24	21.39	17.56	13.90	16.79	15.20	17.53	17.02	19.26	14.43
Fe ₂ O ₃	1.91	2.35	1.77	2.17	2.13	1.93	1.19	1.84	1.61	1.61	1.81	1.76	1.46	2.00	1.93
FeO	7.82	7.56	7.15	6.80	6.54	6.63	2.81	6.88	7.76	7.83	7.06	6.44	6.87	8.58	7.76
MnO	0.14	0.13	0.14	0.15	0.13	0.12	0.06	0.12	0.19	0.18	0.14	0.14	0.13	0.12	0.17
MgO	5.51	6.35	5.79	5.73	4.85	4.73	1.81	3.79	4.00	3.65	4.53	5.49	4.89	9.24	9.06
CaO	7.62	6.84	8.25	9.19	6.14	9.43	8.73	5.78	5.93	7.88	7.23	6.48	6.52	7.95	11.50
Na ₂ O	4.37	3.42	4.67	2.96	3.87	3.35	4.35	4.06	3.03	3.50	3.11	4.37	4.45	4.53	1.86
K ₂ O	1.01	0.67	1.11	0.75	1.80	1.14	1.70	2.25	1.98	1.59	1.47	1.80	1.97	0.96	0.63
P ₂ O ₅	0.22	0.18	0.14	0.06	0.19	0.14	0.10	0.17	0.19	0.20	0.15	0.11	0.13	0.34	0.03
H ₂ O ⁺	0.94	0.79	0.87	1.01	2.71	0.68	1.83	1.79	3.20	1.33	2.23	2.19	2.13	0.61	0.82
Total	100.54	99.30	100.42	99.93	99.92	100.97	99.30	101.34	99.11	99.91	99.79	100.53	100.66	100.29	99.64
Normative minerals (C.I.P.W.), anhydrous phases only															
Or	6.0	4.0	6.6	4.5	10.6	8.7	10.1	13.3	11.7	9.6	8.7	10.6	11.7	5.7	3.4
Ab	36.9	29.0	34.2	25.0	32.7	28.3	36.8	34.3	25.6	29.6	26.3	33.6	37.6	18.6	15.7
An	29.4	32.8	27.0	36.0	27.9	27.7	33.8	23.0	18.4	25.2	22.7	22.9	21.2	29.3	29.1
Ne	-	-	2.8	-	-	-	-	-	-	-	-	-	-	10.7	-
Fo	12.0	0.6	7.2	-	2.1	-	-	-	-	-	-	5.0	6.4	14.7	-
Fa	5.3	0.1	8.8	-	0.4	-	-	-	-	-	-	3.1	2.3	8.2	-
Wo	3.0	-	4.4	3.9	0.6	7.6	3.7	1.9	4.1	5.2	5.1	3.6	4.3	3.3	11.6
En	1.4	-	2.0	2.3	0.5	3.7	1.9	1.1	1.8	2.3	2.3	2.1	2.7	2.2	8.5
Fe	1.5	-	2.4	1.5	0.1	3.8	1.9	0.8	2.3	2.9	2.8	1.6	1.6	1.0	3.1
En	0.5	15.0	-	12.1	8.9	8.2	2.7	9.2	8.2	6.9	9.0	4.1	5.1	-	17.7
Fe	0.6	10.9	-	10.0	9.0	6.3	3.0	8.7	11.6	8.7	9.5	5.4	3.4	-	5.4
Q	-	-	-	0.1	-	2.2	1.7	3.0	8.9	3.9	7.6	-	-	0.1	-
Mt	2.8	3.4	2.6	3.2	3.1	2.8	1.7	2.7	2.3	2.3	2.6	2.6	2.1	2.9	2.8
Ilm	1.1	1.5	1.2	1.4	1.4	0.9	1.0	1.2	1.7	2.0	1.5	1.5	1.4	1.7	1.2
Ap	0.5	0.4	0.3	0.1	0.4	0.4	0.2	0.4	0.4	0.5	0.4	0.3	0.3	0.8	0.1
C	-	1.1	-	-	-	-	-	-	-	-	-	-	-	-	-
Modal composition															
Plag.	69.8	65.4	68.5	66.2	66.9	55.4	78.0	52.5	59.4	57.2	56.1	61.9	59.8	66.4	56.4
Opx.	12.8	9.5	20.4	17.1	10.5	4.8	6.2	-	-	0.4	2.8	-	0.9	14.8	21.8
Cpx.	8.3	10.9	7.4	11.6	4.6	10.4	7.5	1.3	0.3	1.5	10.3	0.6	3.1	9.7	12.0
Hbe.	-	8.4	1.2	1.9	3.2	10.0	2.2	11.6	13.7	19.7	10.6	22.6	13.4	4.9	3.9
Bio.	5.4	2.5	0.7	0.4	9.1	13.6	3.7	18.7	14.0	4.2	12.9	8.2	10.7	2.1	3.4
Qz	1.9	1.3	-	0.3	3.7	5.0	1.4	15.6	11.6	15.4	5.8	6.1	11.8	0.3	2.3
Ore	1.6	2.1	1.8	2.3	2.0	0.8	1.0	0.4	0.4	1.4	2.0	0.2	0.3	1.8	0.4
Ap.	0.2	-	0.1	0.2	-	0.2	-	0.1	0.4	0.3	-	0.4	0.1	-	0.2
Cal.	-	-	-	-	-	-	-	-	0.3	-	-	-	-	-	-

Table 5.1. Chemical analyses, normative and modal compositions of the Saint Quay intrusion.

S4 = central norite, St. Marc, S11 = central norite headland between St. Marc and plage St. Quay; S12 = central norite, 500m. north plage St. Quay; S13 = central norite, plage St. Quay; S9 = hornblende-ferrohypersthene gabbro, 200m north St. Marc; S15b = hornblende-ferrohypersthene gabbro, plage St. Quay; S151 = anorthosite, same locality as S15b; S1 = quartz-hornblende-gabbro, Moulin Plage, S6 = quartz-hornblende gabbro, St. Bec du Vir, S7 = retrogressed quartz-hornblende gabbro, Port Goret; S10 = quartz-hornblende gabbro, 500m. north St. Marc; S20 = quartz-hornblende gabbro, south plage St. Quay; S22 = quartz-hornblende gabbro, Pt. St. Quay; S19 = pyroxene hornfels, plage St. Quay; S26 = pyroxene hornfels, Portrieux harbour.

	I	II	III	IV	V
SiO ₂	51.18	51.45	50.19	50.58	47.88
TiO ₂	0.70	0.34	0.75	2.85	0.64
Al ₂ O ₃	19.04	18.67	17.58	18.67	19.79
Fe ₂ O ₃	2.05	0.28	2.84	3.52	1.40
FeO	7.33	9.04	7.19	7.54	6.92
MnO	0.14	0.47	0.25	0.14	0.12
MgO	5.85	6.84	7.39	2.49	8.57
CaO	7.95	10.95	10.50	8.88	9.99
Na ₂ O	3.85	1.58	2.75	3.75	2.47
K ₂ O	1.13	0.14	0.40	0.40	0.95
P ₂ O ₅	0.15	0.09	0.14	0.36	0.07
H ₂ O+	0.90	0.34	-	1.06	1.12
	100.27	100.19	99.98	100.29	99.92

Table 5.2. Chemical compositions of various high alumina gabbro or basaltic rocks.

- I. = average composition of the central norite, St. Quay intrusion
- II. = hypersthene gabbro, chilled floor phase, Bushveld igneous complex (Hall 1932).
- III. = average composition of the high alumina basalts of Japan (Kuno 1960).
- IV. = quartz-gabbro of the Upper Border Group of the Skaergaard intrusion (anal. A.E. Vincent, B.A. Collett and J.A.V. Douglas; Wager and Brown 1968).
- V. = Augite norite of the St. Peter Port layered intrusion from margin of layered sequence (Roach, Hogg & Drysdall in preparation).

crystallisation of these minerals and was hence solid.

Serpentine, actinolite and anthophyllite were the last minerals to nucleate as they are unaffected by the shearing, whereas the minerals they replace were affected and they must, therefore, be post-deformational. Hence, it appears that the clinopyroxenes altered before the orthopyroxenes.

H. Petrochemistry

15 chemical analyses of samples taken from this intrusion are presented in Table 5.1. It will be noted that the rocks of the first intrusive phase, the norites, are the most basic of the three main rock types. These norites contain higher alkalis and lower CaO than the norites of the Bushveld igneous complex (Hall 1932) and higher alkalis than the high alumina basalts of Japan (Kuno 1960) (Table 5.2). In other respects, however, they are similar to the high alumina basalts (op. cit.) in that they have high alumina, high alkalis, low $\text{FeO}/\text{Fe}_2\text{O}_3$ ratio, little or no normative quartz, and pyroxenes rich in the CaSiO_3 molecule which show iron enrichment. It is possible, therefore, that the parent magma was of the high alumina basalt type and that this had undergone considerable differentiation (as it indicated by the degree of iron enrichment). It is in fact chemically similar to quartz gabbro from the Upper Border Group of the Skaergaard intrusion, which also had a high alumina parent magma (Kuno 1960), (Table 5.2).

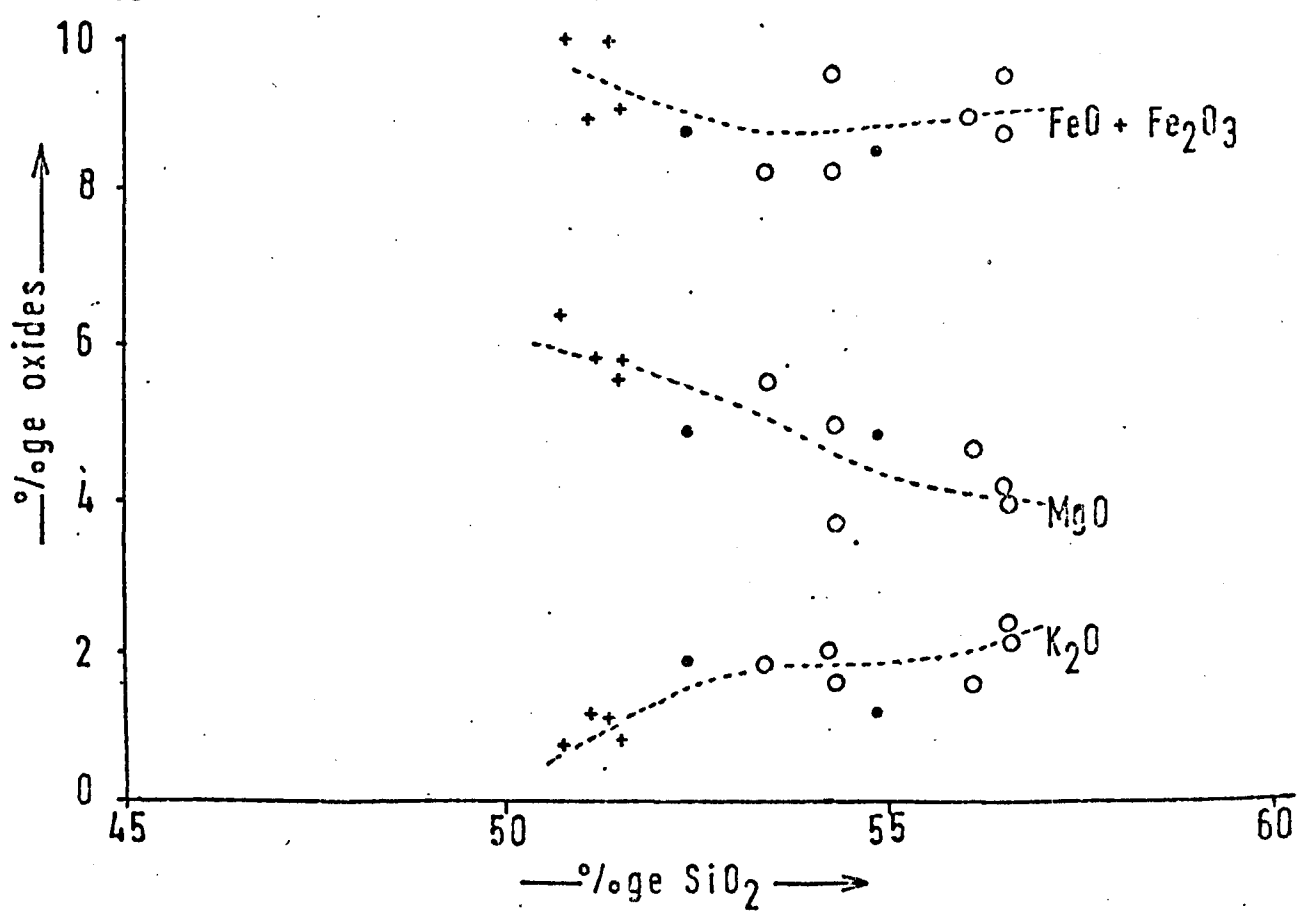
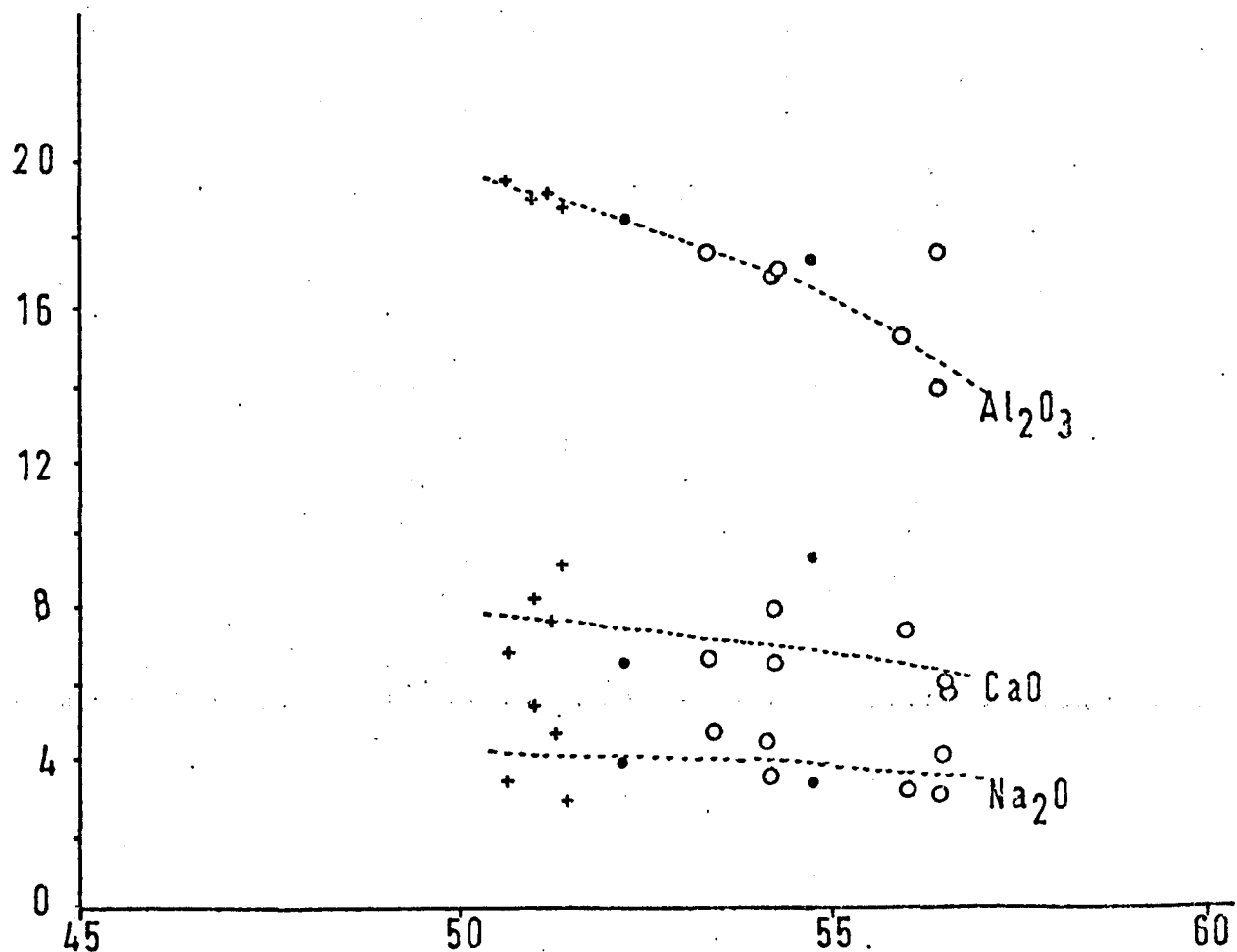


Figure 5.6. Graphs showing the variation in the percentage of the oxide phases with that of SiO_2 for the rock types of the Saint Quay intrusion. Crosses = norite. Dots = hornblende-ferrohypersthene gabbro. Dots and circles = quartz-hornblende gabbro.

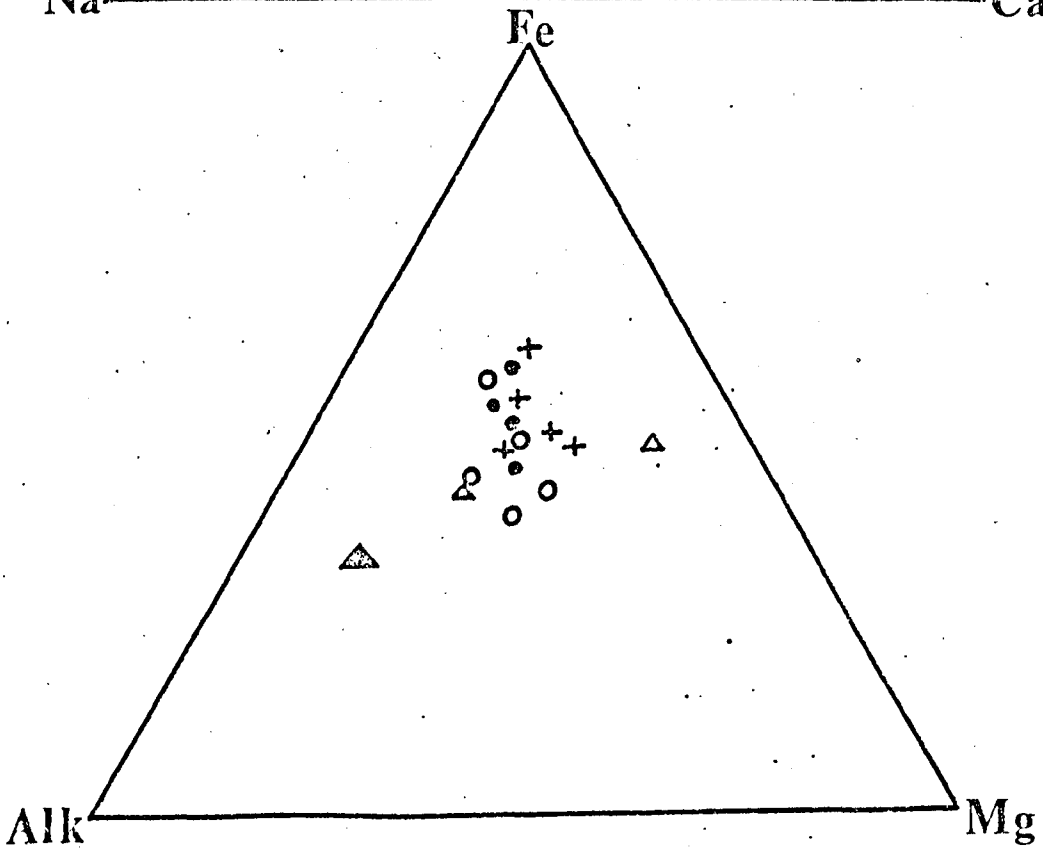
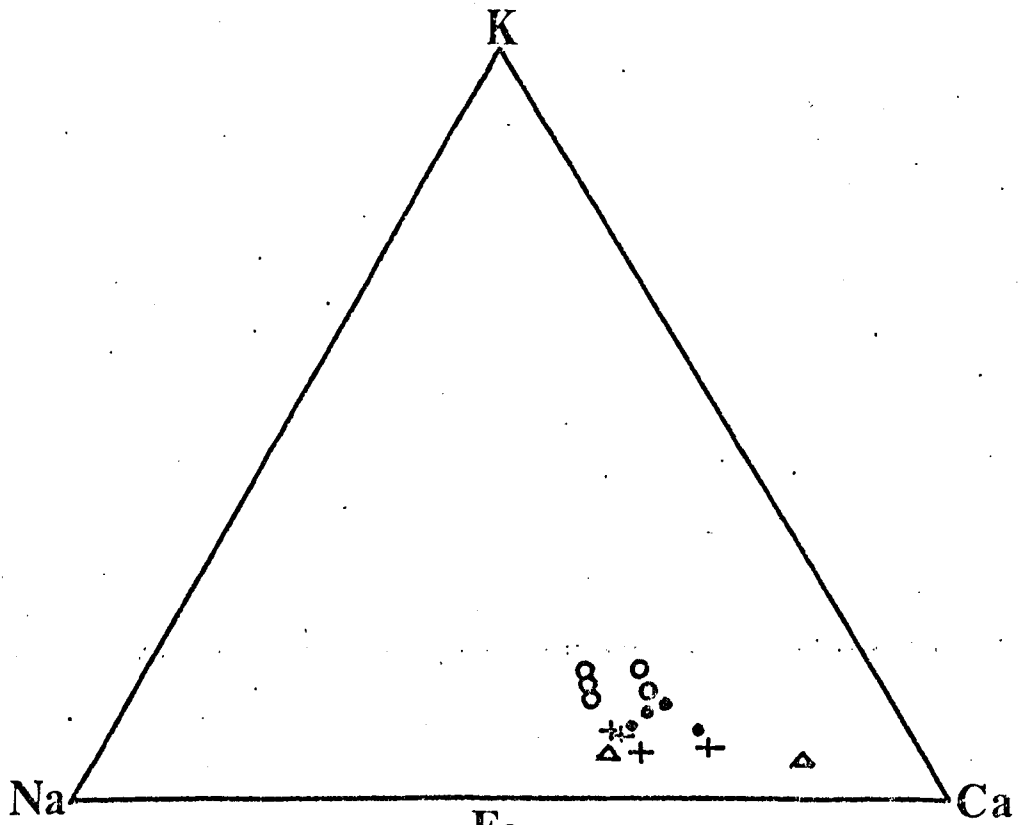


Figure 5.7. K-Na-Ca and F-M-A diagrams for the rock types of the Saint Quay intrusion. Crosses = norite. Dots = hornblende-ferro-hypersthene-gabbro. Open circles = quartz-hornblende-gabbro. Open triangles = pyroxene hornfels and closed triangles = anorthosites.

There is a marked chemical variation between the three main rock types, with the hornblende-ferrohypersthene gabbro showing properties that are intermediate between the norite and the quartz-hornblende gabbro. There is a marked increase in SiO_2 is going from the norite (average 51.2%) to the hornblende-ferrohypersthene gabbro (average 53.8%) and to the quartz-hornblende gabbro (average 59.5%). Associated with this increase in SiO_2 , other oxides such as Al_2O_3 , $\text{Fe}_2\text{O}_3 + \text{FeO}$, and MgO all show a systematic decrease (Figure 5.6) whereas K_2O shows a systematic increase (Figure 5.6). Na_2O and CaO show a slight decrease with increasing SiO_2 but there is no well defined trend. The quartz-hornblende gabbros are richer in H_2O^+ than the norites. K-Na-Ca and Fe-Mg-Alk diagrams (Figure 5.7) show no well defined trends for the rocks analysed although there appears to be a replacement of CaO by K_2O in going from the norites to the quartz-hornblende gabbro.

This chemical variation is reflected in the normative compositions (Table 5.1). There is a marked increase in normative quartz and orthoclase in going from the norite to the quartz-hornblende gabbro, the hornblende-ferrohypersthene gabbro being of intermediate composition. The norite is characterised by normative olivine and nepheline, whereas the other two rock types have normative quartz. Two specimens of the quartz-hornblende gabbro S20 and S22, have no normative quartz and contain normative olivine. This is thought to be due to

the fact that these specimens were collected from a part of the intrusion that is rich in pyroxene hornfels enclaves, many of which are partly digested. Although care was taken to collect samples free from enclaves, reaction between the magma and these enclaves could have led to a local reduction in silica.

The pyroxene hornfels enclaves show no definite chemical characteristics from the two analyses presented although they are poorer in silica than the surrounding rock type, quartz-hornblende gabbro.

1. Discussion

The norites exhibit a fine grained porphyritic chilled margin at their contact with the Port Goret gneisses. This suggests that they intruded these gneisses as a liquid magma which contained some solid phase. The quartz-hornblende gabbro does not show any decrease in grain size at its contact with the gneisses and it contains xenoliths of norite and hornblende-ferrohypersthene gabbro at its contact with the latter. It must therefore, have been intruded between the gneisses and the solidified norite as a crystal mush. The hornblende-ferrohypersthene gabbro of the transition zones, which border the central norite, were probably formed as a result of reaction between the solid norite and the intruding quartz-hornblende gabbro.

The petrology of all three rock types suggests that they all had similar primary igneous solid phases (i.e. labradorite, ferrohypersthene, hedenbergite, magnetite and apatite). However, the quartz-hornblende gabbro is richer in SiO_2 , K_2O and H_2O than the norite. This suggests that the liquid phase of the quartz-hornblende gabbro magma was more differentiated and not in equilibrium with the solid phase. The result was that after its intrusion, the noritic crystal mush reacted with the

more acidic liquid phase. This led to the production of hornblende and biotite at the expense of pyroxene and ore and the precipitation of excess silica as quartz to form the quartz-hornblende gabbro. The hornblende-ferrohypersthene gabbro has an intermediate chemical composition to the other two rock types. This would be expected if it was formed by the limited reaction of the central norites with the liquid phase of the quartz-hornblende gabbro.

The many similarities between the norites and the quartz-hornblende gabbro indicate that they may have originated from the same subjacent magma chamber. The following sequence of events is envisaged. First the norites were intruded to their present level whilst the magma was still fluid. Crystallisation and differentiation by crystal settling then proceeded in this subjacent chamber. When the magma was partly or mostly solid the quartz-hornblende gabbro was intruded between the norites and the gneisses. However, differentiation had led to the formation of a more acidic liquid phase at the upper levels of the subjacent chamber and the noritic crystal mush of the quartz-hornblende gabbro became contaminated with this liquid upon its intrusion.

The sequence of crystallisation of the intrusion would suggest that the magma was subjected to a partial pressure of H_2O in the order of 2,000 to 3,000 bars (Yoder and Tilley 1963). Hamilton, Burnham and Osborne (1964) state that at this $p(H_2O)$ a basaltic magma, saturated with respect to water, could contain 4.5 - 6% (by weight) of water. The patchy zoning and the lack of primary hydrous minerals indicate that the magma was neither saturated nor supersaturated with respect to water. However, the above figures show that even a magma that is unsaturated with respect to water could contain adequate water for the late magmatic development of hydrous phases.

The chemical trends show in figure 5.6, with the exception to

Na_2O , which shows a slight decrease with increasing SiO_2 instead of the expected increase, are consistent with the above hypothesis. This may be due to (1) the decrease in modal plagioclase and the increase in modal quartz in going from norite to quartz-hornblende gabbro or (2) the hornblendes of the quartz-hornblende gabbro being of a low Ca/Na type. The late stage alteration, therefore, appears to be associated with the addition of H_2O , SiO_2 and K_2O to the parent norite and possibly, to a lesser extent, loss of Al_2O_3 , CaO and MgO to the interstitial liquid. Na_2O and total iron appear to have remained relatively constant, but as an overall addition of matter to the parent norite is proposed, their percentage decreases proportionally.

The variation in the Na_2O content of the norite (4.67% in sample S-12 to 2.96% in sample S-13) can only be due to a variation in bulk composition of the plagioclase within the two samples (An_{43} in sample S-12 to An_{58} in sample S-13). This may be due to the local contamination of the norite magma by more highly differentiated sodium rich fluids during intrusion. These fluids may have existed at a higher level in the subjacent magma chamber. Then, as the norite was intruded as a liquid, normal magmatic crystallisation took place and the increased sodium was absorbed by the plagioclase. This variation may also have been due to the local reaction of the norite magma with the pyroxene hornfels enclaves, which are rich in CaO, leading to the growth of more basic plagioclase. It is impossible to estimate the relative importance of the two mechanisms proposed above.

The Saint Quay intrusion was emplaced after the Brioverian sediments were deposited but before the second phase of Cadomian folding F_{2C} . This is obvious from the fact that the contact aureole of the intrusion in the Brioverian is transposed by the S_{2C} foliation. Shear zones were developed in the intrusion during its late to post-magmatic history. The igneous minerals in these shear zones are

cataclased but not retrogressed. The deforming stresses that caused the development of these shear zones must have preceded those which gave rise to the F_{2C} folds and they may have been associated with the first phase of Cadomian folding F_{1C} .

J. Conclusions

The Saint Quay intrusion may be divided into three zones, the central norites, the transitional zone composed of hornblende-ferrohypersthene gabbro and the outer zone of quartz-hornblende gabbro. The Central norites were emplaced first as a liquid magma. The quartz-hornblende gabbro was intruded after the norite had solidified. This crystal mush had a noritic solid phase and a more granitic liquid phase and late to post-magmatic reaction between these two phases produced a quartz-hornblende gabbro. The granitic liquid phase may also have reacted with the margins of the central norite to produce a hornblende-ferrohypersthene gabbro. All these rock types may have originated from one subjacent magma chamber in which a certain amount of crystal settling took place. This intrusion may have been emplaced during the first phase of Cadomian deformation D_{1C} .

CHAPTER VI

SUMMARY OF RESULTS AND DISCUSSION

A. Summary of Results

The existence of Pentevrian rocks in the region has been reported and the lithology, structure and metamorphic history of these rocks have been studied. The Pentevrian has been divided into three lithological units; the Port Goret gneisses, the Plouha Series and the Port Moguer tonalite. The Port Goret gneisses are made up of metamorphosed psammites and pelites that are interbedded with rare calc-silicate bands. The Plouha Series is comprised of metamorphosed sediments, basalts and acid volcanics. The Port Moguer tonalite was intruded into the Plouha Series during the Pentevrian era, post- F_{3p} but pre- F_{5p} , and although original igneous textures are still preserved it is in the main now composed of blastomylonites. Irregular veins of the tonalite have intruded the other two Pentevrian lithological units.

The structural and metamorphic histories of these lithological units have been studied individually and have been found to be very complex, although good correlations between individual events in the different units may be made. In general the Pentevrian has undergone seven phases of deformation that have produced six generations of small scale folds, F_{1p} to F_{6p} , and at least two generations of large scale folds, F_{3p} and F_{5p} . There have been five major metamorphic episodes involved in the pre-Cadomian evolution of the Pentevrian basement, M_{1p} to M_{5p} . The degree of recrystallisation that may be attributed to any one event varies with geographical position within the Pentevrian. The relationship between these structural and metamorphic events is given in Table 2.5. page 2.42.

The first three phases of folding were coaxial and produced tight to isoclinal folds. A penetrative metamorphic foliation S_{1p} was developed throughout the region during the first phase of folding F_{1p} .

The S_{2P} and S_{3P} foliations, which were associated with the F_{2P} and F_{3P} phases of folding respectively, are only locally developed in the hinge regions of these folds. Large scale folds within the Port Goret gneisses were thought to have developed during the third phase of folding F_{3P} . The fourth phase of folding F_{4P} is only locally developed in the Port Goret gneisses. The last main penetrative phase of deformation, D_{5P} , to affect the Pentevrian has produced structures that are orientated $W.10^{\circ}S. - E.10^{\circ}N.$ The style of deformation due to this events shows marked variation, for in the south both large and small scale folds were produced, whereas in the north there was a severe cataclastic deformation. It is thought that this could be due to relative variation in the timing of the deformation and its associated metamorphic events, M_{4P} and M_{5P} .

The Pentevrian is overlain unconformably by the Brioverian. This unconformity is clearly exposed on the coast at Palus plage. The Brioverian has been divided into two lithological units, the Palus plage metavolcanics and metasediments which overstep the Pentevrian basement and the Brioverian of Brehec, Pointe de la Tour and Binic, termed the Binic-Brehec Series. The Palus Plage Brioverian is comprised of interbedded pelites, crystal tuffs, tuffs, and agglomerates. The volcanics are derived from an unknown source and are of acid to intermediate composition. The Binic-Brehec series is comprised of a sequence of regularly bedded turbidites showing such features as to suggest that they were median or distal in nature. This whole series may be regarded as being of "Flysch" type.

The Cadomian orogeny that occurred after the deposition of the Brioverian has affected both the Brioverian and the Pentevrian. Similar structural histories are found in both of the main Brioverian lithological units. Six phases of deformation occurred during this orogeny producing three sets of minor structures, F_{1C} to F_{3C} , two sets of major structures,

F_{1C} and F_{2C} , and three sets of late conjugate minor structures, K_{1C} to K_{3C} . The F_{1C} structures has N-S to NE-SW striking axial surfaces. The main phase F_{2C} structures which control the attitude of the bedding in the Brioverian trend $W15^{\circ}S - E15^{\circ}N$ and were associated with the main metamorphic recrystallisation of the Brioverian M_{2C} . Five phases of metamorphism took place M_{1C} to M_{5C} , M_{3C} being only found in the Palus plage area. In the Binic-Bréhec series the highest grade of metamorphism was of middle greenschist facies whereas the lower amphibolite facies was reached in the Palus Plage area.

Cadomian folding F_{1C} and F_{2C} , has only effected the Pentevrian immediately underlying the unconformity, whereas the later kinks have been developed throughout the region. The earlier phases of Cadomian metamorphism have only effected the Pentevrian near the unconformity, that is at Palus plage, whereas the later events M_{4C} and M_{5C} have effected the whole region. The relationship between the Cadomian structural and metamorphic events is summarised in Table 4.4. page 4.15.

The Port Goret gneisses are invaded by the Saint Quay intrusion. This is a gabbroic body that was emplaced subsequent to Brioverian sedimentation but before the F_{2C} fold phase of the Cadomian orogeny. The body has contact metamorphosed the Series de Binic producing an aureole 1200m in width. It is a composite intrusion, the inner earlier part being made up of norite, and the outer later part being made up of hornblende gabbro that was formed by the late magmatic alteration of a norite that was very similar in nature to that of the inner part. Both phases of the intrusion have such similar geochemistry that it is felt that they have originated from the same magma type that was a moderately well evolved high alumina basalt.

The area is cut by several basic intrusions that are pre- F_{2C} in age

and thought to be associated with the Saint Quay intrusion. Two phases of dolerite dykes are found in the Brioverian, the first was intruded prior to the Cadomian deformation and the second some time after the end of the Cadomian orogeny.

In the north the Brioverian is overlain unconformably by a sequence of red beds that outcrop around Brehec. These were laid down in a shallow water environment and are possibly estuarine. This sequence, which is cut by a small intrusion of augite syenite is only mildly deformed and is of unknown age.

B. Discussion

Although it is realised that the results obtained from such a relatively small region cannot be extended over the whole of the Armorican Massif, they are in contradiction to some of the hypotheses regarding the nature of the Precambrian of the Massif as outlined in Chapter I. It is felt that although these results may help to clarify the general picture it is too early to present a comprehensive picture of the systems analysed.

The Pentevrian of the mainland of France was believed to be made up of dioritic gneisses with a north-south foliation (Cogné 1959). In the region studied they are comprised of paragneisses, orthogneisses, metasediments and metavolcanics. This is a much wider variety of composition than had previously been reported, except for the Pentevrian of Guernsey (Roach 1966) which is comprised of metasediments, migmatites and orthogneisses.

The main structural trend of the Pentevrian in the region studied is almost parallel to that of the later Cadomian structures and both Cadomian and Pentevrian metamorphic episodes achieve the amphibolite facies although the grade of the Brioverian is generally lower. These facts alone are sufficient to invalidate the usage of the criteria of high metamorphic grade or structural trend (north-south) in the recognition of Pentevrian basement. Equally, the criterion of an east-west structural trend is inadequate for the recognition of Cadomian structures.

The only field criteria for the recognition of Pentevrian basement that may be applied are either the demonstration that the particular sequence in question is covered unconformably by rocks of Brioverian age or the proof that this sequence contains structures that pre-date the Cadomian structures found in that region.

The structural history of the Pentevrian in the region studied is a

great deal more complex than that hitherto reported for rocks of this age. In Guernsey a structural history is reported for the Pentevrian (Roach 1966) that whilst not being as complex in detail (this is most likely attributable to the predominance of orthogneisses) actually incorporates two Precambrian orogenic events, the Icartian (2.7 to 2.55 eons) and the Lihouan (2.0 to 1.9 eons) (Roach et al 1972). In view of the lack of radiometric data it is not possible at present to correlate the Pentevrian metamorphic and structural events of the area studied with those of Guernsey. The complex structural history of the Pentevrian basement in this part of the Armorican Massif and the fact that this basement was also affected by the Cadomian orogeny means that if any future age data studies are to be meaningful there must be good geological controls.

Thus it is apparent that a variety of structural histories and lithologies must be expected in any outcrops of Pentevrian that may be subsequently discovered (although it is interesting to note that no limestones have yet been recorded from the Pentevrian) and it is not until such a time that the Armorican Massif has been mapped in detail and all the occurrences of Pentevrian have been recorded and studied that a complete picture of the sequence of events that have affected this Precambrian basement may be drawn up.

No attempt has been made to assign the Brioverian rocks studied to any stratigraphic horizon, although Cogné (1962) and Barrois (1938) have placed the Series de Binic in the middle Brioverian as it contains phtanites and Jeanette and Cogné (1968) have placed it in the upper Brioverian on structural grounds. The author believes that before any lithostratigraphic correlations within the Armorican Massif as a whole can be proposed it is necessary to establish that the various marker horizons were formed as a result of temporal and not geographic

variations within the site of Brioverian sedimentation. Indeed the occurrence of acid volcanics at the local base of the Brioverian at Palus plage is in complete contradiction to previous concepts (Graindor 1957, Cogné 1962) whereby basic vulcanism is said to characterise the lower Brioverian whereas acid vulcanism is typical of the lower part of the upper Brioverian.

Turbidites have been reported in several localities throughout the Brioverian (Bradshaw et al 1967, Bishop et al 1969, Dangeard, Dore et Guignot 1961, Cogné 1962) as well as in the present study. The nature of the sediments in the region studied and those reported elsewhere fits well with the concept that a geosyncline occupied the site of the Armorican Massif during the Upper Proterozoic.

The structures developed during the Cadomian orogeny in the region studied are remarkably similar to those found in the Pays de Leon (Bradshaw et al 1967, Bishop et al 1969). There being a phase of folding about approximately north-south axial surfaces in both regions, which predates the main phase of metamorphism which is associated with the second phase of folding about east-west axial surfaces. This metamorphic event shows rapid variation in grade in both regions. In the region studied the grade appears to increase in those rocks which are in close proximity to the Pentevrian basement. This may be due to the fact that the crystalline basement gneisses are a better conductor of heat than the overlying sequence of clastic sediments. It is interesting to speculate whether other Cadomian 'hot spots' are also associated with outcrops or subcrops of Pentevrian.

The timing of the metamorphism and the folding in this region, as in Pays de Leon, is in direct contradiction to the hypothesis whereby the Cadomian orogeny is divided into two phases, the Constantian and the

Viducastian (Graindor 1964, Cogné 1962). This hypothesis states that the main penetrative foliation should develop before the east-west folds and that it should have had an east-west trend. In both the region studied and in Pays du Leon the penetrative foliation is associated with the second, east-west, phase of folding and it was preceded by folding about north-south axial surfaces. The tectonic sequence reported here is indeed very similar to that found in several other geosynclinal regions and there is no reason to suppose that it was not developed as the result of one orogenic phase that occurred at the end of the Brioverian sedimentation.

The Armorican Massif has so far not been the subject of many detailed structural or lithological studies. Present hypotheses are based on local observations or large scale survey mapping. It is hoped that future researches will enable the full significance of the terms Pentevrian, Brioverian and Cadomian and their relationship to neighbouring Precambrian basements to be elucidated.

APPENDIXMETHODS OF RESEARCH

Geological mapping was carried out upon 1:50,000 scale aerial photographs. The resultant map (Map 1) was prepared from a mozaic of these aerial photographs, as no base maps of less than 1:50,000 scale exist for the area. This map has been checked against the 1:50,000 scale maps for the area (Carte de la France au 50.000^e, type M, sheets numbers VIII/15 "Pontrieux" and IX/15 "Etables") and variations in angle and distance were usually less than 4% of the real value. Larger scale sketch maps (e.g. Map 2 and Figure 3.16) were traced from enlarged copies of these photographs.

The attitudes of planar and linear features were recorded using a Brumpton Transit Compass/Clinometer. Where there was any uncertainty as to the accuracy of the reading, three values were taken and then averaged. Uneven surfaces were smoothed out by placing a flat board upon them. Where these readings are presented on a stereographic projection the lower hemisphere of a Schmidt equal area net was used. These stereograms were contoured using a circular counter whose area was 1% of that of the stereographic net.

The geochemical analyses of the Saint Quay intrusion were carried out using the following methods:

<u>oxide:</u>	<u>author:</u>
SiO ₂	Riley 1958a
TiO ₂	Riley 1958a
Al ₂ O ₃	Shapiro and Brannock 1962
Fe (total)	Riley 1958a
FeO	Shapiro and Brannock 1962
MnO	Riley 1958a
CaO	Esson, J.
MgO	Esson, J.

oxide:author:Na₂O

Riley 1958a

K₂O

Riley 1958a

P₂O₅

Riley 1958a

H₂O+

Riley 1958b

REFERENCES.

- Adams, C.J.E., 1967, K/Ar ages from the basement complex of the Channel Islands (United Kingdom) and the adjacent French mainland: *Earth Planet. Sci. Lett.*, 2, p.52-56.
- Barrois, C., 1895, Le calcaire de Saint Thurial: *Ann. Soc. géol. Nord*, 23, p.38-46.
- Barrois, C., 1896, Légende de la Feuille de Saint Brieuc: *Ann. Soc. géol. Nord*, 24, p. 66-87.
- Barrois, C., 1898, Sur les roches cristallines du massif de Paimpol: *Ann. Soc. géol. Nord*, 27, p.265-270.
- Barrois, C., 1899, Brioverian system. In: *Sketch of the Geology of Central Brittany: Proc. Geol. Assoc.*, 16, p.101-132.
- Barrois, C., 1932, Feuille de Nantes au 1:320,000; chapitre sur les terrains primitifs: *Bull. Carte géol. Fr.*, 36, no. 187, p.38.
- Barrois, C., 1934, Observations sur la carte géologique de Saint Brieuc: *Ann. Soc. géol. Nord*, 59, p. 224.
- Barrois, C., 1934a, Notes sur les gisements des staurotites en Bretagne: *Ann. Soc. géol. Nord*, 59, p.29-65.
- Barrois, C., 1938, Les phanites Briovérien de la Bretagne: *Bull. Serv. Carte géol. Fr.*, 39, no. 197, p.26-30.
- Barrois, C., et Pruvost, P., 1930, Le calcaire de Saint Thurial: *Ann. Soc. géol. Nord*, 54, p.142-185.
- Barrois, C., Pruvost, P., et Waterlot, G., 1938, Revision de la feuille de Saint Brieuc: structure de la Briovérien: *Bull. Serv. Carte géol. Fr.*, 39, no. 197, p.6-10 and 170-174.

- Barrois, C., Pruvost, P. et Waterlot, G., 1939, Les parcours des bandes de phanites graphiteux dans la region briovérienne de Binic (Feuille de Saint Brieuc au 1:80,000): Bull. Carte géol. Fr., 40, no. 199, p.41-53.
- Bertrand, L., 1921, Les anciennes mers de la France et leurs dépôts: Flammarion, Paris.
- Bigot, A., 1890, L'Archéen et le Cambrien dans le nord du Massif Breton et leurs équivalents dans le Pays de Galles: Thèse, Paris, Ed. Le Maout, 202p.
- Bigot, A., 1922, Tectonique de la partie normande du Massif armorican: C.R. XIII^e Congr. geol. intern. Liege, p.382-386.
- Bigot, A., 1923, Observations sur l'existence d'une série compréhensive dans le Massif armoricain: C.R. Somm. Soc. geol. Fr., no. 12, p.117-119.
- Bigot, A., 1925, Sur la présence de Trilobites et d'Archaeocyathidés dans les couches cambriennes des environs de Carteret (Manche): C.R. Acad. Sci. de Paris, 180, p. 1237.
- Bigot, A., 1930, Sketch of the geology of Lower Normandy: Proc. Geol. Assoc., 41, p.363-395.
- Bishop, A.C., Bradshaw, J.D., Renouf, J.T. and Taylor, R.T., 1969, The stratigraphy and structure of part of west Finistère, France: Q. Jl. geol. Soc. Lond., 124, p.308-348.
- Bradshaw, J.D., Renouf, J.T. and Taylor, R.T., 1967, The development of Brioverian structures and the Brioverian/Palaeozoic relationships in west Finistere (France): Geol. Rundsch., 56, p. 567-596.
- Brown, M., Barber, A.J. and Roach, R.A., 1971, Age of the Saint Malo migmatite belt, northern Brittany: Nature (Phys. Sci.), 234, no. 47, p.77-79.
- Brown, M. and Roach, R.A., 1972, Precambrian rocks south of Erquy and around Saint Cast, Cotes du Nord: Nature (Phys.Sci.), 236, no.66, P.77-79.

Bunel, H., 1829-1833, Observations sur les terrains intermédiaires du département du Calvados: Mém. Soc. linn. Normandie, 5, p. 91-100.

Chauris, L., 1956, Sur les relations du Cambrien et du granite du Vir (Calvados): C. R. Acad. Sci. de Paris, 242, p. 3092-3094.

Chauris, L., Dangeard, L., Graindor, M.J. et de L'Apparent, 1956, Les principaux batholiths granitique du bocage normand sont antérieures à la transgression cambrienne: C. R. Acad. Sci. de Paris, 243, p.77-80.

Cogné, J., 1959, Données nouvelles sur l'Antécambrien dans L'Ouest de la France; Pentévrien et Briovérien en baie de Saint Brieuc (Cotes du Nord): Bull. Soc. géol. Fr., ser. 7, 1, p.112-118.

Cogné, J., 1962, Le Briovérien: Bull. Soc. géol. Fr., ser. 7, 4, p413-430.

Cogné, J., 1964, C. R. Sess. extraordinaire de la Soc. Belge Géol. Palaeontol. Hydrol. et la Soc. Géol. Belge.

Cogné, J. et Shelley, D., 1966, Structure géologique du secteur des Abers (Nord Finistère): Bull. Serv. Carte géol. Als. Lorr., 19, p. 1-40.

De Fourcy, J., 1844, Carte géologique du Finistère (text only): Faun et Thunot, Paris, 196p.

Dangeard, L., Doré, F. et Juignet, P., 1961, Le Briovérien supérieur de la Basse Normandie (étage de la Laize) séries à turnidites, a tous les caractères d'un flysch: Rev. Geogr. phys. et Géol. dyn., Ser. 2, 4, p. 251-261.

Dufrénoy, P.A., 1838, Mémoires sur l'âge et composition des terrains de transition d'ouest de la France: Ann. Mines, ser 3, 14, p212-258 & 351-398.

Dzulynski, S. and Walton, E.K., 1965, Sedimentary features of Flysch and Greywackes: Elsevier, London, 274p.

Graindor, M.J., 1954, Note préliminaire sur la glaciation infracambrienne dans le Massif Armoricaïn: Bull. Soc. géol. Fr., ser. 6, 4, p.17-24.

Graindor, M.J., 1957, Le Briovérien dans le nord-est du Massif armoricain: Mém. Serv. Carte géol. Fr., 211p.

Graindor, M.J., 1960, Existence vraisemblable du Pentévrien dans les Îles Anglo-Normandes et la Hague: Bull. Soc. linn. Normandie, ser. 10, 1, p. 44-47.

Graindor, M.J., 1962, Définition du Briovérien sensu stricto: Bull. Soc. linn. Normandie, ser. 10, 3, p.88-91.

Graindor, M.J., 1964, Les tillites anté-Cambriennes de Normandie: Geol. Rundsch., 54, p. 61-82.

Graindor, M.J., 1965, Plissements assyntiens, bakaliens, cadomiens: Bull. Soc. géol. Fr., ser. 7, 7, p. 93-101.

Graindor, M.J. et Wasserburg, G.J., 1962, Déterminations d'âges absolus dans le nord de Massif armoricain: C. R. Acad. Sci. de Paris, 254, p. 3875-3877.

Hall, A.L., 1932, The Bushveld Igneous Complex of the Central Transvaal: Geol. Survey S. Africa Mem. 28, 554p.

Hamilton, D.L., Burnham, C.W. and Osborn, E.F., 1964, The solubility of water and effects of oxygen fugacity and water content on crystallisation in mafic magmas: Jour. Petrology, 5, p. 21-39.

Hérbert, E., 1886, Phyllades de Saint-Lô et conglomérates pourprés du nord-ouest de la France: Bull. Soc. géol. Fr., ser. 3, 14, p. 713-743.

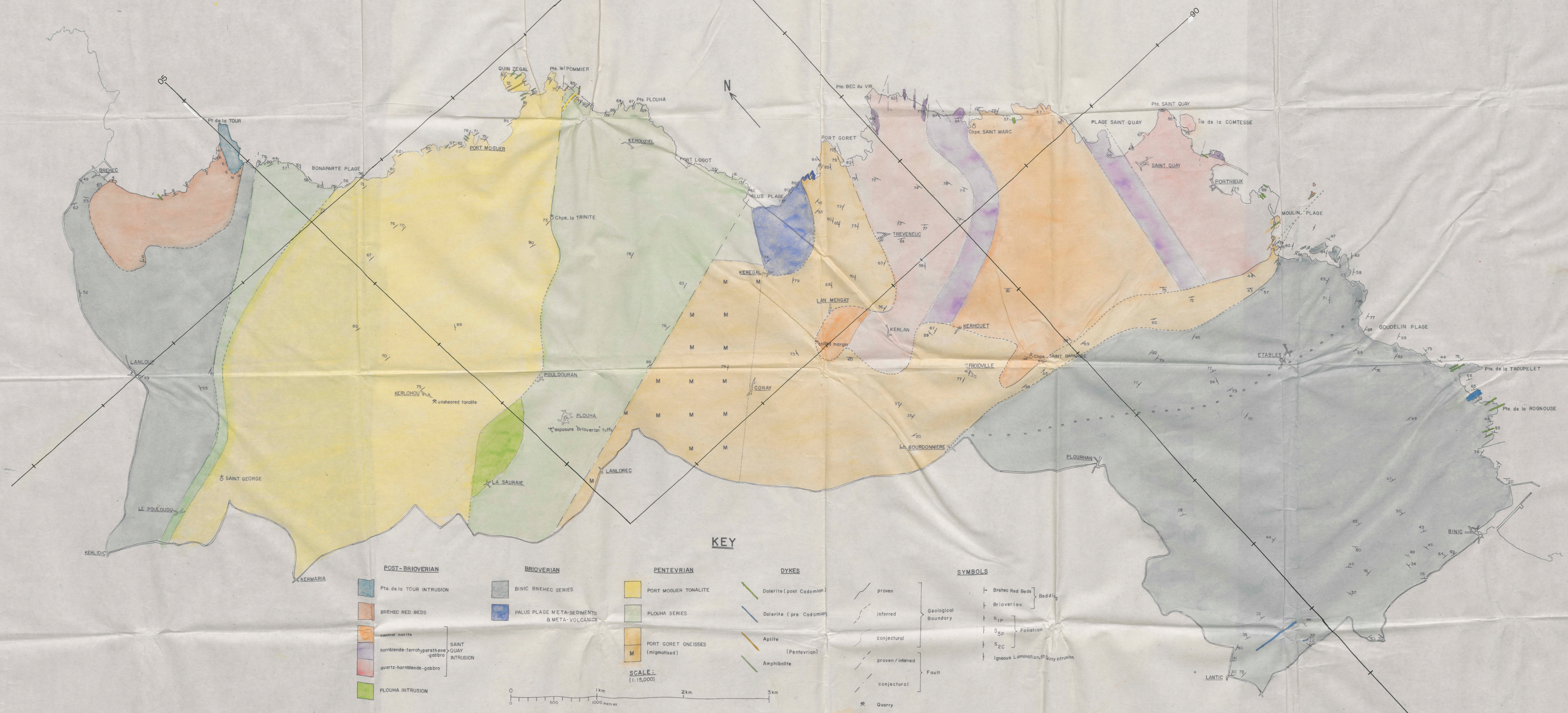
Jeanette, D. et Cogné, J., 1968, Une discordance majeure au sein du Briovérien au flanc ouest de la Baie de Saint Briec: C. R. Acad. Sci. de Paris, 266, p. 2211-2214.

Kaplan, G. et Leutwein, F., 1963, Contribution à l'étude géochronologique du massif granitique de Vire (Normandie): C. R. Acad. Sci. de Paris, 256, p. 2006-2008.

- Kerforne, F., 1923, Le Briovérien dans le massif armoricain: Bull. Soc. Géol. Mineral. Bretagne, 4, p. 123-132.
- Kuno, H., 1960, High alumina basalt: Jour. Petrology, 1, p.121-145.
- Leutwein, F., 1968, Contribution à la connaissance du précambrien récent en Europe Occidentale et développement géochronologique du Briovérien en Bretagne (France). Can. Jour. Earth Sci., 5, p.673-682.
- Leutwein, F. et Sonet, J., 1965, Contribution à la connaissance de l'évolution géochronologique de la partie nord-est du Massif armoricain français: Sci. Terre, 10, (3-4), p. 345-367.
- Leutwein, F., Sonet, J. et Zimmerman, J.L., 1968, Géochronologie et évolution orogénique précambrienne et hercynienne de la partie nord-est du Massif armoricain: Sci. Terre, Mém. no. 11, 84p.
- Mazères, R., 1927, Sur l'existence de roches grésoschisteuses inférieures au poudingues du Bréhec en Plouézec: Bull. Soc. Géol. Mineral. Bretagne, 8, p. 22-26.
- Milon, y., 1927, Le Briovérien et le Cambrien dans l'Anse de Bréhec: Bull. Soc. Géol. Mineral. Bretagne, 8, p. 28-34.
- Mourant, A.E., 1933, The geology of eastern Jersey: Q. Jl. geol. Soc. Lond., 89, p. 273-307.
- Pruvost, P., 1949, Les mers et les terres de Bretagne aux temps paléozoïques: Ann. Hébert Haug, 7, p. 345-362.
- Pruvost, P., 1951, L'Infracambrien: Bull. Soc. Belge Géol. Palaeontol. Hydrol., 60, p. 43-65.
- Puillon-Boblaye, 1827, Essai sur la configuration et la constitution géologique de la Bretagne: Mém. du Muséum, tome 15.

- Ramsay, J.G., 1962, interference patterns produced by the superposition of folds of "similar" type: Jour. Geol., 70, p.466-481.
- Ramsay, J.G., 1963, Structure, stratigraphy and metamorphism in the Western Alps: Proc. Geol. Assoc., 74, p.357-391.
- Ramsay, J.G., 1967, Folding and Fracturing of rocks: McGraw-Hill, New York, 568p.
- Rast, N. and Crimes, T.P., 1969, Caledonian orogenic episodes in the British Isles and North-Western France, and their tectonic and chronological interpretation: Tectonophysics, 7, p.277-307.
- Riley, J.P., 1958a, Rapid analysis of silicate rocks and minerals: Anal. Chim. Acta, 19, p.413-428.
- Riley, J.P., 1958b, Simultaneous determination of water and carbon dioxide in rocks and minerals: Analyst, 83, p.42-49.
- Roach, R.A., 1966, Outline and guide to the geology of Guernsey: Trans. Soc. Guerns., 17, p.751-776.
- Roach, R.A., Adams, C.J.E., Brown, M., Power, G. and Ryan, P.D., 1972, The Precambrian stratigraphy of the Armorican Massif, N.W. France: 24th. International Geological Congress, Montreal, Section 1, p.246-252.
- Robot, M.M. 1962, Sur une coupure stratigraphique à l'intérieur du Briovérien: C.R.Acad. Sci. de Paris., 254, p.3720-3722.
- Shapiro, L. and Brannock, W.W. 1962, Rapid analysis of silicate, carbonate and phosphate rocks: U.S. Geol. Survey Bull., no. 1144A, p. 1-56.
- Shelley, D., 1966, Some aspects of horizontal schistosity: Liverpool and Manchester Geol. Jour., 5, p.185-196.
- Smith, J.V., 1962, Genetic aspects of twinning in feldspar: Norsk. geol. Tidsskr., 42, p.244-262.

- Spry, A., 1969, *Metamorphic Textures*: Pergamon Press, London, 350p.
- Tobisch, O.T., 1967, The influence of early structures on the orientation of late-phase folds in an area of repeated deformation: *Jour. Geol.*, 75, p.554-564.
- Vance, J.A., 1961, Polysynthetic twinning in plagioclase: *Am. Miner.*, 46 p.1097-2006.
- Verdier, P., 1968, Étude pétrographique et structurale de Tregor occidentale (Baie de Lannion, Côtes du Nord, Finistère): Thèse de 3^{ème} cycle, Géologique, Facultie de Science, Universitie de Strasbourg.
- Vidal, P., Auvray, B., Chauvet, J. et Cogné, J., 1972, L'âge radiométrique de la diorite de Saint Quay-Portrieux (Côtes du Nord). Ses conséquences sur le Briovérien de la baie de Saint Brieuc: *C.R.Acad. Sci. de Paris*, 275, p.1323-1326.
- Wager, L.R. and Brown, G.M., 1968, *Layered Igneous Rocks*: Oliver and Boyd, Edinburgh, 587p.
- Walsh, J.N. and Howie, R.A., 1967, Determination of calcium and magnesium in rocks and minerals by atomic absorption spectrophotometry: *Trans. Inst. Min. Metall.*, 76, p. B.119-B.121.
- Wegmann, E., Dangeard, L. et Graindor, M.J., 1950, Sur quelques caractères remarquables de la formation précambrian connue sous le nom de poudingue de Granville: *C.R.Acad.Sci. de Paris*, 230, p.979-980.
- Winterer, E.L., 1964, Late Precambrian pebbly mudstone in Normandy, France: tillite or tilloid: in Nairn, A., (Editor), *Problems in Palaeoclimatology*. Interscience, New York, p.159-158.
- Yoder, H.S. Jr. and Tilley, C.E., 1962, Origin of basaltic magmas: an experimental study of natural and synthetic rock systems: *Jour. Petrology*, 3, p.342-532.



KEY

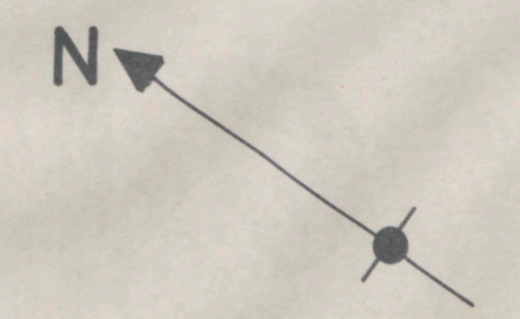
POST-BRIOVERIAN	BRIOVERIAN	PENTEVRIAN	DYKES	SYMBOLS
Pte. de la TOUR INTRUSION	BINIC BREHEC SERIES	PORT MOGUER TONALITE	Dolerite (post Cadomian)	proven
BREHEC RED BEDS	PALUS PLAGE META-SEDIMENTS & META-VOLCANICS	PLOUHA SERIES	Dolerite (pre Cadomian)	inferred
central mafite hornblende-ferrohypersthene-gabbro quartz-hornblende-gabbro		PORT GORET GNEISSES (migmatized)	Aplite (Pentevrian)	conjectural
PLOUHA INTRUSION			Amphibolite	proven / inferred
				conjectural
				Fault
				Quarry
				Trench

SCALE:
(1:15,000)


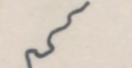
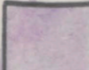
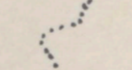

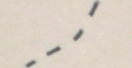
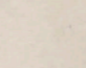
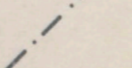
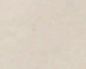
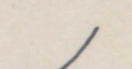
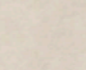

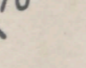
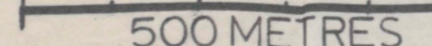
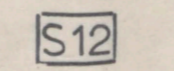
0 500 1000 2000 3000 metres

Geological Boundary
 Bedding
 Foliation
 Igneous Lamination, St. Quay intrusion

MAP 2
 MAP OF THE SAINT QUAY INTRUSION
 [coastal section]



key

- | | | | |
|---|-------------------------------------|---|---------------------|
|  | NORITE |  | CLIFF LINE |
|  | HORNBLÉNDÉ-FÉRRÓ-HYPERSTHÉNE GABBRO |  | ROCKY FORESHORE |
|  | QUARTZ-HORNBLÉNDÉ GABBRO |  | LOW-TIDE LINE |
|  | PYROXÉNE HORNFÉLS |  | FAULT |
|  | NORITE XENOLITHS |  | GEOLOGICAL BOUNDARY |
|  | GNEISS XENOLITHS |  | GNEISS |
|  | ATTITUDE FLUXION STRUCTURE |  | 500 MÈTRES |
|  | GEOCHEM. SAMPLE | | |